CORROSION PERFORMANCE OF EPOXY-COATED REINFORCEMENT–MACROCELL TESTS

by

Khaled Z. Kahhaleh, Enrique Vaca-Cortés, James O. Jirsa, Harovel G. Wheat, and Ramón L. Carrasquillo

Research Report No. 1265-3

Research Project 1265

STRUCTURAL INTEGRITY OF EPOXY-COATED BARS

conducted for the

Texas Department of Transportation

by the

CENTER FOR TRANSPORTATION RESEARCH
BUREAU OF ENGINEERING RESEARCH
THE UNIVERSITY OF TEXAS AT AUSTIN

November 1998

DISCLAIMERS

The contents of this report reflect the views of the authors, who are responsible for the facts and the accuracy of the data presented herein. The contents do not necessarily reflect the official views or policies of the Federal Highway Administration or the Texas Department of Transportation. This report does not constitute a standard, specification, or regulation.

There was no invention or discovery conceived or first actually reduced to practice in the course of or under this contract, including any art, method, process, machine, manufacture, design or composition of matter, or any new and useful improvement thereof, or any variety of plant, which is or may be patentable under the patent laws of the United States of America or any foreign country.

NOT INTENDED FOR CONSTRUCTION, BIDDING, OR PERMIT PURPOSES

James O. Jirsa, Texas P.E. #31360

Research Supervisor

ABSTRACT

A macrocell corrosion experimental program was conducted to study the performance of bent epoxy-coated bars. The damage to the epoxy coating was varied from no visible to the unaided eye (small pinholes) to large gaps of 6x6 mm. The coated bars were embedded in concrete prisms and linked electrically to uncoated bars to set up macro-corrosion cells. Concrete was contaminated with chlorides by ponding salt water in a cyclic wet and dry regime. Corrosion currents flowing from coated steel to uncoated steel were monitored over a period of 4.5 years. The corrosion rate of coated bars was determined and compared to that of uncoated bars. Forensic examinations were conducted at 1, 2, and 4.5 years to relate corrosion measurements to actual bar condition. Based on the findings, recommendations are provided for modifying current specification limits on acceptable damage to coating and improving bar fabrication and coating repair procedures.

PREFACE

This report is one of a series of reports on a project to evaluate the integrity and performance of epoxy-coated reinforcing bars used in transportation structures in the State of Texas. The report describes an investigation of the corrosion performance of fabricated coated bars embedded in concrete prisms and subjected to chlorides in a macrocell setup. Some replicate specimens were maintained in a corrosive environment for about 4.5 years-some of the longest running tests of epoxy-coated reinforcement to date. Companion specimens were autopsied at different times. Findings have been transmitted to TxDOT throughout the project to permit implementation of practices that should help extend the service life of transportation structures.

SUMMARY

Regardless of coating condition, epoxy-coated bars performed much better than uncoated bars. Based on the measured charge flux in the macrocell tests, the worst coated bar performed about 2.3 times better than an uncoated bar. None of the specimens with coated bars experienced extensive cracking, rust staining, delamination, and scaling of the concrete surface as specimens with uncoated bars did. Nevertheless, epoxy-coated bars were not immune to corrosion. The combination of bar fabrication and coating damage was detrimental to corrosion performance. Bars with more damage tended to perform worse. Exposed areas played an important role in the corrosion initiation and mechanism of coated bars. Corrosion in most bars spread from the outer and lower bends towards the inner bend and straight bar legs. Regardless of the level of corrosion, the epoxy coating extensively debonded from the steel substrate, especially at the bent portion. Patching coating damage slightly reduced but did not prevent corrosion in most specimens. The effectiveness of patching was reduced with longer exposure times. Patching damaged areas on the outside of the bend only was not sufficient. Corrosion also propagated from mandrel indentations at the inside of the bend and at the outside of one straight leg. Larger bars experienced higher corrosion than smaller bars. No clear trend was found in the performance of bars with different deformation (bar lug) patterns.

Quality and consolidation of the surrounding concrete had an important influence on the corrosion of epoxy-coated bars. More corrosion was observed at surfaces surrounded by less dense, very porous concrete with more and larger voids. The practice of mixing coated and uncoated bars in the same concrete member may lead to undesirable performance. Any incidental continuity between coated and uncoated bars could establish large macrocells that would be conducive to extensive corrosion. Uncoated bars, even if away from the exposed surface, can corrode regardless of electrical continuity conditions.

IMPLEMENTATION

The study revealed that damage to coating was a dominant factor for performance. Means to improve the quality of coating and minimize damage during production, fabrication, and placement were proposed. Coating bars after fabrication, and following stricter specification requirements regarding coating damage were recommended. Macrocell action between different types of reinforcement could be eliminated in practice by avoiding mixing coated and uncoated bars. Patching all visible damage is advisable to improve performance. The study recommendations were incorporated in guidelines for epoxy-coated reinforcement (Research Report 1265-S). Based on the study findings, additional studies in Project 1265 were focused on improving the materials and methods of patching (Research Report 1265-5), and on improving concrete consolidation around the coated bars (Research Report 1265-2).

TABLE OF CONTENTS

List of Figures

List of Tables

CHAPTER 1

INTRODUCTION

1.1 GENERAL

The effects of coating damage and debonding on the long-term corrosion performance of epoxy-coated reinforcement are major concerns to the industry. Damage to coating during fabrication, transportation, handling, storage, and concrete vibration is almost inevitable. Damage due to fabrication is particularly important because damage and debonding may coexist at critical regions. During bending, bars may be damaged either mechanically or by forming small fissures or holidays, or both, in the stretched coating. Hence, steel becomes exposed within the bent portion. In addition, the common practice of bending coated bars to tight radii results in weakening of the coating adhesion to underlying steel. Although damaged spots are normally patched manually, little has been done to prove the effectiveness of patching. Bent bars are particularly vulnerable because they may be located where chlorides are most likely to attack.

In Florida bridge substructures, the first signs of corrosion of coated reinforcement were observed on fabricated bars. Subsequent investigations revealed that fabrication of coated bars reduces their protection abilities. The susceptibility of coated bent bars to early corrosion development became a major concern. This necessitated evaluating the allowable coating damage limits in the specifications.

This study focuses on assessing earlier specification limits on acceptable damage to epoxy-coated bent bars. These specification limits were current when the study began and are discussed in Section 1.3.5. In order to evaluate the criteria of the specifications, the effects of the following factors on corrosion initiation and progression were considered:

- Use of epoxy-coated and black bars in the same specimen
- Debonded coating in tightly bent bars
- Level of mechanical damage
- Repair of damage
- Bar size
- Bar deformation pattern.

An accelerated corrosion test was designed to study these variables in view of governing standards and specifications. This test utilized the concept of macrocell formation between different reinforcing layers in concrete to aggravate corrosion.

Details of the test, such as steel preparation, material characteristics, specimen design and preparation, test setup, routine monitoring, and postmortem examination procedure are included in Appendix A. Some of this information is presented here for clarity.

1.2 TEST CONCEPT

1.2.1 Macrocell Action

Corrosive cells are set up in concrete structures by differences in concentration of chlorides, alkalies, moisture, oxygen, and metallic ions on different zones of the steel reinforcement.[4,5] In the electrochemical corrosion process, the availability of a cathodic area drives corrosion at anodic sites. Therefore, depending on the relative size and location of the anodic and cathodic areas, corrosion cells may occur in a micro and/or macro scale. In a macro scale, large quantities of cathodic steel are apt to drive high corrosion at anodic steel. In addition, the anode and cathode can be separated by a few centimeters or by several meters, forming macrocells. Such macrocell activity is very destructive in concrete. It is the primary cause of early bridge deck deterioration (concrete cracking and spalling) where chloride-based deicing salts are used[6–8]. (Figure 1.1) The top mat, which is closer to the road surface, is subjected to increased concentration of chlorides and moisture, and oxygen is available at the bottom mat. The top mat becomes an anode and the bottom mat a cathode. Macrocell corrosion is particularly severe because of the availability of a large cathodic area with respect to the smaller anodic areas. The smaller the anode/cathode ratio, the more severe the corrosion.[4,10]

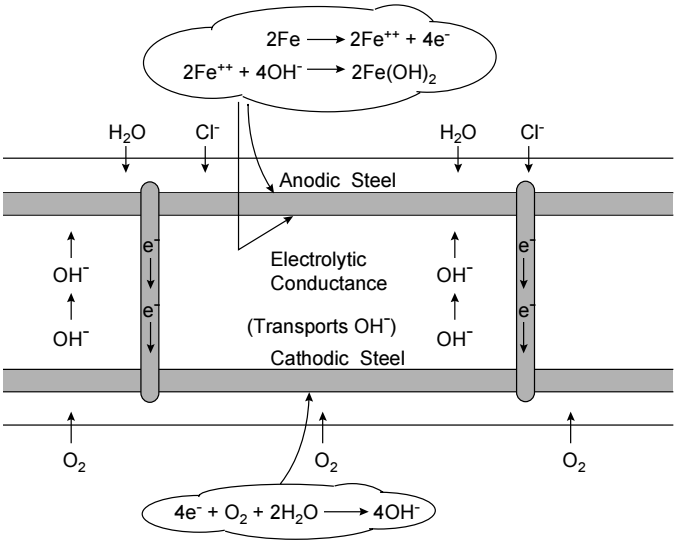

Figure 1.1 Macrocell corrosion cell in bridge deck.

In concrete structures with epoxy-coated reinforcement, macrocell corrosion was originally thought to be unlikely. The rationale was that the epoxy coating would provide not only a physical barrier to the ingress of chlorides to the rebar surface, but would also electrically isolate the protected rebar from other portions of the reinforcement because of its dielectric properties. Because of this assumption, in early applications in which bridge decks were reinforced with epoxy-coated reinforcement, only the top mat was coated (Figure 1.2). Nevertheless, the destructive action of macrocell formation is also envisaged as a possible major cause of corrosion of epoxy-coated reinforcement mainly in bridge decks and marine applications. When damaged coated bars in contact with chlorides are electrically coupled to uncoated bars away from chlorides, the large cathode (uncoated steel) may drive corrosion on the small potentially active anode (damaged spots). However, corrosion of epoxy-coated steel may be governed by physical restraint of ion transport to the damaged spots. This restraint can lead to different corrosion performance characteristics compared to uncoated steel.

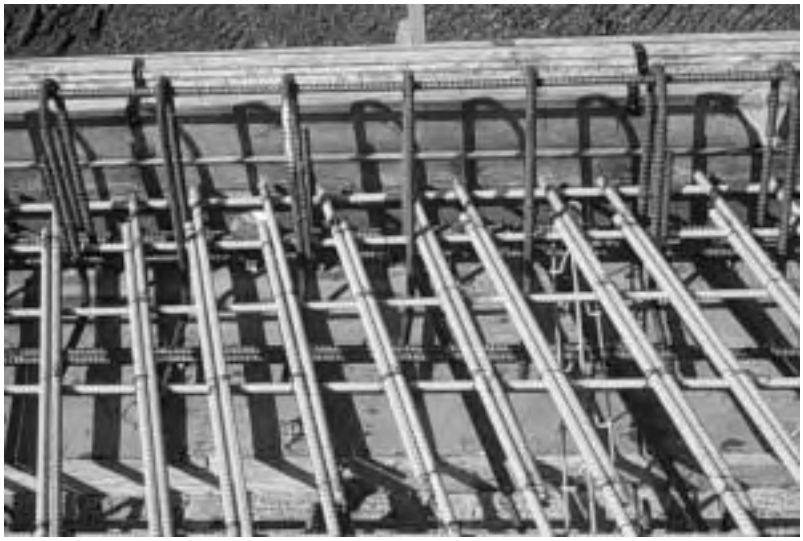

Figure 1.2 Bridge deck construction showing mix of coated and black bars.

Progression of corrosion after initiation is also related to anode potential. The kinetics of anodic polarization can dictate the severity of corrosion activity. Therefore, it is important to investigate the performance of coated bars at the anodic end of corrosion macrocells in concrete. With the availability of cathodic steel, the mechanism of corrosion of coated steel may be controlled by anodic polarization. The macrocell test provides an opportunity to study the anodic performance of fabricated epoxy-coated bars in concrete.

1.2.2 Test Conditions

In order to simulate a bridge deck for macrocell testing, and accelerate corrosion at the same time, the following factors were implemented:

- *High permeability concrete (W/C= 0.57).* The diffusion of chloride ions is faster in less water-tight concrete.
- *Reduced concrete cover (25 mm).* The time of penetration of chlorides to steel level is reduced.
- *A large cathodic steel area coupled to a small anodic steel area.* This ensures a large corrosion driving force.
- *Reduced concrete path between anode and cathode.* The ionic flow path through concrete becomes shorter.

The reality of having a direct electrical contact between reinforcing layers, in the form of metal to metal contact, can be demonstrated by previous field observations. In bridge decks that contained uncoated steel, top and bottom, contact was available in virtually every instance. [7,11] Such contact was provided by truss bars, tie wires, bar chairs, bar ends in contact with expansion dams or scuppers, or both. [7,8,11,12]

On the other hand, partial contact was the most common situation found with epoxy-coated bars. [7,11,12] Even when nonmetallic-coated tie wires and bar chairs were used, mat-to-mat coupling was not always eliminated. Therefore, assuming full contact between reinforcing layers covers the worst conditions. Sagüés[13] has recently found a considerable degree of electrical contact between epoxy-coated bars in the same structure.

Damage to epoxy coating is expected. A damage level of 1% of bar surface area was considered to be representative of the unavoidable mechanical damage prior to casting. Damage introduced during concrete placement may, moderately, add another 1%.[15] Thus, coating damage may eventually reach as high as 2%. This percentage is equivalent to the highest allowable damage limit in earlier specifications.

Subjecting concrete to a wet-dry cyclic regime using a chloride solution promotes corrosion. An earlier study showed that the drying period locally concentrates chloride and oxygen and eventually leads to corrosion initiation[16]. Concentration of chlorides is favorable in corrosion testing for triggering corrosion activity in a short period.

When chlorides penetrate concrete, their accumulation at reinforcing bar level is gradual and nonuniform. The rate of accumulation affects the initiation and development of corrosion and should be accounted for when designing a laboratory experiment. Therefore, ponding a relatively strong salt solution on the concrete surface with shallow depth to reinforcement will reproduce the exposure conditions in the field in a shorter time.

The test represents an artificial situation that may not accurately represent field conditions. The difference between test and field conditions should be kept in mind when analyzing and interpreting the data. It should also be emphasized that the epoxy coating material used for the bars was produced in the early 1990's. Epoxy coatings have been continuously developed since then and today's materials have improved properties compared to earlier formulations. Test results reported herein may not necessarily reflect the potential performance of materials more recently developed.

1.3 TEST VARIABLES

1.3.1 General

The test variables were selected after reviewing practice and governing standards and specifications of epoxy-coated reinforcement that were current when the study began. Bars with standard bends were used in all the macrocell tests because they represent a category of bars most vulnerable to coating damage and increased susceptibility to corrosion.

1.3.2 Reinforcement

Uncoated and epoxy-coated steel bars were included to compare corrosion performance. The performance of "as received" uncoated steel was the standard against which the performance of coated steel, with different surface conditions, was compared.

1.3.3 Bar Diameter

Two diameters, 13 mm (#4) and 25 mm (#8) were selected. Small bars represent reinforcement used in bridge construction for decks and for transverse reinforcement (ties and stirrups). The large bars are typical of longitudinal reinforcement in support structures.

1.3.4 Bar Deformation Pattern

Bars with parallel and cross rib patterns were chosen for the study. The deformation pattern may affect the quality of coating and coating defects produced during bending.

1.3.5 Level of Coating Damage

Previous testing of bent bars reported in the literature has shown that considerable coating damage and debonding may seriously impair the corrosion resistance. Therefore, the degree of mechanical damage to the epoxy coating was the principal variable in the macrocell study.

Epoxy-coated bar specifications, such as ASTM A775,[17] ASTM D3963,[18] and AASHTO M284,[19] and the CRSI guidelines for inspection and acceptance of epoxy-coated reinforcing bars at the job site,[20] set limits on acceptable coating damage. The limits specified by ASTM D3963-87 and incorporated in AASHTO M284-86 (governing specifications when the study began) form the basis of the selected

damage for corrosion testing. The damage level was selected to verify the adequacy of these limits, and to assess whether or not stricter specification requirements were needed.

One category of damage was spots on the outside of bends with a loss of coating slightly greater than 6 x 6 mm (1/4 x 1/4 in.), the acceptable damage size limit. Another category included bars with smaller, but more frequent, damage spots. In this case, the percentage of total damaged area to bar surface area in contact with concrete was slightly above the 2% permissible limit. Hairline cracking along the transverse ribs on the outside of the bend (which is permissible) was the third category. Here, the total percentage of damage did not exceed 1% of the bar surface area. Pinholes or small damaged spots, and sometimes the "as received" condition, constituted the fourth damage category marked by damage percentage less than 1% or 2%. In all cases, damage on the inside of bends, in the form of small mandrel impressions, was included in calculations of percentages.

1.3.6 Repair of Damage

The damaged areas of coating on the outside of the bend were either repaired or left unrepaired as another variable in the test. Repairs (patching) were done according to the manufacturer's instructions using a liquid epoxy patching material and recommended touch-up techniques. To evaluate the effectiveness of repair, the damaged areas on some bars were repaired while similar damaged areas on other bars were not. The intent was to examine the patched areas because the application process is quite different from the plant-applied, fusion-bonded epoxy coating.

1.4 TEST SETUP AND PROCEDURE

Concrete prisms were designed and prepared to simulate the conditions of a bridge deck slab exposed to salt solution. A model of the test specimen and a view of actual specimens are shown in Figures 1.3 and 1.4, respectively. Test bars were divided into two series, denoted A and B, referring to the two bar diameters 13 mm (#4) and 25 mm (#8), respectively. Two different prism configurations were designed for these two series. Only one coated bent bar was used in each specimen at the top, and two (for series A) or three (for series B) uncoated straight bars were placed at the bottom. In control specimens, uncoated bars were used for the top and bottom layers. A third series of smaller plain concrete prisms, denoted C, was designed to provide additional specimens for the determination of chloride content in concrete over the duration of exposure testing.

Series A and B each had 11 groups of three replicate specimens distinguished by the test variables summarized in Table 1.1. With two additional specimens, a total of 68 macrocell specimens was included in the test. The exposure conditions consisted of cycles of ponding a 3.5% NaCl solution on the top surfaces followed by removing the solution and allowing the specimens to dry in a temperature-controlled room. Each cycle lasted four weeks, with two weeks wet and two weeks dry.

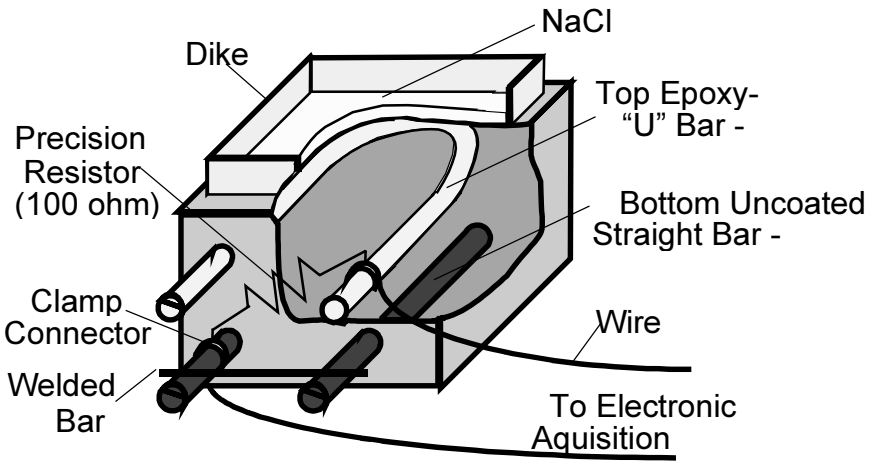

Figure 1.3 Macrocell specimen model.

Figure 1.4 Macrocell test setup.

In order to monitor the macrocell corrosion current, the two reinforcing layers were linked via a known resistor and the voltage drop across this resistor was measured periodically. The voltage was converted to current using Ohm's Law. Corrosion potentials of the top bars were monitored for the last 10 months of the exposure for the last group of triplicates only.

The concrete surfaces were inspected periodically to detect the first signs of corrosion-induced staining and cracking. Concrete deterioration with time was documented to indicate the level of corrosion activity. Macrocell specimens were opened after 1, 2, and 4.5 years to examine the condition of the test bars.

Table 1.1 Summary of Macrocell Study Variables, Series A [13-mm (#4) bent bars] and B [25-mm (#8) bent bars].

Group No.	Deformation Pattern		Epoxy Coating Damage Level[a]					Damage Condition	
	Parallel Ribs	Cross Ribs	Spots >6x6mm	Spots > 2%	Cracks < 1%[b]	Spots < 2%	Pinholes < 1%[c]	Patched	Not Patched
1	●		Control Specimens - Uncoated Bars						
2	●		●					●	
3	●		●						●
4	●			●				●	
5	●			●					●
6	●				●				●
7	●					●			●
8		●	Control Specimens - Uncoated Bars						
9		●	●					●	
10		●	●						●
11		●					●		●

a: Refer to either the size of damaged spots or percentage of damaged area to bar surface area embedded in concrete.
b: Hairline cracks along the transverse ribs on the outside of bends.
c: Fine intermittent tears or pinholes along the rib bases on the outside of bends.
Groups 1 through 7: Parallel Ribs
Groups 8 through 11: Cross Ribs

CHAPTER 2

TEST RESULTS

2.1 GENERAL

Time development of macrocell corrosion was studied over a 4.5-year period. Time-to-onset of corrosion, and time-to-cracking were the two important observations of particular interest during the first year of the test.

The measured macrocell current served as an excellent indicator of time-to-corrosion. Some of the control (uncoated steel) specimens exhibited steadily increasing currents shortly after the test was started. Others showed a delay in the onset of corrosion. In Table 2.1 the time periods elapsed before increasing corrosion currents began to flow are listed.

Table 2.1 Time to Corrosion and Cracking (Time in Days).

Group No.	Damage Category and Condition	Series A, 13-mm bars		Series B, 25-mm bars	
		Time-to-Corrosion	Time-to-Cracking	Time-to-Corrosion	Time-to-Cracking
1	Control	63–98	350–518	7–56	210–224
2	Spots > 6 x 6 mm, Patched	N[a]	-	182–350	-
3	Spots > 6 x 6 mm	469	-	154–266	-
4	Spots > 2%, Patched	N	-	266–462	-
5	Spots > 2%	23–350	-	98–154	-
6	Cracks < 1%	53–616	-	245–280	-
7	Spots < 2%	294	-	84–399	-
8	Control	14–126	343 - 532	7–42	210
9	Spots > 6 x 6 mm, Patched	N	-	203–294	-
10	Spots > 6 x 6 mm	245–504	-	98–273	-
11	Pinholes < 1%	N	-	182–231	-

a N means consistently very low (below 10 μAmp) corrosion current.

Periodical visual inspection of the concrete specimens allowed the determination of time-to-cracking. The first signs of concrete staining and cracking due to corrosion were visible on the large bar control specimens. The small bar control specimens also exhibited similar corrosion manifestations but after a longer period of exposure. The recorded time-to-cracking for all the specimens are also shown in Table

2.1. Further descriptions of crack initiation and propagation are given in Section 2.3.1. The epoxy-coated bar specimens remained uncracked during the initial (2 year) observation period.

Measuring the macrocell current between anode bars and cathode bars offered quantitative means to evaluate the corrosion rate of the anode bars. The corrosion rate was used to study the relative performance between the coated and uncoated bars and within the variably damaged coated bars.

2.2 MACROCELL CORROSION CURRENTS

2.2.1 General

Graphs showing the trend of corrosion current data over time for all specimens are included in Figures 2.1 and 2.2. Each diagram displays three curves corresponding to the three replicate specimens in a group. The corrosion currents illustrate macrocell development as a function of exposure time. The results provided valuable information on corrosion behavior. Monitored currents were useful in assessing the relative performance of specimens before autopsy and complemented the findings after the autopsies. Current plots were generally jagged curves with a series of low and high peaks. Such peaks corresponded to the end of the wet (high values) and dry (low values) periods.

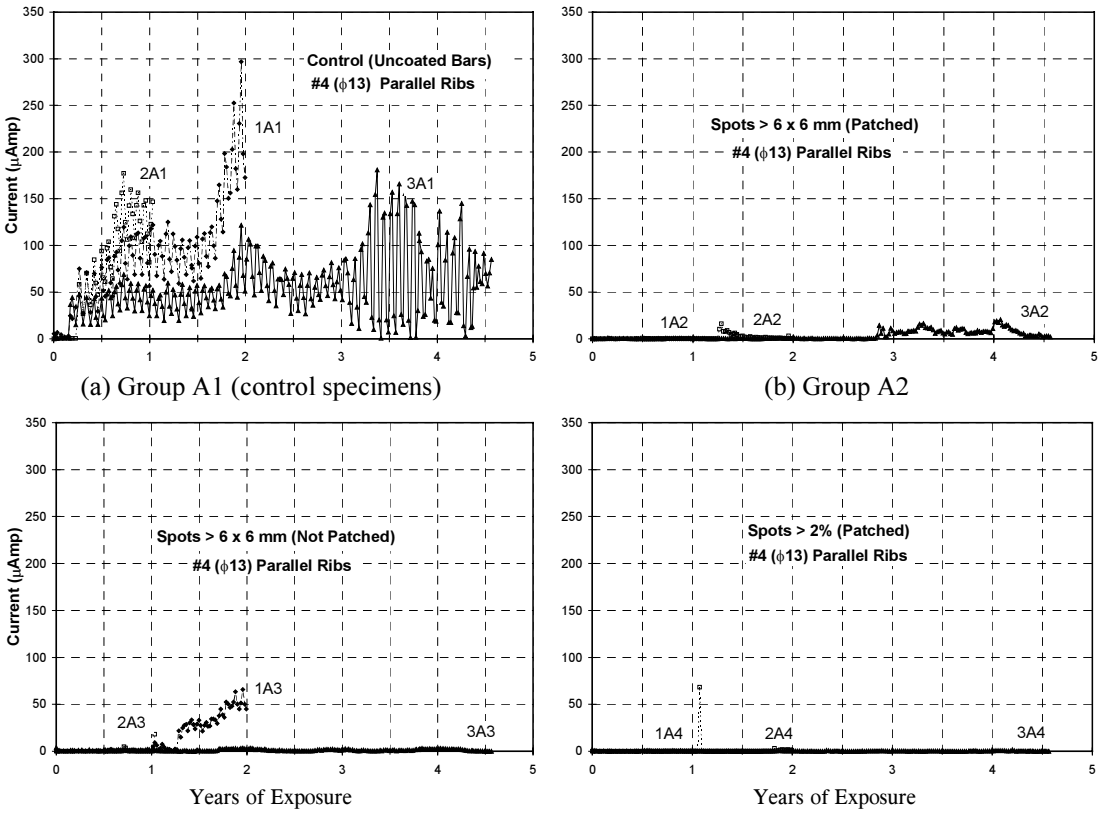

Figure 2.1 Current vs. time of series A (13-mm) bars (con't.).

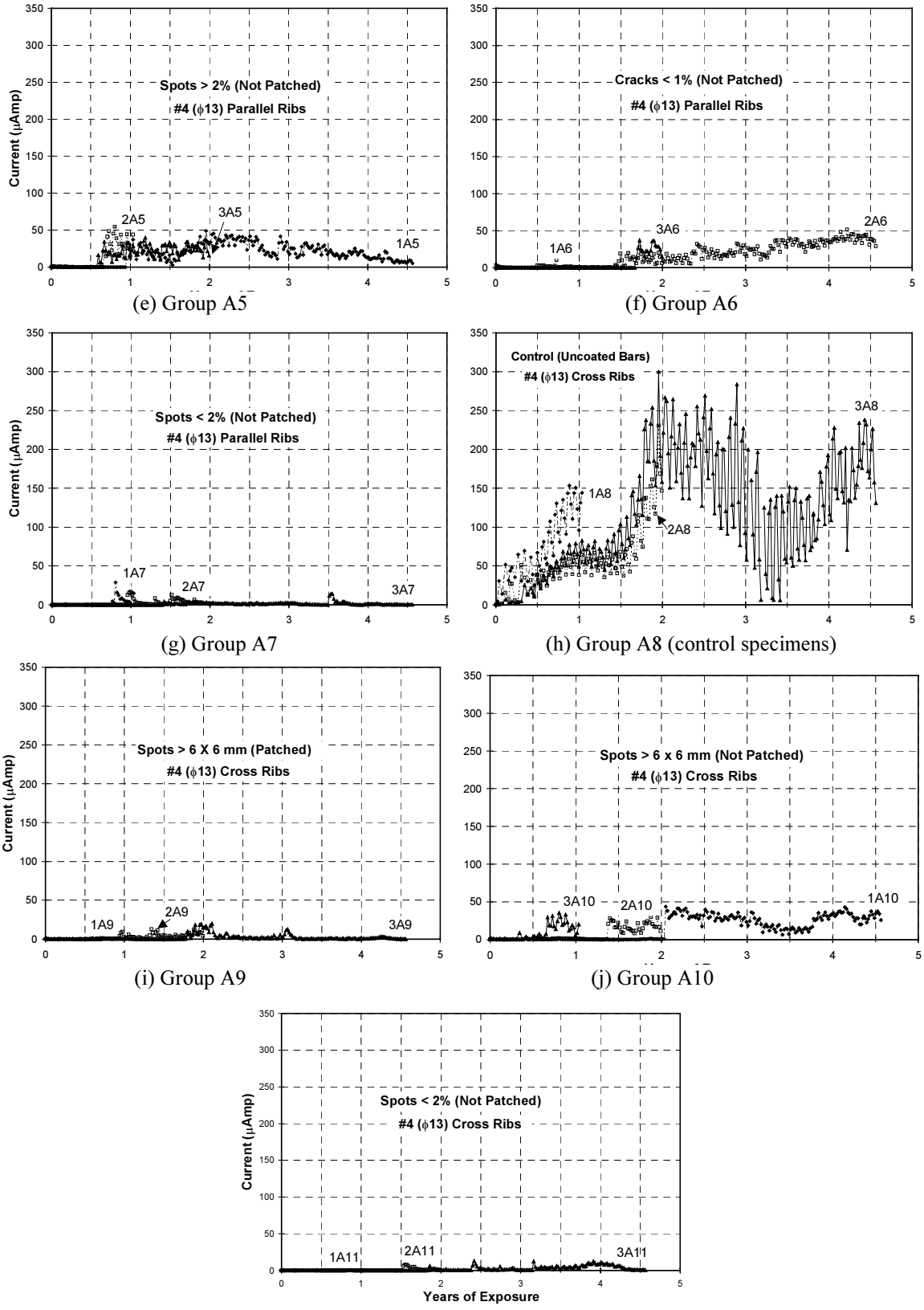

Figure 2.1 Current vs. time of series A (13-mm) bars.

2.2.2 Control Bar Specimens

Uncoated bars showed higher currents than epoxy-coated bars. Initially, all control specimens appeared to develop consistent macrocell current patterns after some time of exposure, with the small bar specimens showing less variation in currents than the large bar specimens. However, all bars showed more scattered and erratic behavior after 2 and 3 years of exposure. The jumps between high and low peaks became significantly larger. This was especially noticeable in the 13-mm (#4) bar with parallel ribs. Larger bars experienced higher corrosion currents than smaller bars.

Interestingly, macrocell currents for 13-mm (#4) bars with parallel ribs [Figure 2.1(a)] were not very high (in the range of 60-90 μA) despite the evident surface deterioration and cracking of the specimen. At about 2.5 years, the 13-mm (#4) bar with cross ribs [Figure 2.1(h)] started to show a continuous drop with wide jumps between high and low peaks after reaching maximum currents (200 to 250 μA) between 2 and 2.5 years. However, at about 3.5 years the current continuously increased again until the end of the exposure (range of 150 to 230 μA).

Jumps between high and low peaks tended to be less pronounced in 25-mm (#8) bars but the specimens experienced relatively sudden, large increments of activity at certain periods. The specimen with parallel ribs [Figure 2.2(a) reached a steady-state behavior (between 200 and 300 μA) at about 3.5 years when there was an abrupt increase in current (up to 700 μA). Thereafter, the behavior showed wide variations between high and low values (range of 400 to 600 μA). The specimen with cross ribs [Figure 2.2(h)] showed declining currents from 2 to 3 years, but after 3.5 years the currents suddenly increased about 200% in a 9-month period and remained high until the end.

2.2.3 Epoxy-Coated Bar Specimens

Plots of corrosion currents for epoxy coated bars did not show as large variations between high and low readings as those for uncoated bars, possibly due to the smaller current levels. From Figures 2.1 and 2.2, clearly, the specimens with larger bars developed much higher current levels than specimens with smaller bars. Group B.5 specimens (25-mm bars with coating damage slightly exceeding 2%) showed the worst performance of all coated bar specimens. Series A specimens with total coating damage less than 2%, and patched bars, exhibited the best performance with negligible currents. The patched bars of series B exhibited activity much lower than identical unrepaired bars after 2 years, but the difference in currents between repaired and unrepaired bars decreased after 4.5 years. Even though repaired specimens tended to develop less current than unpatched specimens, there were a few cases where patched bars had similar or higher currents than damaged bars. There was no appreciable difference in performance between bars with different deformation patterns.

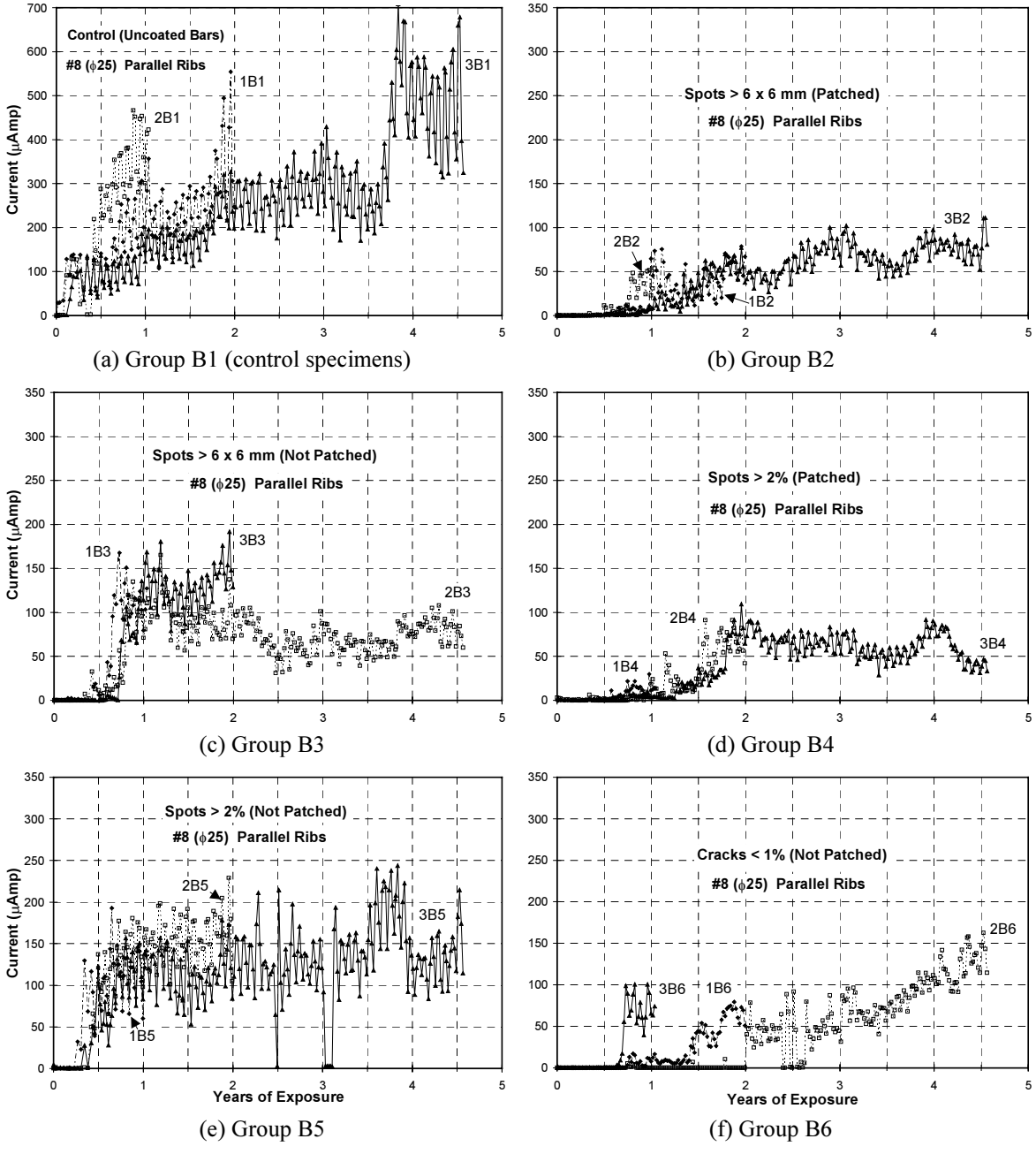

(a) Group B1 (control specimens)

(b) Group B2

(c) Group B3

(d) Group B4

(e) Group B5

(f) Group B6

Figure 2.2 Current vs. time of series B (25-mm) bars (con't).

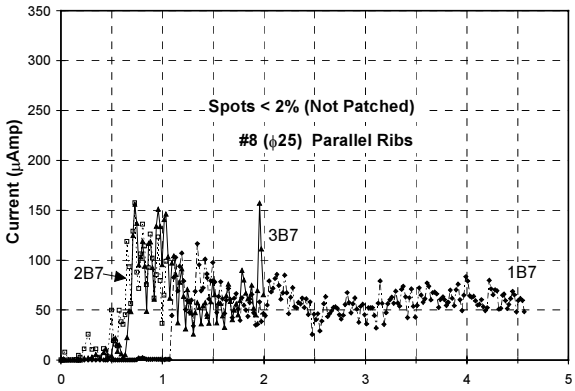

(g) Group B7

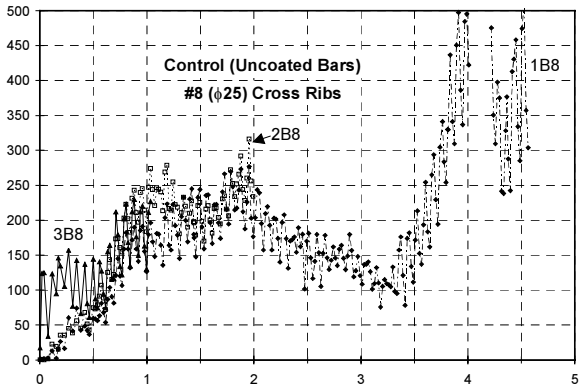

(h) Group B8 (control specimens)

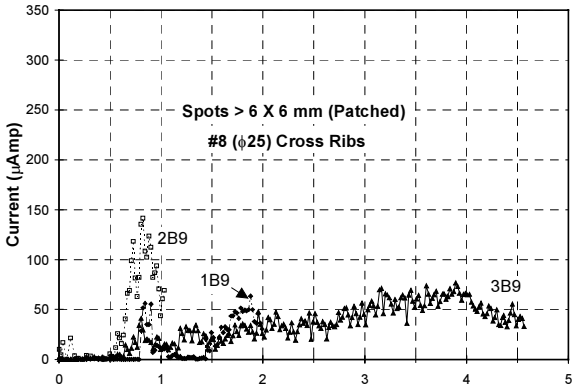

(i) Group B9

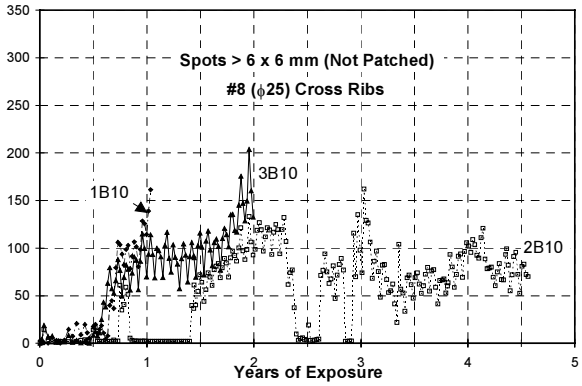

(j) Group B10

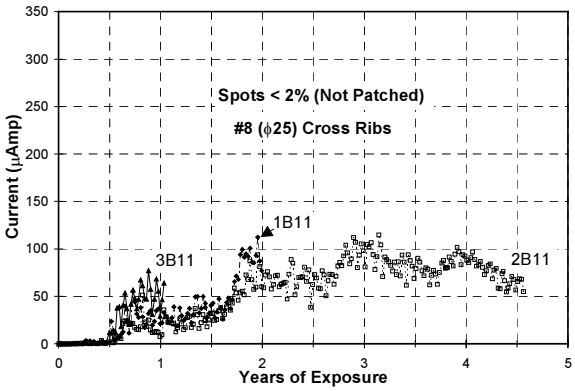

(k) Group B11

Figure 2.2 Current vs. time of series B (25-mm) bars.

If corrosion rate is defined as the increment of corrosion per unit time (the slope of the curves), most specimens showed small corrosion rates and seemed to have reached a steady-state behavior. The few specimens that were showing increasing corrosion rates at the end of the exposure were 13- and 25-mm bars with cracks in the coating and damage less than 1% (coating is cracked alongside the ribs and the amount of exposed steel is less than 1 %).

For all specimens where corrosion activity was evident, the electric currents flowed from the top reinforcing bar to the bottom bars as expected. This pattern was maintained throughout the test period.

The differences in currents observed within one group reflect variations in the extent of corrosion activity experienced during the time period of testing. These differences could be attributed to variations in concrete cover due to finishing after concrete pouring. Generally, the differences in behavior tended to even out with time.

2.3 CORROSION POTENTIALS

A few, typical plots of corrosion potentials measured over time of exposure are shown in Figures 2.3 and 2.4. For the majority of specimens, there was little variation between readings and potential curves had reached steady-state behavior. Any corrosion process (large or small) is expected to be well established by the time measurements were first taken (after 3.5 years of exposure).

Figures 2.5 and 2.6 show average corrosion potentials for all specimens from series A and B. All uncoated bars (13 and 25 mm) had more negative average potentials than coated bars (from -530 to -565 mV vs. SCE). Corrosion potentials were similar for both 13- and 25-mm black bars. For coated bars in series A (13-mm bars), average corrosion potentials ranged from -205 mV to -480 mV vs. SCE. For coated bars in series B (25-mm bars), average potentials ranged from -325 mV to -425 mV vs. SCE. Clearly, larger bars developed more negative and more uniform average potentials than smaller bars.

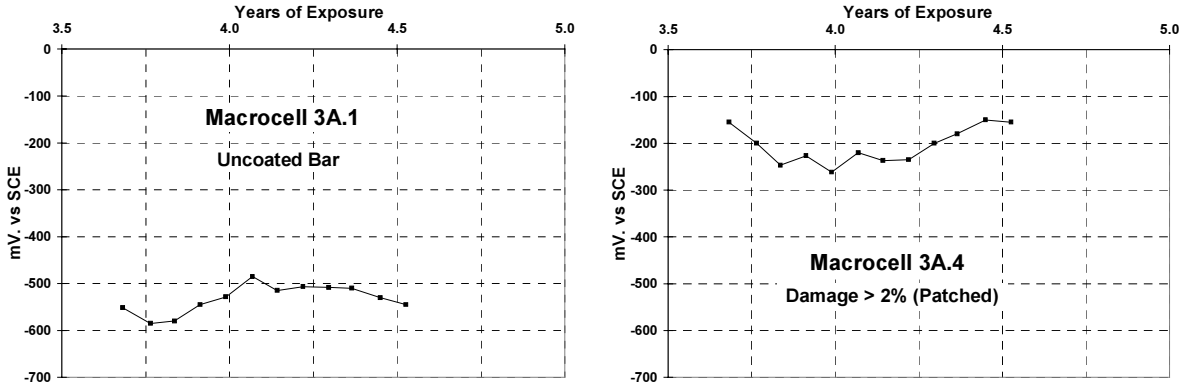

Figure 2.3 Average corrosion potentials vs. time of typical specimen A [13-mm (#4)] bars.

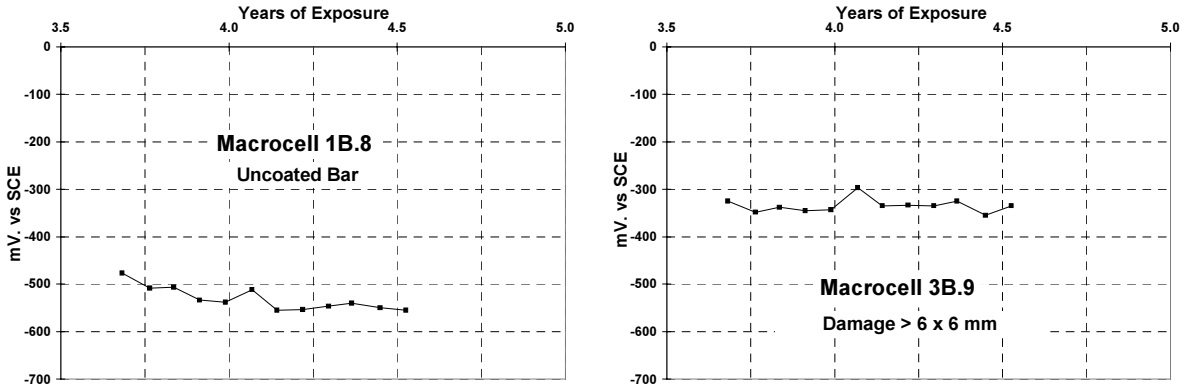

Figure 2.4 Average corrosion potentials vs. time of typical specimen B [25-mm (#8)] bars.

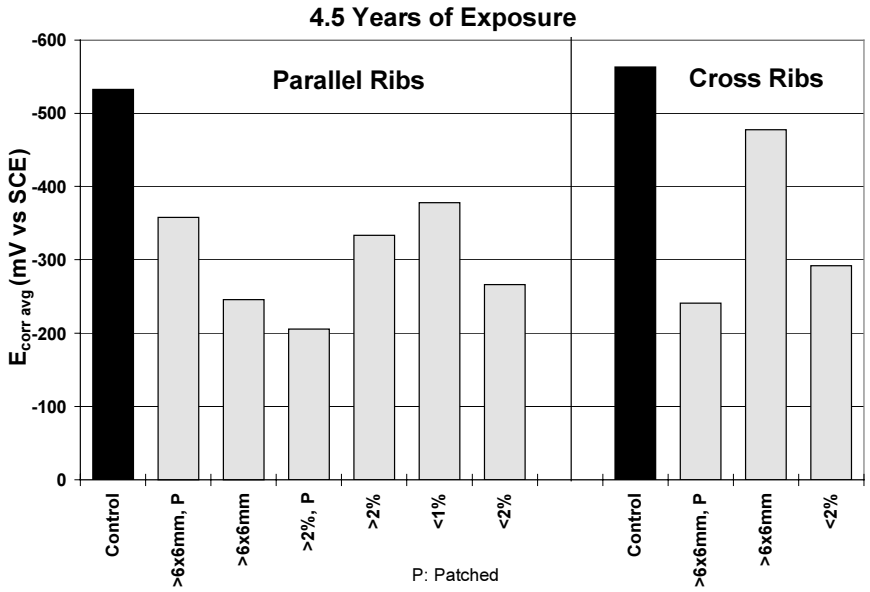

Figure 2.5 Average corrosion potentials of all specimen A [13-mm (#4)] bars.

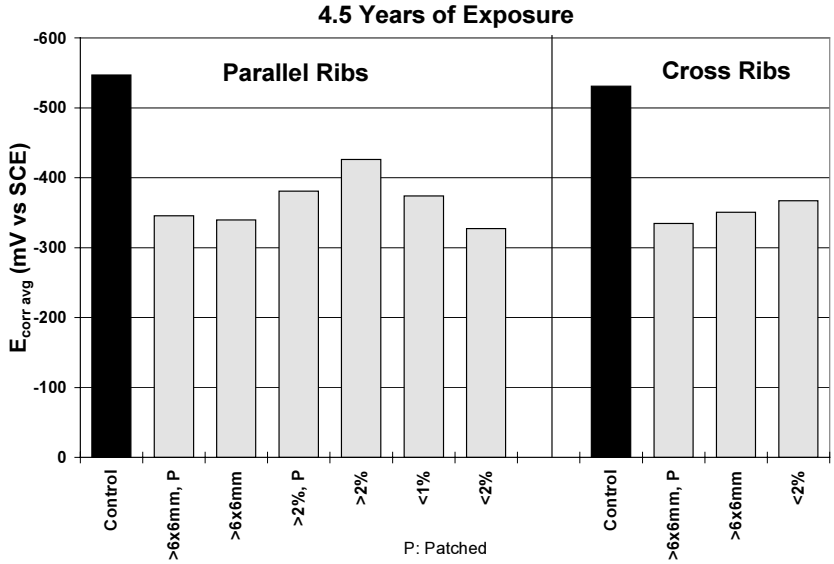

Figure 2.6 Average corrosion potentials of all specimen B [25-mm (#8)] bars.

2.4 CONDITION OF CONCRETE SURFACE

2.4.1 Control Bar Specimens

All specimens with uncoated bars underwent extensive deterioration after 4.5 years of exposure, including concrete cracking, rust staining, and surface scaling, as shown in Figures 2.7 and 2.8. The first outward signs of corrosion became apparent after about 100 days of exposure. The large bar specimens, in particular, showed minor brown spots on the concrete surface around the protruding ends of top bars. After about 170 days of exposure, larger brown stains were apparent at the same locations. Rust staining on the top concrete surfaces was visible after about 200 days of exposure. The small bar specimens

showed staining on the top concrete surfaces after about 330 days of exposure. Rust stains were of different sizes and colors (light to dark brown, reddish and orange brown) and generally formed along cracks on the top surface. Their appearance constantly changed during exposure. At different periods during the third and fourth years, fine orange brown rust powder exuded on the surface, especially on cracks. The top surface of all control specimens had an overall yellowish appearance, probably due to contamination by dissolved rust products in the solution.

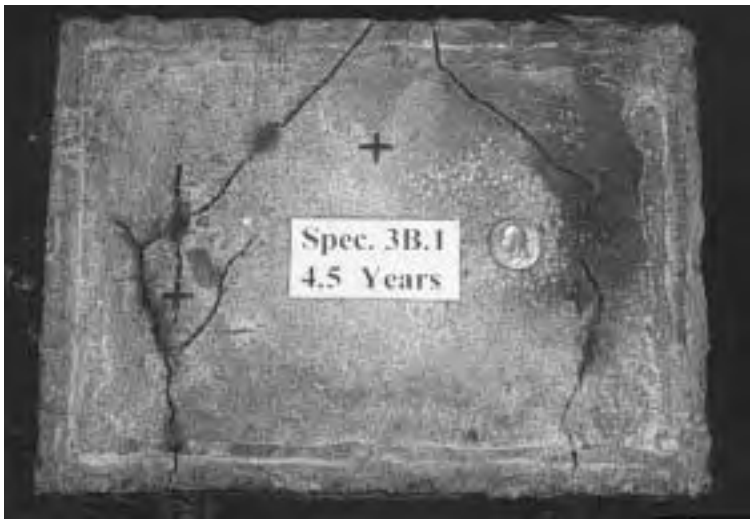

Figure 2.7 Surface condition of specimen with uncoated bar.

Fine corrosion-induced cracks showed up on the top concrete surfaces of some of the large bar specimens at approximately 210 days. The fine cracks gradually developed larger areas of rust staining and widened. The cracks generally formed parallel to the embedded bars and along the straight portions of the bars. Cracking was first evident on the top surfaces of the smaller bar specimens after about 340 days of testing. None of the specimens developed early cracking due to plastic shrinkage. Cracking generally occurred along the path of the top bar, starting at the straight regions of the bar next to the front face and later extending towards the bent zone of the bar.

In all cases, cracks propagated on the front face above the protruding bar legs. In specimen 3A1 (13-mm bar with parallel ribs) horizontal cracking developed on the front face between the 2 bar legs, which is a symptom of concrete delamination. In specimen 3A8 (13-mm bar with cross ribs), the crack above the left bar leg propagated on the front face all the way down to the bottom of the specimen and was visible at the bottom surface, along the left cathodic bar (Figure 2.8). Horizontal cracks appeared on the two lateral surfaces of specimen 3B1 (25-mm bar with parallel ribs) at a section slightly below the top bar location. The maximum crack width was 1.0 mm in specimens with 13-mm bars and 1.25 mm in specimens with 25-mm bars.

Figure 2.8 Surface condition of specimen with uncoated bar.

Concrete scaling on the lateral surfaces developed mostly during the third year and worsened during the fourth year of exposure. Scaling was always worse and more extensive on the lateral surface closer to the zone of more extensive cracking on the top surface. Scaling was so severe at some surfaces that concrete aggregate particles were exposed. Fine granules of salt exuded on scaled areas at different depths, indicating that solution permeated to a considerable depth from the top surface.

After the first signs of concrete cracking and rust staining, deterioration of the specimens progressed gradually during the first two years of exposure and worsened noticeably during the third and fourth years. Rust staining seemed to have reached its peak during the third year of exposure, and concrete cracking and scaling continuously progressed until the end of exposure.

2.4.2 Epoxy-Coated Bar Specimens

Unlike specimens with uncoated bars, specimens with coated bars maintained very good surface conditions after 4.5 years (Figure 2.9). Some specimens cracked but widths were narrower than in control specimens. Twenty percent of specimens with 13-mm bars and 80% of specimens with 25-mm bars developed cracking. In the first two years of exposure, none of the epoxy-coated bar specimens showed surface staining or cracking beyond the plastic settlement and shrinkage cracks detected at the beginning of the test. These initial cracks are described in Appendix A.

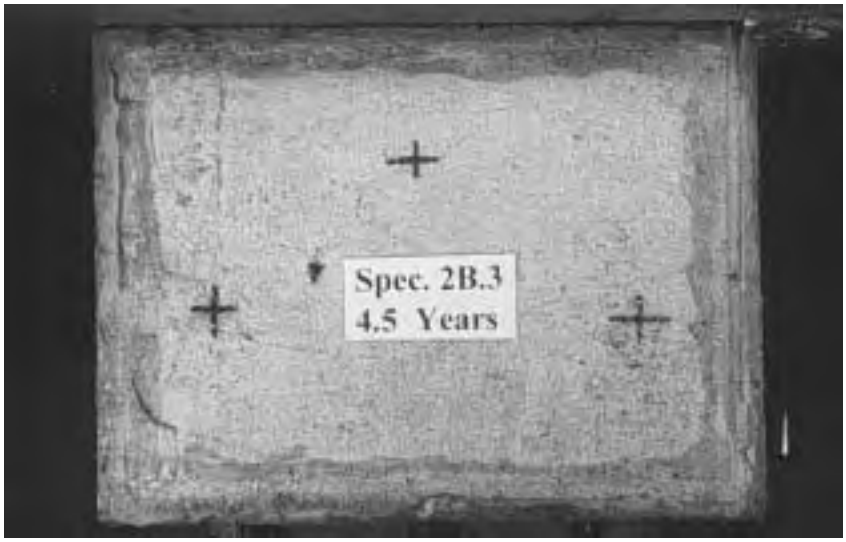

(a) Top surface

(b) Front surface

Figure 2.9 Surface condition of specimens with coated bars.

Crack formation is summarized below:

For series A (13-mm bars):

- Specimen 2A6 (bar with exposed damaged area less than 1%): Plastic settlement cracks were noted before the first day of exposure. Cracking progressed after 3 years of exposure.
- Specimen 3A9 (bar with exposed damage greater than 6x6 mm): Cracking initiated after 3.5 years.

For series B (25-mm bars):

- The two specimens with damage greater than 2% (patched and not-patched) had plastic settlement cracks. In specimen with unrepaired damage, cracking progressed after 2.5 years.

- Two specimens started to crack at the end of 3 years (bars with damage less than 2%, both parallel and cross ribs).
- Three specimens cracked during the last 10 months of exposure (bar with parallel ribs and patched damage greater than 6x6 mm; bar with damage less than 1%; and bar with cross ribs and damage greater than 6x6 mm).

Most coated bar specimens cracked between the end of the third year and the fourth year of exposure. In 2 specimens with plastic settlement cracks, cracks progressed after about 3.5 years. Maximum crack width was 0.20 mm, but most cracks had widths of 0.08 mm (hairline cracks). In fact, among cracked specimens with coated bars, only two specimens had the maximum crack width of 0.20 mm (25-mm bar with damage > 2% and 13-mm bar with cracks < 1%). The rest of specimens had very fine, hairline cracks with a maximum width of 0.08 mm.

Concrete scaling was mostly superficial, not severe, and not widespread on the surface of specimens with coated bars. Scaled areas were hardly noticeable and of small size on most specimens with 13-mm bars. Scaling was a little bit more severe and scaled areas were larger on specimens with 25-mm bars. Scaling was first observed on a specimen with 25-mm (#8) bar after about 2.8 years of exposure.

Specimens with coated bars did not develop significant rust stains on their top surface. The largest manifestation of rust staining occurred on the front face of specimens with 25-mm bars. Solution with rust products exuded on the exterior surface of protruding bars near the concrete face (Figure 2.10). When the solution dried, a formation of very brittle rust products was noted. Frequently, some of the solution oozed down the concrete face. Almost all specimens with 25-mm bars exhibited this phenomenon which was first observed after about 1.5 years of exposure in one specimen, and after 2.5 to 3.5 years of exposure in others. The solution had a pH between 3 and 4. A small sample of solution was obtained for chemical analysis. Such analysis disclosed the presence of hydrochloric acid in the solution.

Overall, there was good correlation between crack width and concrete deterioration with measured corrosion currents. Most specimens with 13-mm (#4) coated bars did not develop cracks, maintained excellent surface condition, and exhibited very low corrosion currents. Most specimens with 25-mm coated bars developed fine cracks, experienced exudation of acidic solution with rust on the front face, underwent light to moderate concrete scaling, and had medium corrosion currents. Specimens with uncoated bars experienced extensive concrete scaling and cracking, developed extensive rust staining, and exhibited larger corrosion currents.

Figure 2.10 Brown solution exuding from protruding bar at front face of specimen.

2.5 CHLORIDE PENETRATION

Chloride penetration in concrete over time was monitored by measuring the acid-soluble chloride content in companion concrete prisms at different depths. Companion prisms were made from the same concrete used in the specimens.

A graph showing the history of chloride profiles for selected years of exposure is included in Figure 2.11(a). Chloride content at a depth of 3.5 cm (1.375 in) vs. time is plotted in Figure 2.11(b). The chloride contents shown are not the chloride contents in the actual specimens, but give a good indication of chloride penetration with time because the samples were made from the same concrete mix used for the specimens and the exposure cycles were the same. Chloride penetration increased with time, and the penetration was accelerated in the last 2.5 years of exposure. The increase was significant deeper into the concrete. Note in Figure 2.11(a) that the chloride content at a depth of 7 cm (2 7/8 in.) after 4.5 years was higher than that at a depth of 1 cm (3/8 in.) after 2 years. The chloride content at the level of the coated bars was quite high towards the end of the exposure period.

By comparing the trends of chloride contents and corrosion currents, chloride concentrations associated with the onset of corrosion of uncoated bars were estimated in the range from 0.08 to 0.12% by weight of concrete. The corresponding average chloride content for onset of corrosion of epoxy-coated bars was estimated at about 0.18%. In general, it was difficult to find a clear relationship between increases of chloride content and spikes in the corrosion current. The following two observations illustrate this point:

1) The chloride content remained relatively constant from 6 months to 2 years of accelerated exposure [Figure 2.11(b)]. Within that period, a number of specimens experienced a gradual

increase of current (Figures 2.1 and 2.2). Apparently, the presence of a steady level of chloride ions had a corrosive effect over time.

2) The steady increase of chloride content observed in the last 2.5 years of exposure was not associated with an increase in the amount of current for the majority of the specimens.

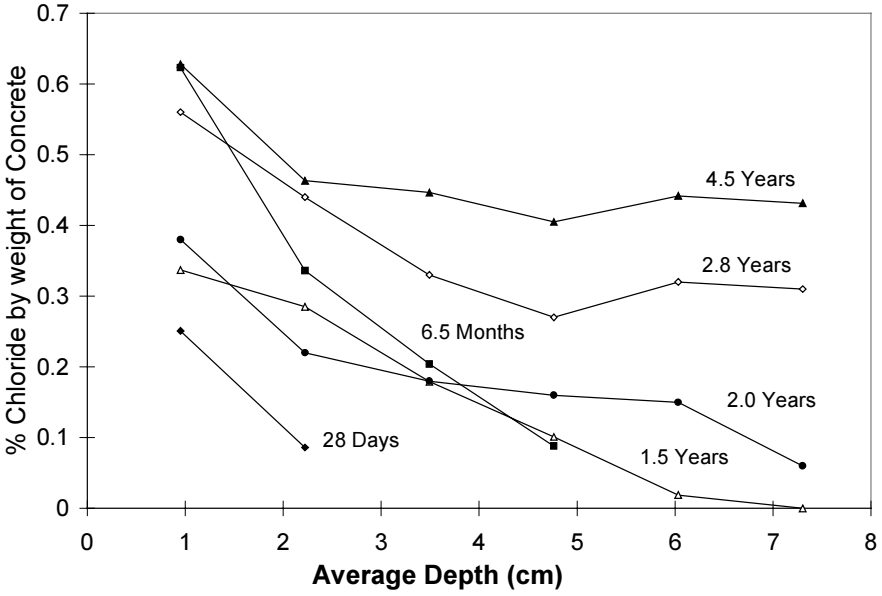

(a) Chloride profiles at different times of exposure.

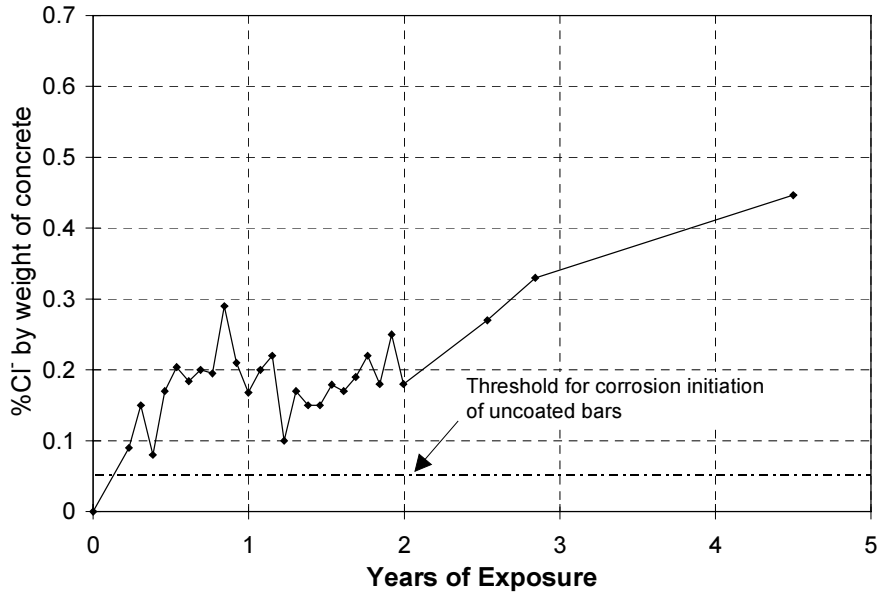

(b) Chloride content at the bar location vs. time of exposure.

Figure 2.11 Chloride measurements over time on concrete blocks cast with same concrete mix as in macrocells.

2.6 FORENSIC EXAMINATION

2.6.1 General

Forensic examination was carried out for three reasons:

- To correlate the corrosion current measurements with actual bar condition
- To determine the relative corrosion activity on bars with different levels of damage to the epoxy coating, and
- To investigate the condition of the epoxy coating.

One specimen in each group of three was removed from the saline environment for autopsy after 1, 2, and 4.5 years of exposure. Generally, the specimen selected was the one showing maximum corrosion activity indicated by the history of the macrocell corrosion current. The bars were carefully removed following the procedure outlined in Appendix A. The forensic examination was documented by visual observations, examination with microscope, and photographs. Four specimens with 25-mm bars (cross ribs) were not autopsied because they were diverted to another corrosion experiment for exposure for an additional year. The condition of the bar after exposure was described and the location of damage was identified using the notation described in Figure 2.12.

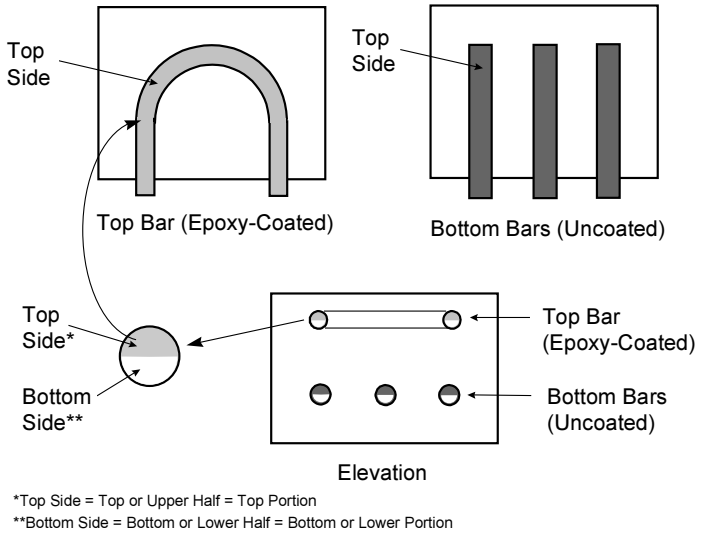

Figure 2.12 Convention for identifying bar locations.

2.6.2 Concrete Delamination

Before breaking open the specimens, signs of concrete delamination were detected by tapping the surface with a hammer. Three of the control specimens developed concrete delamination: The two specimens with 13-mm bars and a specimen with 25-mm bars (parallel ribs). Delaminated areas were confined and

generally coincided with lateral surfaces and wide cracks. Delamination was localized. None of the specimens with coated bars developed concrete delamination.

2.6.3 Chloride Content at Steel Level

Chloride samples were removed from each specimen before demolishing. The concrete surfaces at the drilled locations were uncracked; therefore, the chloride concentrations should represent quite closely the general distribution of ingressive chlorides. The measured acid-soluble chloride concentrations are tabulated in Appendix A.

The chloride contents at the top steel level varied considerably among specimens. Chloride profiles (based on average chloride percent by weight of concrete) of specimens autopsied after 1, 2, and 4.5 years are plotted in Figures 2.13 and 2.14. There was a slight increase in the amount of chlorides from 1 to 2 years of exposure for both 13- and 25-mm bar specimens, but from 2 to 4.5 years, there was a significant increase for all specimens. At the end of 4.5 years, the average chloride content by weight of concrete at the top bar location was 0.34% for series A specimens and 0.33% for series B specimens. This contrasts with 0.23% and 0.21% of chlorides at the top bar location for series A and B, respectively, at the end of 2 years. The respective values after one year were 0.17% and 0.19%. At a depth of 8 cm (3¼ in.), the average amount of chloride after 4.5 years was similar to that at the level of the top bar after 2 years.

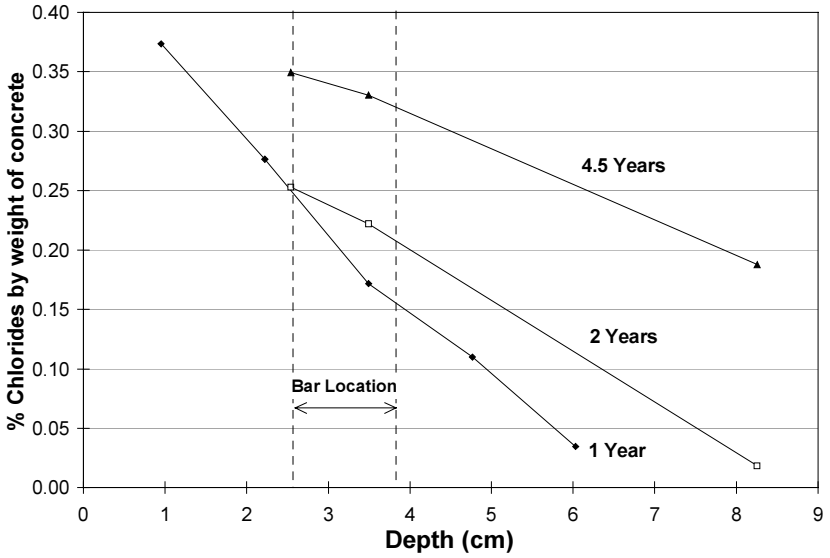

Figure 2.13 Average chloride profiles for A specimens [13-mm (#4) bars].

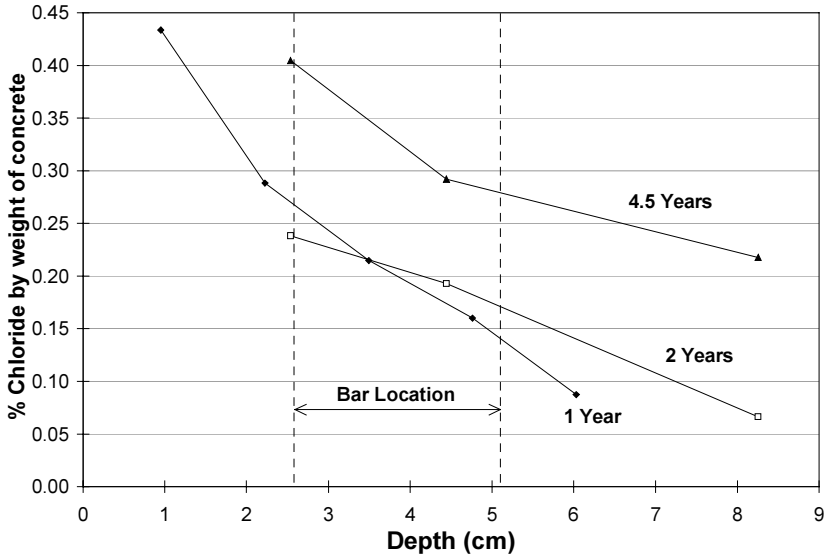

Figure 2.14 Average chloride profiles for B specimens [25-mm (#8) bars].

There is no agreement as to the chloride threshold level that triggers corrosion of steel in concrete.[21,22] For reference, reported chloride thresholds for corrosion initiation fall in the range of 0.02–0.05% by weight of concrete.[23] These numbers indicate that the exposure conditions were particularly severe for the top bars, especially during the last 2.5 years of exposure.

2.6.4 Appearance at Removal from Concrete

CONTROL BARS

The uncoated bars showed relatively high levels of corrosion with discernible extensive degradation and localized loss in section, especially after 4.5 years. Figure 2.15 shows the top and bottom sides of one uncoated bar after removal. Immediately after opening the specimens, corroded metal had a black or dark appearance with randomly distributed areas of reddish-brown rust and several smaller areas of dark-green and bluish-green rust. After being exposed to oxygen, all dark- and bluish-green areas changed to bright orange-brown or yellowish-brown rust.

The accumulation and build-up of rust products was evident in the most corroded areas. Corrosion was concentrated mostly at the straight portions of the bar, exhibiting appreciable loss of metal and pitting (Figure 2.16). On bent areas, a relatively clean, non-corroded metallic surface was visible over most of the top half of the bar and over a portion of the bottom side. After 1 and 2 years, more pitting corrosion occurred on the top side than the bottom side of the bar. However, corrosion spread more on the bottom side than on the top side of the bars after 4.5 years. Larger bars were more severely attacked than the smaller bars.

(a) Top side

(b) Bottom side

Figure 2.15 Uncoated bars after autopsy.

Pitting corrosion worsened after 4.5 years of exposure. Several large pits, ranging from 0.5 to 2.0 mm deep, developed on the straight legs of both 13-mm bars [(Figure 2.16(b)], outside of the bent portion on a 13-mm bar with cross ribs, and on the right side of the bent portion in a 25-mm bar with parallel ribs. A large, deep pit on the top side of a 13-mm bar with parallel ribs caused a significant reduction in bar area at that location.

On specimen 3A1 (13-mm bar with parallel ribs), a series of brown drops of acidic solution (pH = 3) appeared on the straight portion. The solution was very similar to the solution oozing from the front faces of specimens with 25-mm coated bars. An interesting phenomenon that occurred on most specimens was that about 24 hours after removal from the concrete, drops of brown, acidic solution, similar to the drops found on specimen 3A1 after autopsy, formed on the bar surfaces.

Fragments of concrete of different size remained adhered to several portions of bar surfaces, evidence of good adherence between concrete and uncoated steel.

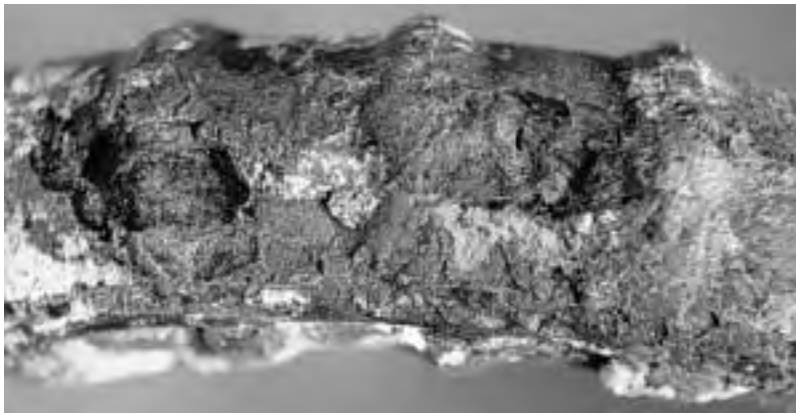

(a) Severe pitting on 25-mm (#8) uncoated bar after 2 years of exposure.

(b) Severe metal loss and pitting at straight leg of 13-mm (#4) uncoated bar after 4.5 years of exposure.

(c) Pitting at straight leg of 25-mm (#8) uncoated bar after 4.5 years of exposure.

Figure 2.16 Loss of metal and pitting of uncoated bars.

EPOXY-COATED BARS

The following observations pertain to the appearance of the epoxy-coated bars before peeling the coating to uncover the metallic surface underneath. Results from such examination are shown later. Here, the condition of the coating surface and of the damaged areas is described. As was found later, the condition of the coating surface usually differed from the condition of the metallic surface beneath the coating. Summarized descriptions of the bar surface condition are tabulated in Appendix A. It was decided that the commonly used ratio of area covered by red rust (ratio of corroded area to bar surface area) as a measure of the state of corrosion was inaccurate for coated bars. The apparent corrosion at coating breaks does not represent the actual extent of substrate metal corrosion.

One Year of Exposure

After one year of exposure, the small coated bars showed either no apparent corrosion or minor surface corrosion on the introduced damage and other defective areas of coating (inside and outside of bend). Figure 2.17 shows two examples of the 13-mm (#4) bars exposed for one year. At the damaged locations, steel was only discolored or had suffered minor (shallow) loss of metal.

(a) Specimen 1A.4

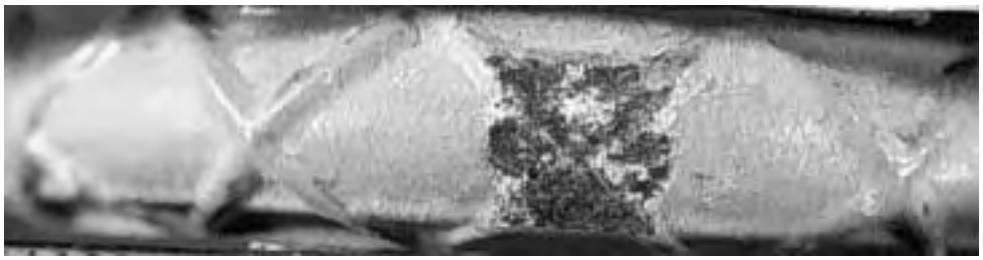

(b) Specimen 3A.10

Figure 2.17 Examples of 13-mm (#4) coated bar specimens autopsied after one year of exposure.

The large bars showed relatively more corrosion activity; however, metal loss was minor as shown in Figure 2.18. Rust spotting at some patched areas was visible. On the majority of the large bars, many variable size blisters distributed on the coated surface were noted. The blisters formed at spots facing air voids in concrete as shown in Figure 2.19. Based on appearance, the worst bars, from both series, were those with exposed damaged areas slightly exceeding 2% of the bar surface area.

Figure 2.18 Example of 25-mm (#8) coated bar specimens after one year of exposure.

(a) Blister on a coated bar surface

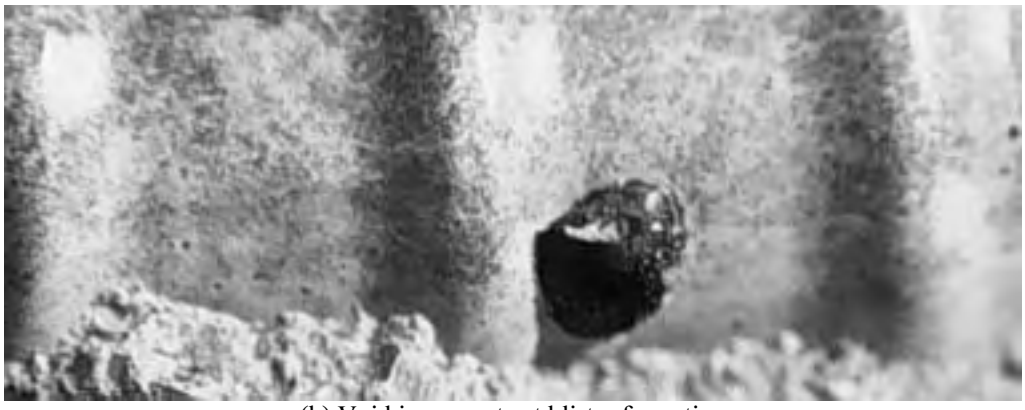

(b) Void in concrete at blister formation

Figure 2.19 Coating blistering at voids in concrete.

Two Years of Exposure

More corrosion activity was visible after two years than after one year. After two years, it was clear that pitting corrosion was occurring on the exposed areas of some specimens. Rust spotting at some patched areas was also observed, particularly on the larger size bars. These observations are illustrated in Figure 2.20. Again, blisters of variable sizes formed on the coated bar surface at locations facing voids in concrete. These voids were more concentrated on the underside of the bar as shown in Figure 2.21. The blisters were also much more apparent after two years than after one year for the corresponding specimens indicating further breakdown of the coating with longer exposure. Figure 2.21 shows a bar with many blisters formed on the bottom side.

As for the specimens examined after one year, small size bars examined after two years exhibited less corrosion than the large size bars. The only bars that appeared in excellent condition were the small bars with parallel deformations and repaired damaged areas. One of the damaged small bars showed fine cracking of the coating along the longitudinal rib in the bent area.

After one and two years, corrosion products were dark green-black and brown solid products. However, upon exposing the epoxy-coated bars, in many instances, a dark greenish-blue corrosion product was found in a soluble form. The dark greenish product rapidly converted to brown on contact with air. In addition, a clear solution spilled from damaged spots and pinholes at the bottom side of some bars. Furthermore, steel corroded spots almost always coincided with gaps in the surrounding concrete through which the corrosion products dispersed as shown in Figure 2.22. In addition to corrosion on the exposed steel areas (inside and outside of bend), the bottom side of bar generally showed the worst rust spotting and blistering.

(a) Pitting corrosion on specimen 3B.3

(b) Rust spotting on specimen 1B.2

Figure 2.20 Examples of 25-mm (#8) coated bar specimens after two years of exposure.

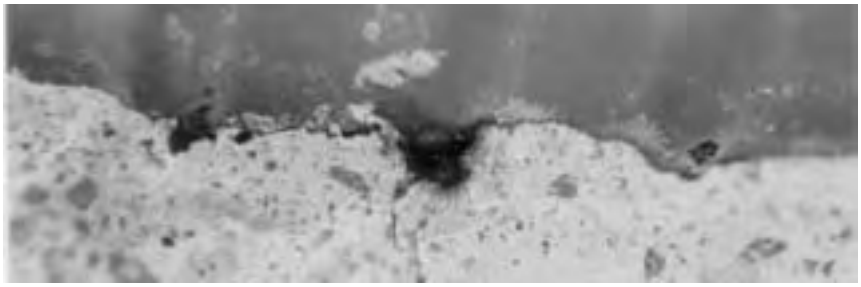

(a) Specimen 3B.7

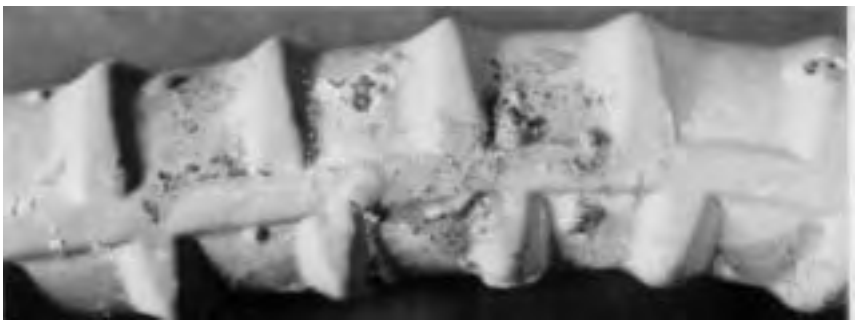

(b) Specimen 2B.5

Figure 2.21 Blister formation at bottom side of coated bars after two years of exposure.

One interesting phenomenon was that a soft swelling spot with rust stain exudations formed on the coated bar surface either exactly where the bar protruded from the specimen, or about 3 mm (1/8 in.) from the concrete edge. These spots were first observed after about 600 days of testing and only on the larger size bars. The solution filling these spots must have passed under the coating from the embedded portions where damage existed or corrosion was taking place. Figure 2.10 shows one of the swelling spots.

4.5 Years of Exposure

As expected, corrosion of coated bars progressed with time. Corrosion was more extensive after 4.5 years, especially in larger bars. Rust staining, coating blistering, and corrosion of exposed areas were noted (Figure 2.23). The color of rust stains ranged from dark to light brown, and their appearance varied from dense to tenuous. Blisters of different sizes formed but small ones were prevalent. In some bars, a few small stain lines with dull appearance (indicating coating distress or cracking) were detected next to longitudinal lugs. Corrosion did not always occur at the damaged, exposed areas of smaller bars. In contrast, all exposed areas of larger bars corroded severely. Rust at damaged spots on the outside of the bend was uniformly dark. Traces of bright or dull reddish-brown rust were found inside the darkly rusted damaged areas. At some of the damaged spots, metal depletion was evident. Traces of acidic (pH = 3) brown solution were observed on several damaged areas. In contrast, generally minor corrosion was observed on patched areas. Patched areas were frequently discolored, had medium-sized to small dark-brown or reddish-brown rust spotting, and tiny blisters (See Figure 2.29 later in Chapter). Fine reddish-brown rust products (in small amounts) were deposited at several patched spots.

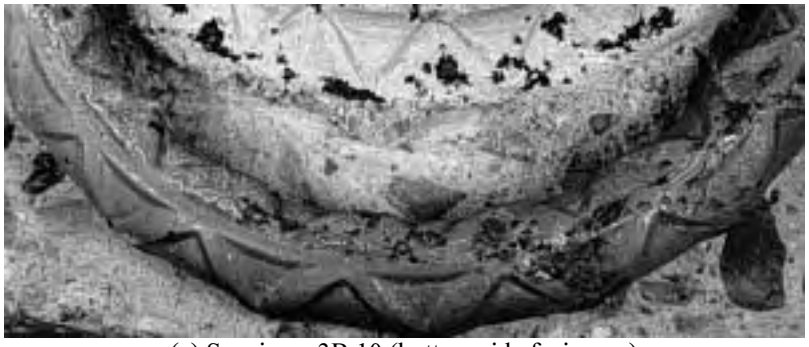

(a) Specimen 3B.10 (bottom side facing up)

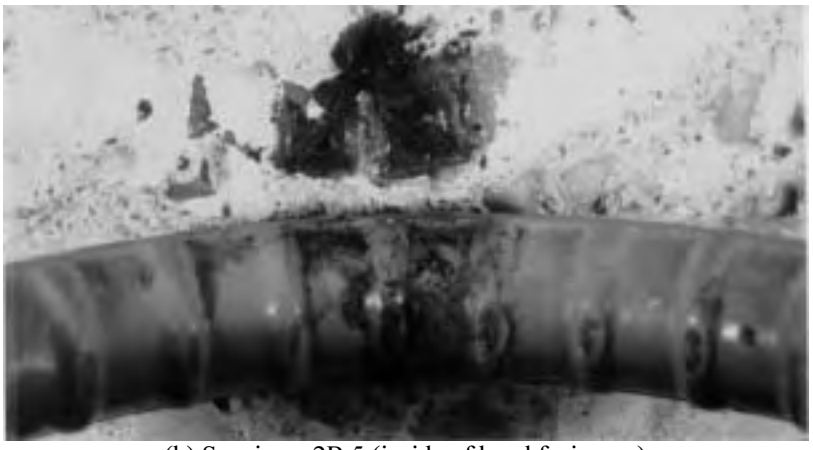

(b) Specimen 2B.5 (inside of bend facing up)

Figure 2.22 Rust spotting on bottom sides of coated bars coincident with voids in concrete.

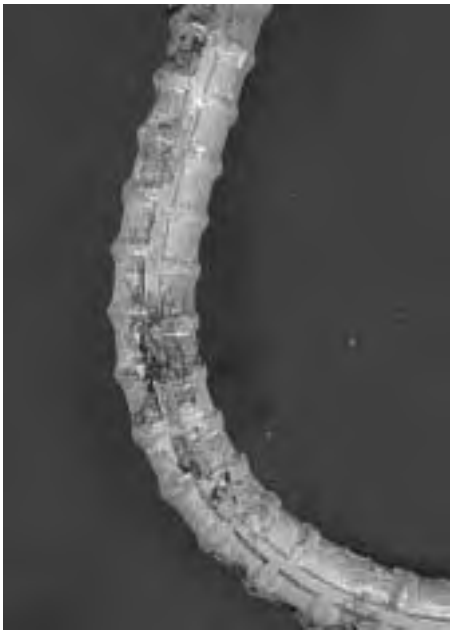

(a) Rust staining and blistering on epoxy-coated bar.

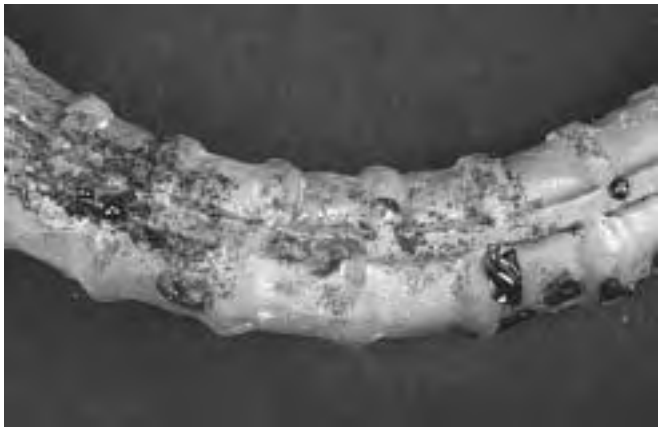

(b) Rust staining and exudation of brown liquid on epoxy-coated bar.

Figure 2.23 Corrosion of epoxy-coated bars after 4.5 years of exposure.

Except for bar 3B.5 (25-mm bar with damage greater than 2%), all bars experienced more rust staining or spotting and blistering on the bottom surface than on the top (Figure 2.24). In most cases, more corrosion developed on the bent area than on the straight portions. Blistering and rust staining tended to concentrate next to the longitudinal lugs. Most damaged areas on the inside of the bend (produced by the mandrel during fabrication) did not show much corrosion, only superficial rusting. There was almost always a void in the concrete where a blister formed. However, corrosion did not occur at all voids. As with 1-year and 2-year specimens, smaller bars corroded less than large bars.

(a) Top side.

(b) Bottom side.

Figure 2.24 Appearance of top and bottom sides of epoxy-coated bars.

In group A (smaller bars), bar 1A.5 (damage > 2%) experienced the most corrosion, followed by bars 2A.6 (cracks with damage < 1%), and 1A.10 (damage > 6x6mm). There were traces of dark rust along coating cracks of bar 2A.6. The coating condition on remaining bars was good with few rust stains and blisters. The bars with the best appearance were 3A.3 (damage > 6x6 mm) and 3A.7 (damage < 2%). It was a significant contrast to find that the exposed steel areas at damaged spots in specimens 3A.3 and 3A.7 were completely free of corrosion after 4.5 years of exposure and displayed a shiny, bright surface (Figures 2.25 and 2.26). No voids were visible in the concrete adjacent to the exposed areas. The overall condition of bars 3A.3 and 3A.7 away from the damaged areas was good, with only a few blisters and small brown stains.

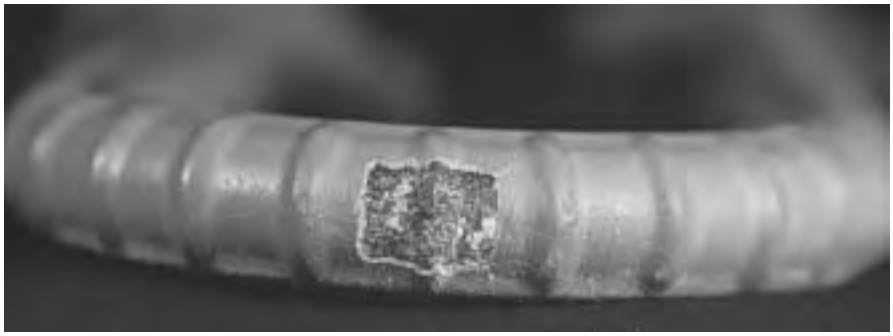

Figure 2.25 Clean, uncorroded damaged area after 4.5 years of exposure (Bar 3A.3).

Figure 2.26 Clean, uncorroded damaged areas after 4.5 years of exposure.

In group B (larger bars), bars 2B.3 (damage > 6x6 mm), 3B.5 (damage > 2%), and 1B.7 (damage < 2%) exhibited the highest corrosion. Dark, dense stains formed on the top portion of bar 3B.5 [Figure 2.27(a)]. Diluted, dark and brownish stains appeared at the bottom side around the bent zone and on one bar leg [Figure 2.27(b)]. Damaged areas at the outside of the bend had a dark rust accumulation (Figure 2.28). For comparison, Figure 2.29 shows the appearance of patched areas at the outside of the bend on box 3B.4.

A common phenomenon was that a few days after the bars were removed from the concrete, a series of drops of brownish, acidic solution (pH between 3 and 4) formed on the surface of the bars (Figure 2.30). In several cases the drops dried and formed beads of brittle rust. An unsuccessful attempt was made to obtain samples of the acidic solution for analysis, but the amount of liquid in the drops was too small to

be sampled. In most bars, remains of whitish concrete paste adhered to the bottom side of the bars while the coating remained cleaner and glossy on the top portion.

(a) Top side.

(b) Bottom side.

Figure 2.27 Bar 3B.5 after 4.5 years of exposure.

Figure 2.28 Corrosion of damaged areas at outside bend on bar 3B.5.

Figure 2.29 Corrosion of patched areas at outside bend on bar 3B.4.

Figure 2.30 Brownish, liquid solution exuded on surface of epoxy-coated bars.

CATHODIC BARS

One- and Two-Year Specimens

Cathodic bars were removed from a few selected specimens and their condition was examined. The appearance of the cathodic bar trace in concrete was also examined. The cathodic uncoated bars at the bottom were, as expected, free of rust after 2 years of exposure, as shown in Figure 2.31. However, a number of cathodic bars experienced corrosion after 4.5 years of exposure, as described in the following paragraphs.

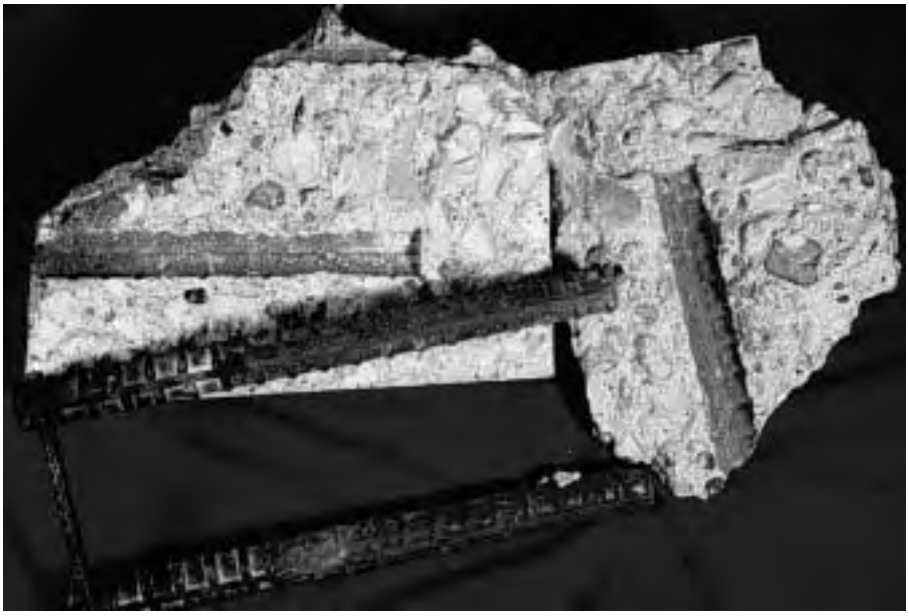

Figure 2.31 Cathodic uncoated bars at bottom of macrocell specimens.

4.5-Year Specimens

Control Specimens

Most cathodic bars from control specimens experienced corrosion after 4.5 years of exposure. Corrosion tended to be more severe and extensive on one of the bars for each specimen. For instance, the left bar of specimen 3A.1 had a clean, uncorroded surface. Bar trace in concrete above and below the bar was clean, with a grayish appearance. In contrast, the right bar experienced reddish-brown rusting mainly on its right and bottom sides. Two medium-sized pits were observed: One pit was located at the top side close to the front face of the specimen and was 36 mm^2 big, 1.5 mm deep. The other pit was located at the bottom side close to the back end of the bar and measured 16 mm^2 of area, 0.9 mm of depth.

The left bar in specimen 3A.8 underwent very extensive and severe corrosion, characterized by uniform dark or black rust with large areas of evident rust volume accumulation, causing cracking of concrete at the bottom of the specimen (Figure 2.32). Corrosion was slightly more severe below than above the bar. The right bar experienced more limited corrosion at a few spots. Most of the bar surface was non-corroded, with a dark grayish aspect, especially at the bottom side. Concrete adjacent to uncorroded areas had a grayish appearance.

Cathodic bars from specimen 3B.1 showed widespread black or dark and reddish-brown rusting on their surface. More corrosion was found at one side of the left bar and at the bottom of the right bar. Several sizable pits formed on the right bar: One medium-sized (24 mm^2) and several small, shallow pits (0.4 mm deep) were observed on the top side. One large, deep pit (0.84 cm^2, 1.3 mm deep) and two large, shallow (0.2 or 0.3 mm deep maximum) pitted areas were observed on the bottom. The trace of corroded bars in

concrete showed extensive dark and reddish-brown rust staining, similar to the corrosion observed on the bars. Sites adjacent to pitted locations in the bars showed accumulation of solid rust products, usually inside concrete voids.

Figure 2.32 Corrosion at bottom side of cathodic, bottom bars of specimen 3A.8.

Epoxy-Coated Bar Specimens

Most cathodic bars from selected specimens with epoxy-coated bars had a clean metallic surface without corrosion (Figure 2.33). Most bars experienced slight surface darkening within 1.0 to 2.0 cm from the front face of the specimen. At some portions of the bottom side of two bars (specimen 1A.5), dark-grayish stains giving the appearance of solution trace were observed. Small concrete paste residues remained adhered to the bottom side of the bars. One of the cathodic bars in three specimens with top epoxy-coated bars experienced corrosion: The left bar of specimen 3A.3, the right bar of specimen 2B.3, and the middle bar of specimen 3B.5. The left bar of specimen 3A.3 experienced light but widespread dark-brown rust staining at the bottom side. No pitting was observed. The right bar of specimen 2B.3 had a relatively large, dark rust spot exactly at the point of contact with the bar chair. Examination of the adjacent bar trace under the bar showed that the bar chair was visibly rusted. It is possible that localized galvanic corrosion took place at the contact zone between the two metals.

The middle bar of specimen 3B.5 experience the largest corrosion among cathodic bars in coated specimens. The bar exhibited dark and reddish-brown rusting on the bottom, on a 6.0 cm-stretch from the embedded end of the bar, including the embedded cut end surface. One medium-sized, shallow pit (25 mm^2, 0.7 mm deep) was observed at the bottom side close to the back end. Interestingly, grayish and

darks stains appeared at the uncorroded portion on the bottom side (a 11.5-cm long zone closer to the front face of the specimen). Laitance was present at the adjacent bar trace in concrete, suggesting that something occurred at the metallic surface (ions that were generated by the cathode may have reacted with concrete). Macrocell currents in specimen 3B.5 experienced incidental large drops between cyclic high and low peaks after 2 years. This suggests that corrosion of the cathodic bar started to affect the currents measured.

Figure 2.33 Appearance of bottom side of cathodic, bottom bars of specimen 2B.3.

2.6.5 Coating Removal

The coating was removed around exposed spots and from originally undamaged areas using a sharp blade. A cut was made with a utility knife alongside one longitudinal rib (generally the rib located at the more corroded bottom side). The coating was then lifted by inserting the blade tip of the knife under the coating at the cut sections and applying prying action. The removal process provided a rough indication of the remaining adhesion of the coating to the steel substrate. In general, loss of adhesion along the bend for both bar sizes was extensive (Figure 2.34). Coating debonding progressed from the bent areas towards the straight bar legs. The debonded areas were relatively easy to pry and were characterized by noticeable separation from the metal. In contrast, cutting through the well-bonded coating near the straight ends was difficult and caused cohesive separation of the coating material itself. However, even the straight portions of the bars became mostly debonded after two years of exposure.

Scraping the coating after two years was easier than after one year and resulted in larger chipped off pieces. The extent of coating debonding after 4.5 years was slightly greater than after 2 years. Extensive adhesion loss was observed more frequently on large bars than on small bars. Four small bars developed complete coating debonding throughout their whole length (bent and straight zones). At the remaining

small bars, debonded areas included the bent zone and an adjacent portion of the straight bar legs. Coating adhesion was preserved in the portion of straight bar legs closer to the protruding ends, away from the bent zone (a 4- to 7.5-cm stretch extending from the front face). In contrast, all large bars experienced complete loss of adhesion throughout their length. Only in bar 1B.7, a short piece of coating (about 2.5 cm long) adjacent to the protruding end of one leg remained adhered to the steel substrate.

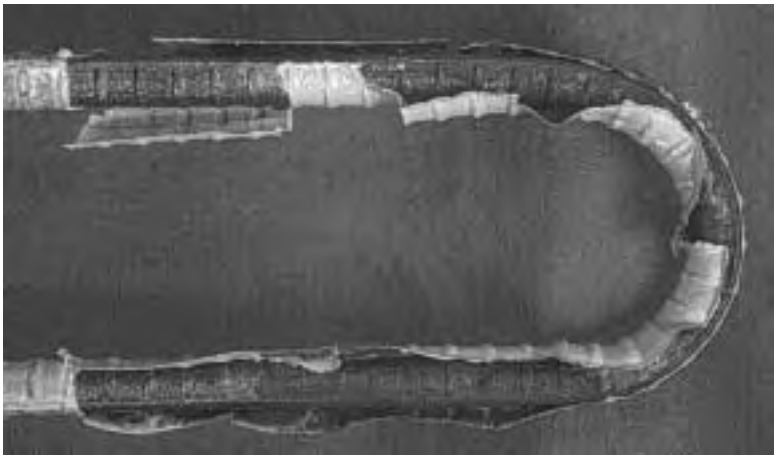

Figure 2.34 Coating debonding on 13-mm (#4) bar.

In areas where coating adhesion was preserved, the steel surface beneath the coating maintained its original condition (bright, shiny surface) without corrosion. The steel surface beneath the coating at debonded areas changed appearance and corrosion was observed, as will be discussed in the following section.

2.6.6 Underfilm Corrosion

It was observed that the greater the amount of rust staining on the epoxy coating, the greater the degree of corrosion on the steel surface beneath the coating. However, the amount of staining on the coating surface was not always indicative of the severity of corrosion of the metal substrate. Corrosion of the steel surface was generally more severe and extensive than was apparent from the coating surface. Short descriptions of the condition of steel substrate are given in Appendix A.

Examination of steel surfaces indicated trends similar to those found upon examination of coating surfaces. Larger bars corroded more extensively and severely than smaller bars. Corrosion was more severe on the outside than inside of the bend. Corrosion at the bend zone tended to be worse than along straight bar legs and bottom sides corroded more than top sides.

The appearance of the steel surface varied depending on the severity of corrosion and will be classified as: 1) Debonded, non-corroded surfaces, and 2) Corroded surfaces.

DEBONDED, NON-CORRODED SURFACES

The designation of "non-corroded" is possibly a misnomer because corrosion may be in an initial stage. The steel surface showed a very unique characteristic: A sort of a mottled, glittery or twinkling appearance with a golden-brown or similar brownish color. An example of such a surface is illustrated in Figure 2.35. The condition of such steel surfaces was very good, with no discernible pitting or metal attack. The term "non-corroded" was used to describe the good condition of the steel. The loss of coating adhesion, though, may indicate that corrosion may already be in early stages. Mottled surfaces were found mainly in the less corroded small bars and occurred more often at straight bar legs than at bent zones. Debonded areas with mottled surfaces underneath were suspected to have undergone cathodic disbondment, as will be explained later.

(a) Left leg of bar 3A.2.

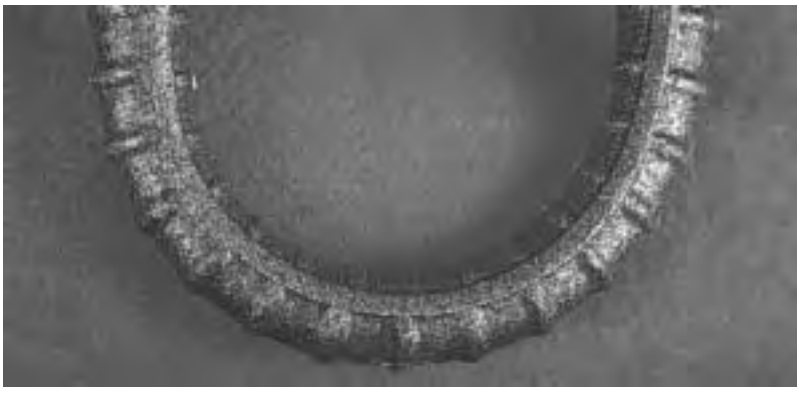

(b) Top side of bar 3A.3.

Figure 2.35 Mottled, glittery surface with golden-brown (or similar brownish) appearance under the coating.

CORRODED SURFACES

The appearance of corroded surfaces varied from bar to bar. In most cases, a uniformly black or dark rusted surface developed. The degree of darkness varied from specimen to specimen and it also changed with time for the same specimen. In several bars, the corroded surface looked darker one or two days after the coating was removed. Depending on the length of exposure and severity of corrosion, shallow pitting and metal depletion, rust volume increase, and blistering may have developed in varying degrees (Figure 2.36). In many specimens, spots of whitish matter with pasty consistency, sometimes combined

with brownish rust, were observed. Whitish products would turn yellowish-brown, orange-brown, light-brown, and reddish-brown after several hours of being exposed to air.

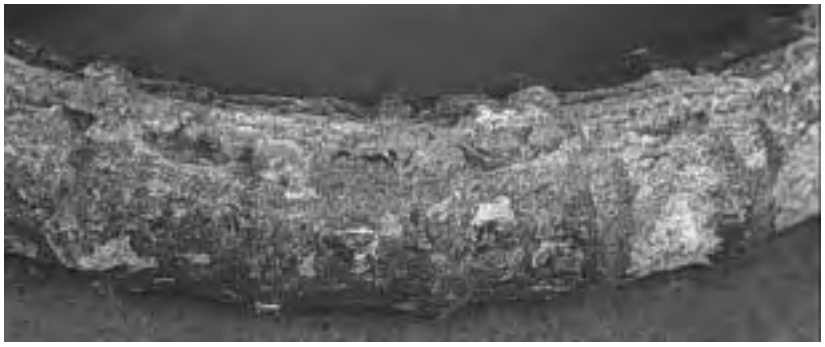

Figure 2.36 Shallow pitting and accumulation of rust products on steel surface under the coating (outside bend).

One-Year Specimens

Generally, the small bars, after one year of exposure, appeared in good condition. The substrate metal either remained bright with no visible corrosion activity, or was slightly discolored with minor surface disruption.

Many of the large bars, however, exhibited moderate to widespread underfilm corrosion starting from the exposed steel areas and defects on both the inside and outside of bends. The metal underneath the coating, including patching, appeared dull and darkened with some brown rust spotting. A thin black layer was observed, particularly in the cases with a high percentage or large size of coating damage. Despite this appearance, surface rusting was light without significant loss of bar section. Additionally, a clear or whitish trapped solution was found underneath the coating of many bar specimens. The solution dried fast upon exposure to the atmosphere leaving whitish deposits, which turned to orange, and then to brown. Figure 2.37 shows an example of undercutting on a large bar specimen after one year of exposure.

Two-Year Specimens

After two years, specimens showed moderate underfilm activity and pitting. There was a clear distinction between the appearance of the top and bottom sides of the bar. The top side was black, and sometimes moist, while the bottom side was dull with sporadic rust spotting as shown in Figure 2.38. Even the patched large bars showed surface darkening with minor metal loss or slight pitting as shown in Figure 2.39. Whitish and orange residue was occasionally observed in some pockets forming alongside the bottom continuous rib as shown in Figure 2.40. The blisters were often full of corrosion products and some had an acidic (pH 2 to 4) trapped solution. Figure 2.41 shows a close up of the solution detected underneath the coating.

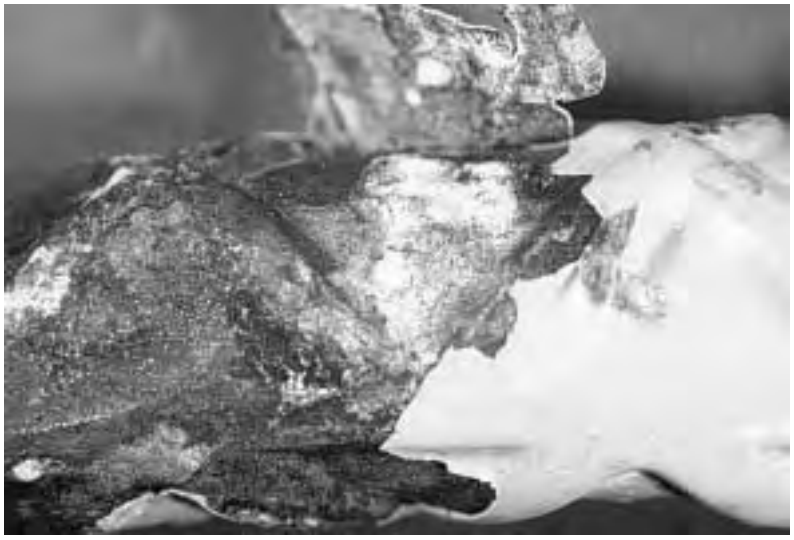

Figure 2.37 Underfilm corrosion (undercutting).

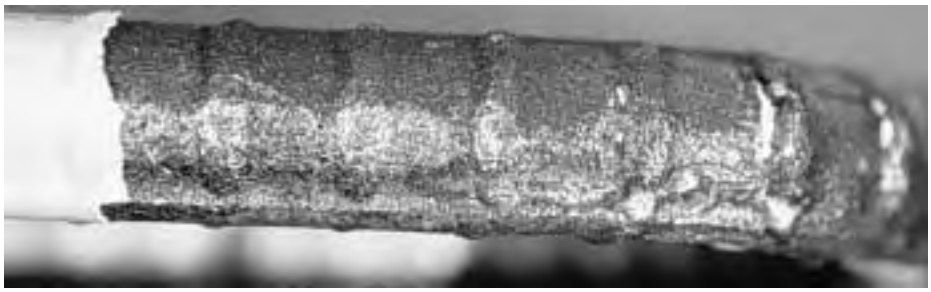

Figure 2.38 Thin black layer on top side of steel surface.

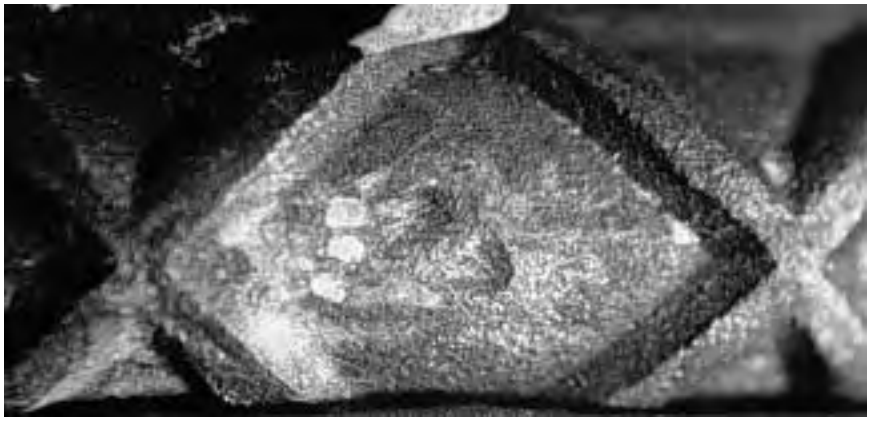

Figure 2.39 Darkening and pitting underneath patching.

Figure 2.40 Corrosion deposits on bottom side of steel surface.

Figure 2.41 Trapped solution beneath epoxy coating.

4.5 Year Specimens

Underfilm corrosion progressed with time, particularly in larger bars. However, no severe, localized, deep pits were found in any bar. The largest pits were less than 0.5 mm deep. No drastic reduction of cross-sectional area was found in any coated bar. The volume increase (due to rust formation) appeared to be less than for uncoated bars. Variable amounts of dark rust powder came off during removal of the coating, more noticeably in larger bars. In larger bars, damaged sites at the outside of the bend experienced accumulation of orange- and reddish-brown rust. Such rust products were more brittle at some spots. Corrosion beneath patched areas was rather superficial and not severe. Corrosion spread and tended to be worse at portions adjacent to repaired areas, showing shallow pitting and loss of metal. Most

blisters formed below the bent portions and had a very hard, solid consistency. Smaller blisters were more abundant than larger blisters. In small bars, bottom sides corroded more than top sides but the difference in corrosion severity between top and bottom sides was less pronounced than indicated by the coating surface appearance. In large bars, corrosion at top and bottom sides tended to be similar (the bottom sides corroded slightly more than the top sides in most cases) and in one specimen (3B.5), corrosion seemed to be worse at the top side.

Areas with rust deposits or pockets of varying size, shape, appearance, color, and amount were usually present along the bar surface above the uniform black rusted surface (Figures 2.42 and 2.43). The size of such rust spots ranged from very large, occupying large areas of the bar surface, to small flecks. Appearance of rust spots was dependent on rust concentration, varying from a light film of rust, similar to a stain, to thicker layers of rust deposits. Rust layers at some spots were bulky enough to cause a bulge in the coating, but in most instances, rust amounts in such areas were light. At the time of autopsy, whitish products were the most prevalent. After a few days of being exposed to air, more commonly found colors were light-brown, reddish-brown, orange-brown, and yellowish-brown. Many of the larger and medium-sized rust stains often had shapes with clearly delineated boundaries, giving the appearance of traces or remains of a solution (Figure 2.43). Several rust spots or stains appeared to be wet. In one case (bar 3B.5), a silver-colored stain was detected (top side of bar between bent zone and right straight leg) immediately after removing the coating. One hour later its color changed to whitish, and 2 days later changed to dull-brown and orange-brown. At the bottom side of bar 1A.5, a whitish substance found alongside a longitudinal lug (bent zone and straight right leg) turned yellowish-brown a few hours after coating removal. Such matter was deposited along a strip, giving the appearance of a solution trace (Figure 2.44).

Figure 2.42 Various rust products above uniformly black corroded surface under the coating.

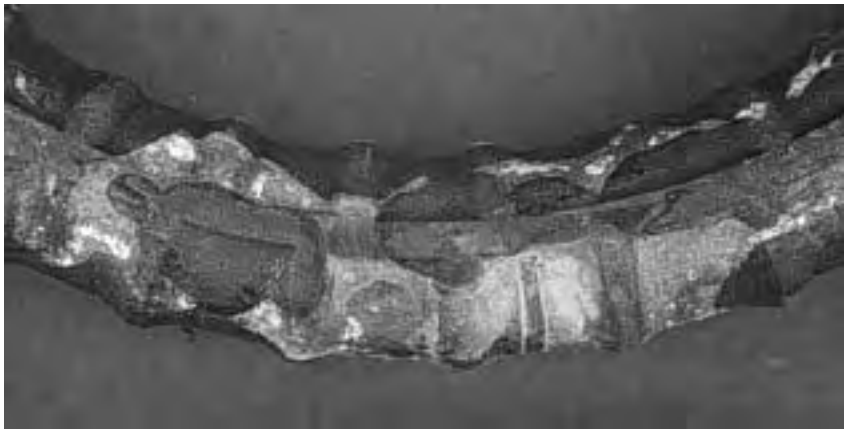

(a) Top side of bar 1B.7

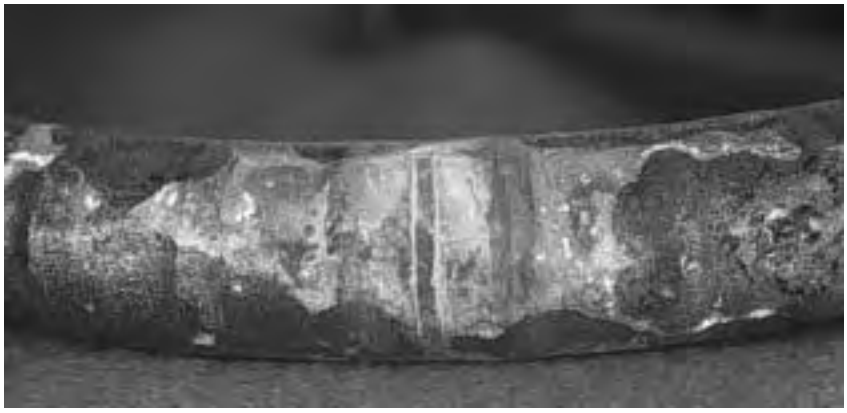

(b) Outside bend of bar 1B.7

Figure 2.43 Rust products or stains with clearly delineated boundaries, with the appearance of solution trace.

Figure 2.44 Whitish products alongside longitudinal lug at bottom side of bar 1A.5.

Wet areas and drops of brownish, liquid solution formed on the surface of most bars, similar to those found above the coating. This phenomenon occurred in more bars as days after coating removal passed. As before, some of the drops had dried and formed driblets or beads of brittle rust with wet consistency. The measured pH was between 3 and 4, indicating that the solution was acidic. This phenomenon was more common in larger bars.

Bars with the best surface condition (generally smaller bars) were characterized by a mottled surface with glittering golden-brown appearance. In these bars, the coating usually adhered along a portion of the straight legs next to the protruding bar ends. The steel surface beneath the adhered coating was in its original condition, with a shiny, bright appearance.

Among smaller bars, specimen 1A.5 (damage > 2%) suffered the worst corrosion (Figure 2.45), followed by bars 2A.6 (cracks with damage < 1%) and 1A.10 (damage > 6x6 mm). The bar with best condition was, amazingly, 3A.3 (damage > 6x6 mm) (Figure 2.46), followed by bar 3A.7 (damage < 2%). Among larger bars, specimen 3B.5 (damage > 2%) suffered the worst corrosion (Figure 2.47), followed closely by bar 3B.4 (damage > 2%, patched). The extent and severity of corrosion was similar for the remaining bars. Interestingly, in bars with damage greater than 6x6 mm, corrosion spread much more on the repaired bar (3B.2) than on the unrepaired bar (2B.3).

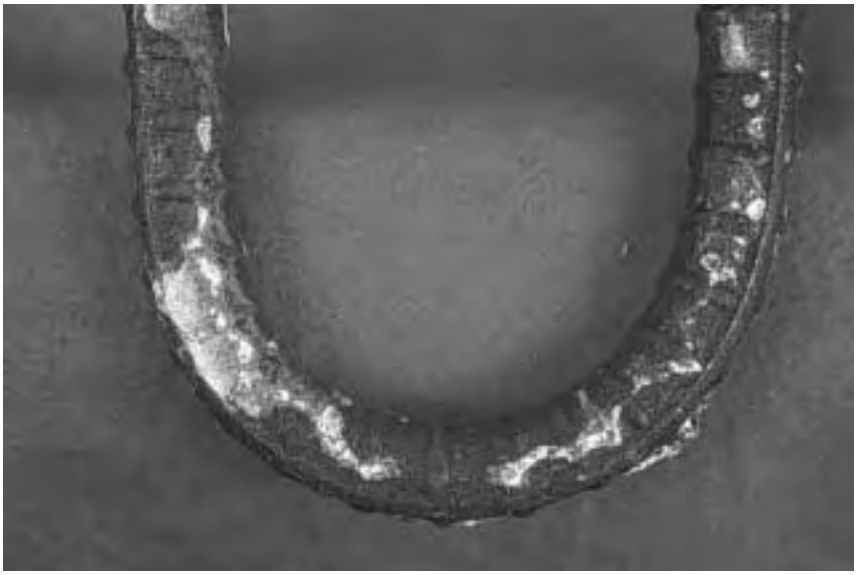

(a) Top side.

(b) Bottom side.

Figure 2.45 Whitish and yellowish-brown corrosion products on bar 1A.5.

(a) Top side.

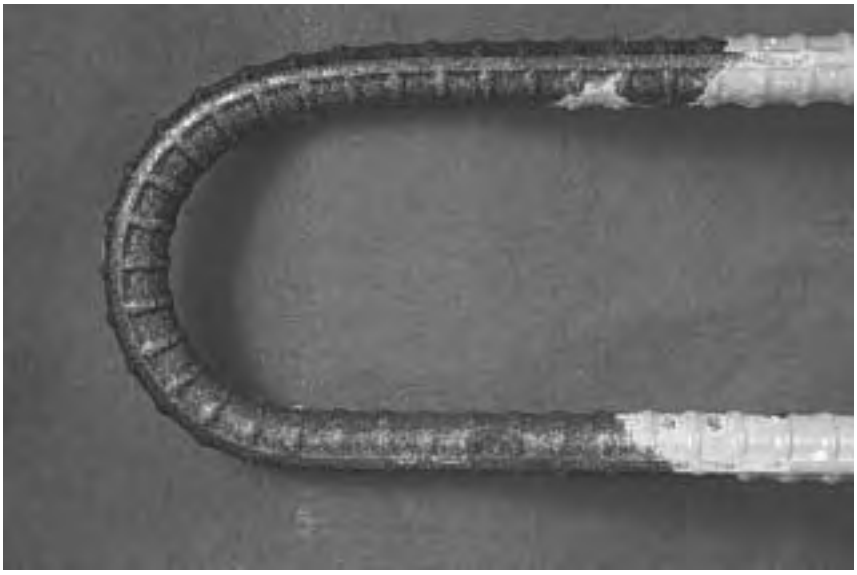

(b) Bottom side.

Figure 2.46 Steel surface condition beneath the coating of bar 3A.3.

(a) Top side.

(b) Bottom side.

Figure 2.47 Steel surface condition under the coating of bar 3B.5.

2.6.7 Appearance of Concrete Fragments and Bar Trace in Concrete

CONTROL BARS

Concrete surrounding the top bar (above and below the bar) was extensively rust stained (Figure 2.48). Rust stains were very large, mostly black or dark and reddish-brown colored. Sometimes, reddish-brown stains had a black rim. Other observed stains were bluish, bright orange, brownish, yellowish-brown, and whitish. In specimen 3B.1, a few dark-greenish spots were observed immediately after autopsy, and hours later turned bluish or dark. In specimens with small bars, concrete around straight bar legs experienced more rust staining than concrete around the bend zone. Black and reddish-brown rust usually accumulated and hardened in concrete above straight bar legs. Staining distribution seemed more uniform in concrete around large bars. Rust staining was more extensive in concrete above smaller bars, especially in the portion closer to the front face of the specimen, where stains penetrated the concrete far beyond the bar location at either side or both sides of bar legs (Figure 2.48). Rust staining was more extensive in concrete below large bars. In general, rust stains penetrated the concrete far beyond the bar location along different portions of the bar. Stains penetrated cracks and expanded towards the top concrete surface (Figure 2.49). Rust staining was mostly reddish-brown and orange-brown at areas closer

to the upper surface while it tended to be dark or black at the rebar level. Reddish-brown and dark rust was also observed inside large concrete voids above and below the bar.

Figure 2.48 Rust staining on surrounding concrete under uncoated bar 3A.8.

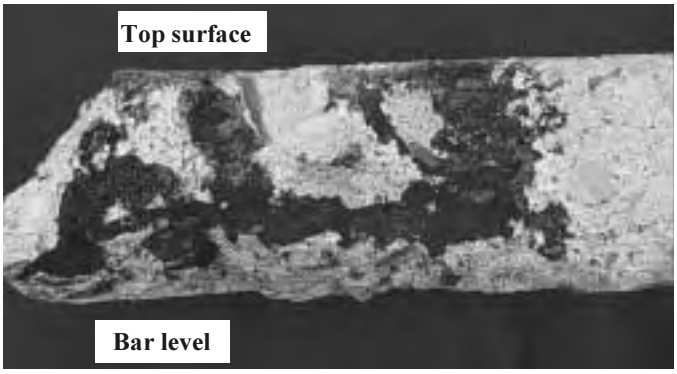

(a) Rust inside crack surfaces in concrete cover.

(b) Another aspect of rust inside crack surface.

Figure 2.49 Rust products penetrated through cracks and rose to the upper surface in specimens with uncoated bars.

In non-stained areas, the bar trace in concrete above the bar looked porous with a grayish-like appearance, the rib imprints were not clearly defined, and there were few voids. The bar trace in concrete below the bar had also a grayish-like appearance, but looked more porous and dusty with the presence of laitance and more voids of different size. Concrete adhered well to black bars as evidenced by the chunks of concrete that remained stuck to the bar surface.

EPOXY-COATED BARS

Concrete surrounding epoxy-coated bars showed much less rust staining than specimens with uncoated bars. Rust staining was generally confined to the concrete-bar interface and did not spread inside the concrete beyond the bar location. Among specimens with coated bars, concrete around 25-mm bars experienced more extensive rust staining than concrete around 13-mm bars. In all specimens, rust staining was more extensive in concrete below the bars than in concrete above the bars. In most specimens, rust staining in concrete spread more around the bend than along straight bar legs. Distribution of staining in concrete tended to be more uniform in specimens with larger bars.

The size of rust stains ranged from large to very small. The largest stains were in the bend zone. Color and appearance of stains varied widely. Very often, colors of stains were combined: brown or reddish-brown areas inside black stains, brown or reddish-brown with a black rim, black with reddish rim, stain ranging from dark reddish-brown to light brown, and stain ranging from black to reddish-brown. The most common stains were dark or black, reddish-brown, and black with reddish-brown areas. Dark-greenish stains were found mainly in specimens with 25-mm bars: Only one specimen with 13-mm bars had a dark-greenish stain versus four specimens with 25-mm bars. The appearance of dark-greenish stains changed within minutes or hours after specimen autopsy, i.e. after being exposed to the atmosphere. The color of dark greenish stains changed to one of the following colors: Reddish-brown, brown, reddish-brown combined with dark or black, and light-brown. In specimen 2B.6, one dark-greenish spot turned brown within minutes, then gradually turned reddish-brown within a day. Another greenish spot in the same specimen turned yellowish-brown within minutes and then reddish-brown within a day.

Rust stains in concrete in most cases were at the following locations: At and near concrete voids, next to coating imperfections and discontinuities (intentionally damaged spots, patched areas, as-received damage, cracks in the coating, pinholes, and mandrel-induced nicks), and alongside the path of the longitudinal lug on the bottom of the bar (Figure 2.50). Rust staining below the bar sometimes extended along a strip. Stains at other locations were more sporadic, such as at straight bar legs (above and below the bar). There was almost always a blister in the coating next to a rust-stained void in the concrete. However, there were many concrete voids, large and small, which were free of any rust products or staining.

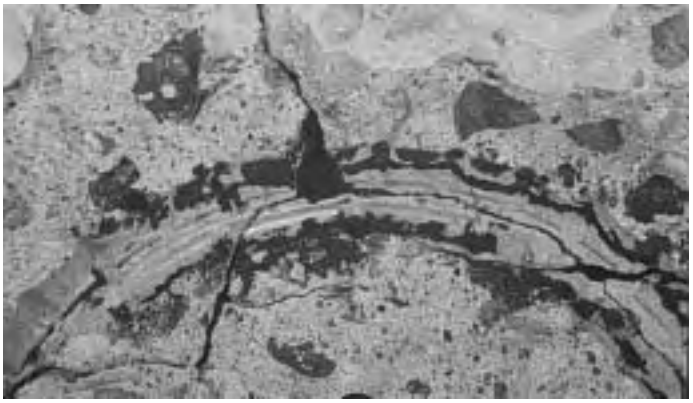

(a) Concrete above the bar.

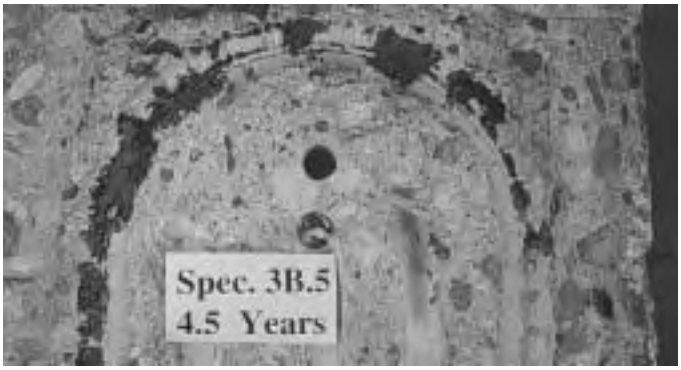

(b) Concrete below the bar.

Figure 2.50 Bar trace in concrete of specimens 3B.5.

The bar trace in concrete above epoxy-coated bars consisted of a smooth, shiny, glossy surface with a grayish-like appearance, the rib imprints were clearly defined, and there were few voids (Figure 2.51). The bar trace in concrete below epoxy-coated bars had a whitish-like appearance, looked more dusty and porous with presence of laitance, and had much more voids of different size (Figure 2.52). Sometimes white deposits, probably salt, accumulated on the underside bar trace as shown in Figure 2.53. Chemical adhesion to concrete was lost, as evidenced by the ease with which the bar was removed from the concrete and lack of concrete adhering to the bar. Only a film of white dust from the concrete paste adhered to the bottom of the bars.

Figure 2.51 Bar trace on top of coated bar in concrete.

Figure 2.52 Bar trace on bottom of coated bar in concrete.

Figure 2.53 White deposits accumulated under coated bar.

CATHODIC BARS

The trace of uncorroded bars in concrete had a grayish-like appearance, with a darker gray within 1.0 to 2.0 cm from the front face. This appearance was probably the result of the alkalinity produced by cathodic activity at the steel surface. Concrete at the top side of the bar was smoother with few concrete voids. Concrete on the bottom of the bars was more porous with many more voids. Figure 2.54 shows the cathodic bar imprint in concrete.

Figure 2.54 Cathodic bar trace in concrete

CHAPTER 3

ANALYSIS AND DISCUSSION OF TEST RESULTS

3.1 GENERAL

Variables in the macrocell study, such as bar size, deformation pattern, level of coating damage, and patching could have affected the test results significantly. Other factors, including the chloride distribution, coating thickness, and material properties could have also played a role in the corrosion process. These factors may act together or individually, leading to complex behavior of the corrosion systems. In this chapter, the results from corrosion monitoring, visual examinations, chloride analysis, and post-mortem examination are analyzed and discussed and the effects of the various factors are evaluated.

The macrocell corrosion phenomenon was studied in terms of the corrosion system parameters and how they influenced the corrosion mechanism. Time development of the corrosion process, level of corrosion activity and intensity, and observations of the corroded metal and its environment were systematically evaluated. The causes of coating debonding and loss of integrity which led to corrosion of the metal substrate were discussed. The data and observations were used to develop a hypothesis for the corrosion mechanism.

3.2 TIME DEVELOPMENT OF CORROSION

3.2.1 Time-to-Corrosion

Time-to-onset of corrosion varied considerably. It was noted that the less the degree of damage to coating, the longer corrosion initiation was delayed. In other words, the more steel area was exposed, the higher was the potential for earlier corrosion initiation. Nearly all specimens with patched damage in series A, the 13-mm (#4) bars, showed negligible activity throughout the 4.5-year period. Patching of bars in series B, the 25-mm (#8) bars, merely delayed the onset of corrosion compared to bars with exposed steel areas.

In general, earlier corrosion initiation was noticed in series B than in A. This reflects the combined effects of many factors: bar size and area of exposed metal; steel metallurgy; variation in coating thickness; and variability of the surrounding concrete environment. The smaller bars had smaller total area of steel exposed, better mechanical properties (yield strength), slightly thicker coatings, and better concrete consolidation.

Epoxy-coated reinforcement showed a greater tolerance to chloride accumulation in the surrounding concrete than uncoated reinforcement. The epoxy film isolated the steel from the contaminated

environment and delayed corrosion. When sufficient amounts of chloride ions reached the exposed steel areas, corrosion was initiated. Acid-soluble chloride concentrations associated with the onset of corrosion in the control specimens ranged from below 0.08 to 0.12% by weight of concrete, which is equivalent to 1.8 to 2.7 kg/m^3 (3.0 to 4.6 lb./yd^3). The corresponding average chloride content for onset of corrosion of the epoxy-coated bar specimens was about 0.18%, *i.e.* 4.0 kg/m^3 (6.7 lb./yd^3). Hence, corrosion started on the damaged epoxy-coated bars when chlorides had reached about 1.5 to 2 times the levels corresponding to uncoated bars.

3.2.2 Time-To-Cracking

The control specimens showed surface cracking and staining at ages that varied between approximately 210 and 532 days of exposure. Not surprisingly, the large bar specimens cracked much earlier than the small bar specimens at the same cover depth. This observation agrees with previous findings that the smaller the cover-to-bar diameter ratio, the earlier cracking will occur.[24] Corrosion activity increased noticeably after concrete cracking. Corrosion currents for the small bar specimens increased after about 1.5 years which is roughly the average time to cracking for the six control specimens.

Based on the established relation that each amp-hour of corrosion current consumes 1.04 gm (0.037 oz.) of iron,[7] the average consumption of iron of the control bars at the time of cracking was 0.6 gm (0.021 oz.). As a percentage of the total bar weight or volume, the consumption was as low as 0.05% for 25-mm (#8) bars and 0.1% for 13-mm (#4) bars. This consumption yields an average yearly rate of thickness loss from the metal surface area of 3.6 μm/yr for all control bars.

As stated earlier, the epoxy-coated bar specimens exhibited limited corrosion-related staining or cracking during 4.5 years of exposure. Coated bar specimens cracked between the end of the third year and the fourth year of exposure. Exudation of acidic solution on the front face of the specimens with large bars was first observed after about 1.5 years of exposure. Interestingly, some of the coated bar specimens reached higher levels of metal consumption than those associated with control bar cracking and yet did not crack. Possible explanations of this phenomenon are presented in Sections 3.4.4 and 3.7.1.

Concrete cracking occurred at a much lower rate of consumption of iron than stated by other researchers. Clear and Virmani[7,12,25] indicated that concrete cracking occurs at total iron losses as low as 0.5–2% of bar volume. Broomfield *et al.*[24] found that cracking can occur at steel consumption of 10–100 μm/yr depending on geometry (cover to bar diameter), concrete quality, and oxygen access.

However, Spellman and Stratfull, as reported in Reference 26, showed that a conversion of as little as 25 μm (1 mil) of steel into its characteristic corrosion products can cause cracking in a 22 mm (7/8 in.) thick concrete layer. More recently, Hime[27] has indicated that although cracking was suggested to occur

at a rust thickness of 25–500 μm (1–20 mils), evidence has been gathered that even below 2.5 μm (0.1 mil) cracking can occur. These observations indicate that cracking may occur at significantly lower metal losses than often reported in literature. In this study, the main reasons why cracking occurred at a low metal consumption rate may be attributed to the low strength of concrete and small cover to reinforcement.

3.3 CORROSION ACTIVITY

3.3.1 General

In principle, a direct measurement of the corrosion current can be obtained by reading the voltage drop across the resistor in the macrocell specimen. The magnitude of the current reflects the severity of corrosion activity. When monitored versus time, the corrosion current indicates the amount of iron consumed from the top anode bar under macrocell action.

Besides the cathodic bottom bars in the macrocell specimen, other cathodes may also have developed at the top bar. In this case, the net reaction of the anodes and cathodes on the same bar would not result in a net current flowing to the bottom reinforcement. Such activity is not expected to be critical for coated bars because of the very limited surface area available for oxygen reduction. For uncoated bars, the actual corrosion activity would be underestimated by the measured corrosion current. It is conservative then to compare the performance of coated bars to that of uncoated bars on the basis of the measured macrocell currents.

The rate of corrosion can be expressed in different forms. The commonly-used expressions are: weighted average current; corrosion current density; and amount of metal consumed. These are discussed in subsequent sections.

3.3.2 Macrocell Current and Corrosion Potentials

Figures 3.1 through 3.6 show graphs of macrocell currents comparing relative performances of different damage conditions for specimens with both 13- and 25-mm coated bars. Among 13-mm bars with parallel ribs, specimens with damage greater than 2% and specimens with coating cracks and damage less than 1% underwent the highest corrosion currents. Interestingly, the specimen with cracks in the coating and damage less than 1% tended to have increasing currents at the end of the exposure, while the specimen with damage greater than 2% had lower, declining currents at the end of 4.5 years (Figure 3.3). Specimens with parallel ribs and damage greater than 6x6 mm had very low currents and, paradoxically, the repaired specimen showed slightly greater currents [(Figure 3.1(a)]. This agreed well with the observed lack of corrosion at damaged spots noted previously. For 13-mm bars with cross ribs, specimen with damage greater than 6x6 mm experienced the greatest current, as expected.

Among 25-mm bars with parallel ribs, the specimen with damage greater than 2% and the specimen with cracks less than 1% experienced the highest currents, as was the case for 13-mm bars (Figure 3.6). Again, the specimen with cracks and damage less than 1% experienced increasing macrocell current at the end of 4.5 years while other damaged specimens seemed to have reached a steady-state behavior. Apparently, when there are cracks in the coating, the corrosion mechanism may differ from that for other types of damage. Among 25-mm bars with cross ribs, the specimen with damage less than 1%, which met previous specifications in terms of limiting damage, showed currents very similar to the specimen with damage greater than 6x6 mm. Among all 25-mm bars (parallel and cross ribs), except for damage greater than 2% [Figure 3.4(b)], patched specimens underwent macrocell currents similar to unrepaired specimens after 4.5 years of exposure (Figures 3.4(a) and 3.5). It seemed that patching provided some initial protection during the first 2.5 years but currents for both patched and non-patched specimens were similar thereafter.

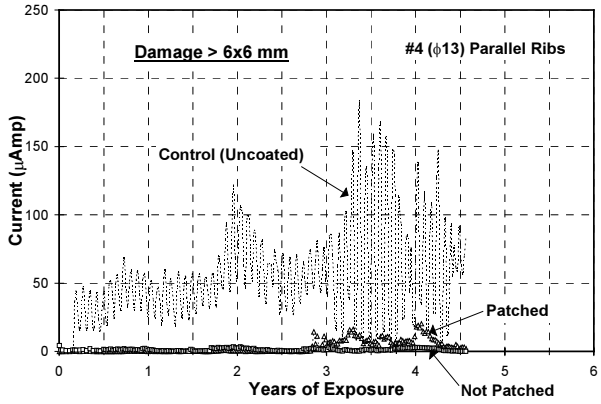

(a) Damaged areas larger than 6x6 mm.

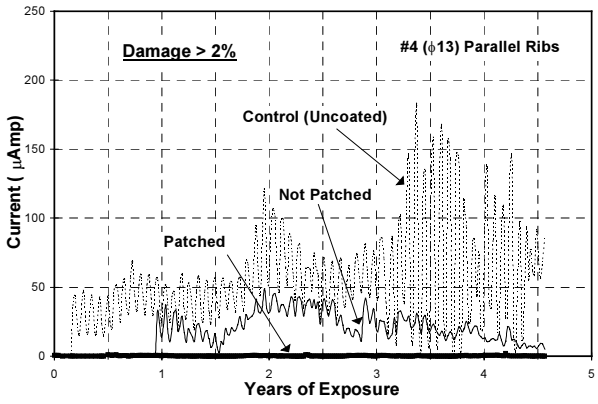

(b) Damage greater than 2% of bar surface.

Figure 3.1 Current vs. time for various combinations of epoxy-coating condition of A specimens [13-mm (#4) bars] with parallel ribs.

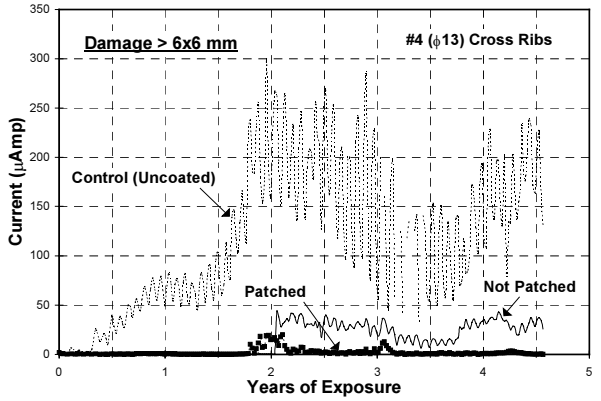

Figure 3.2 Current vs. time of A specimens[13mm (#4)bars] with cross ribs and damaged areas larger than 6x6 mm.

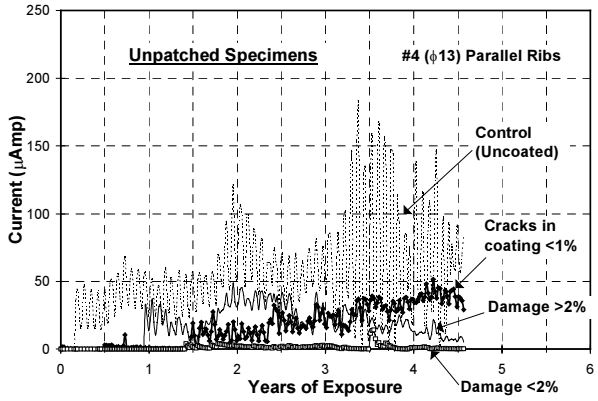

Figure 3.3 Current vs. time of A specimens [13mm (#4) bars] with different damage levels or cracks in the coating.

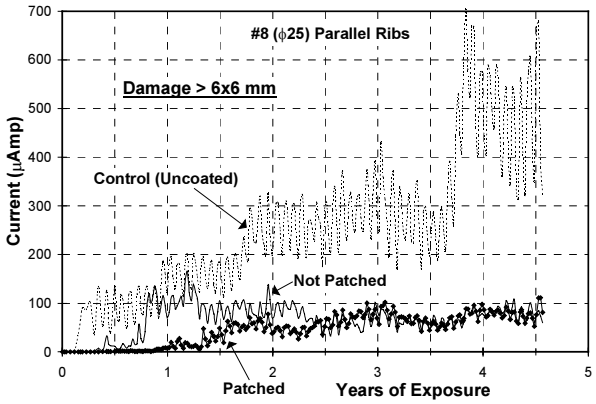

(a) Damaged areas larger than 6x6 mm.

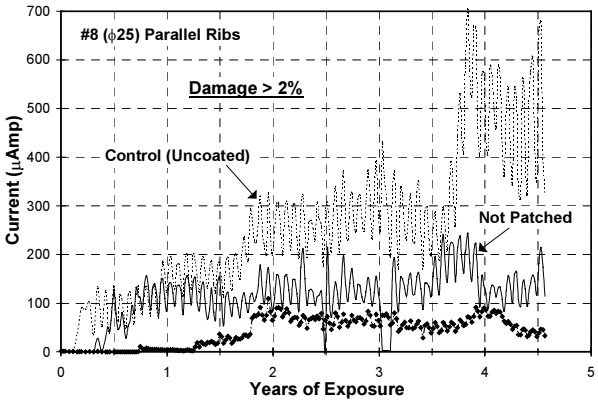

(b) Damage greater than 2% of the bar surface.

Figure 3.4 Current vs. time for various combinations of epoxy-coating condition of B specimens [25-mm (#8) bars] with parallel ribs.

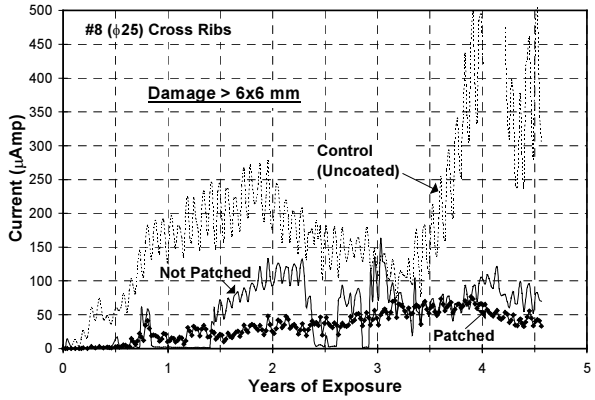

Figure 3.5 Current vs. time of B specimens [25mm (#8) bars] with cross ribs and damaged areas larger than 6x6 mm.

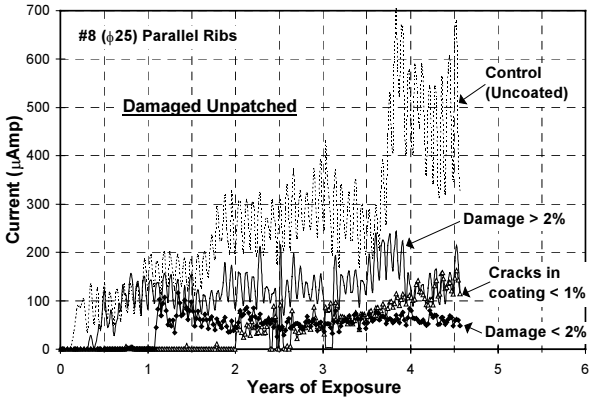

Figure 3.6 Current vs. time of B specimens [25mm (#8) bars] with different damage levels or cracks in the coating.

Corrosion potentials correlated well with measured currents in terms of the relative performance of different groups with the same bar type and damage. Plots of corrosion potentials over time of bars with the same type of damage and of the respective control bar are shown in Figures 3.7 and 3.8. Corrosion potentials were measured for only the last ten months of the exposure test periods. A comparison of these graphs with those of Figures 3.1, 3.2, 3.4, and 3.5 indicates that the order of relative performance among specimens is the same for both potential and current measurements. The average corrosion potential of each specimen is plotted in Figures 3.9 and 3.10. In the same graphs, the average current density (calculation of this parameter is explained in subsequent sections) of each specimen is also plotted for comparison. Both corrosion potential and current density curves have very similar shapes, indicating comparable trends. With a few exceptions, more negative corrosion potentials correlated with higher current densities for a given set of bars with the same type of damage.

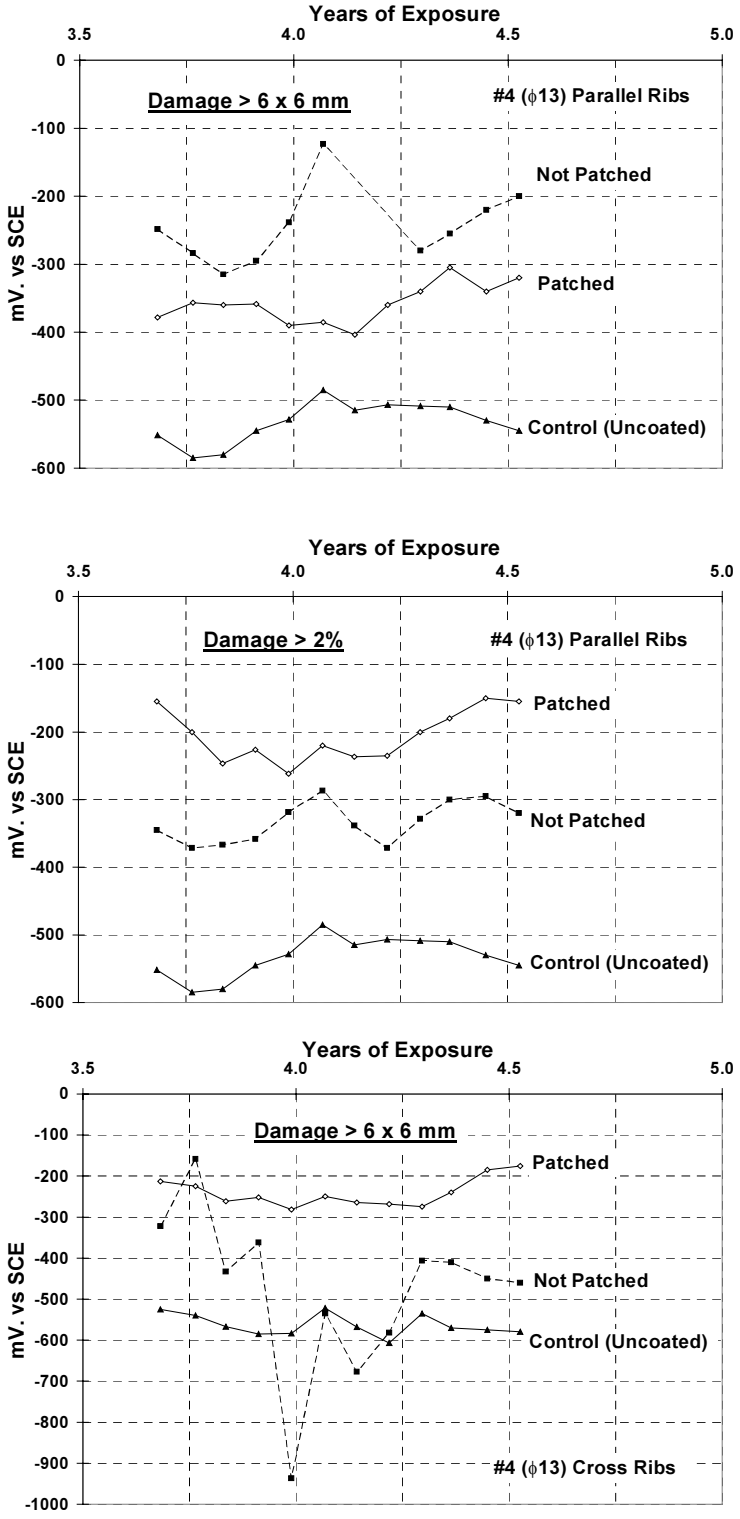

Figure 3.7 Three graphs of corrosion potential vs. time of various epoxy-coating condition of A specimens [13-mm (#4) bars].

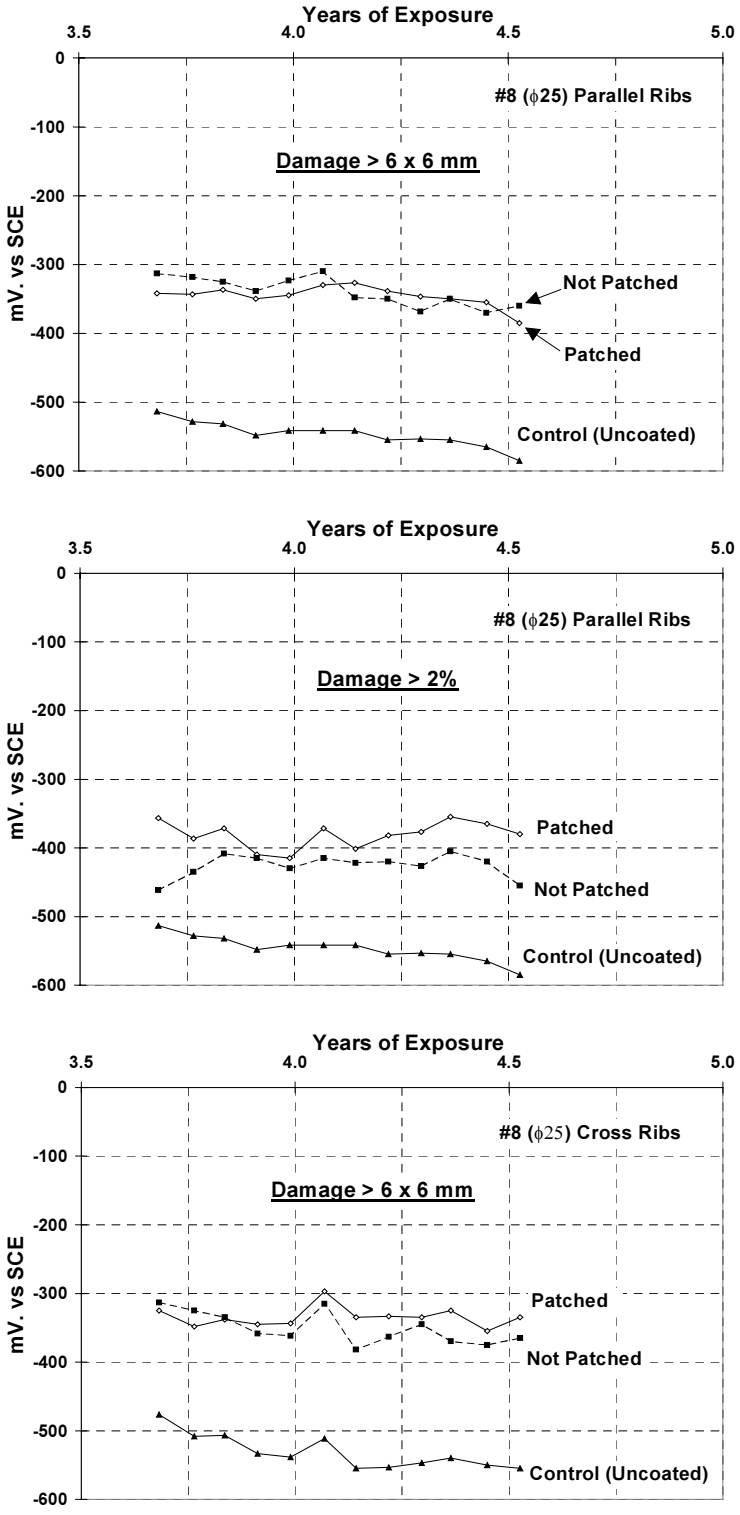

Figure 3.8 Three graphs of corrosion potential vs. time of various epoxy-coating condition of B specimens [25-mm (#8) bars].

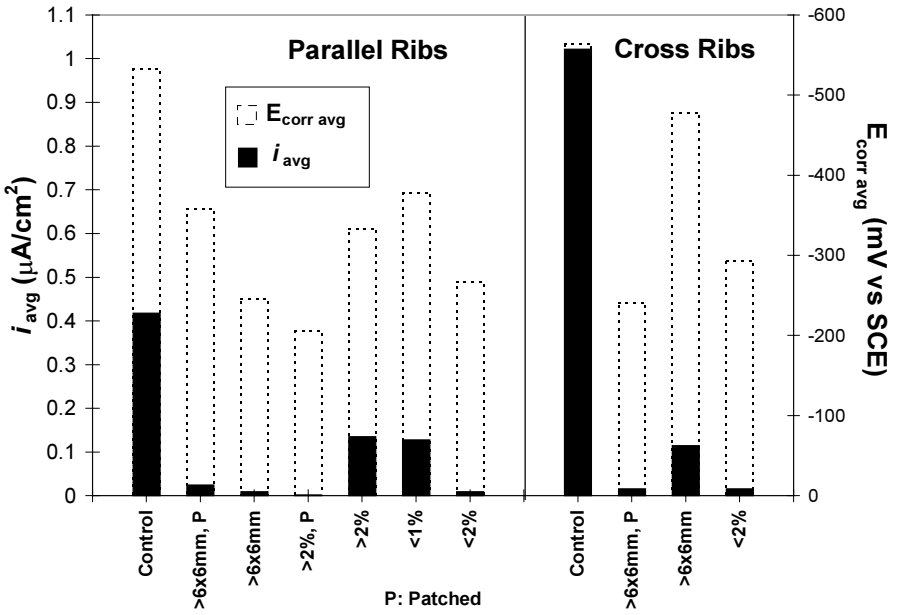

Figure 3.9 Graphs of average corrosion potentials and current densities of all A specimens [13-mm (#4) bars].

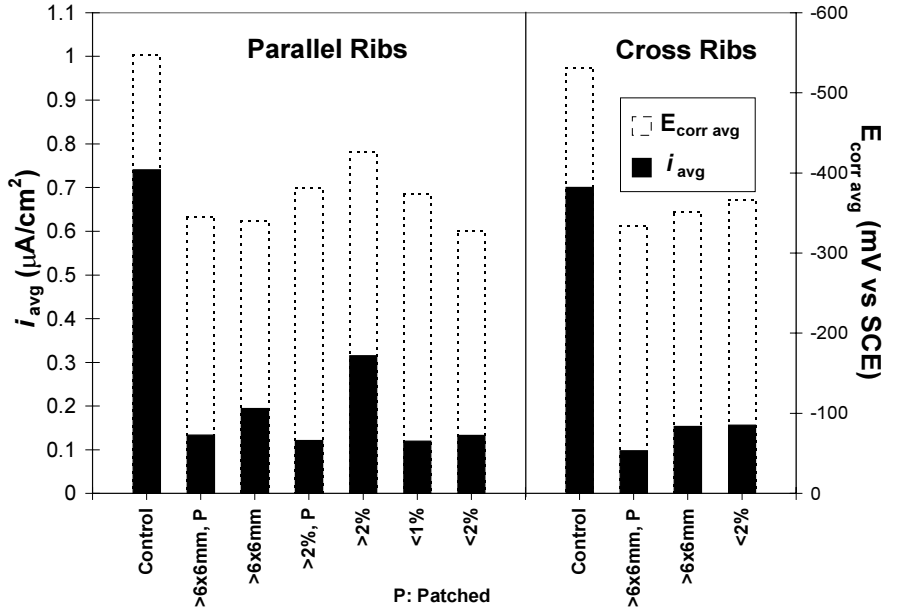

Figure 3.10 Graphs of average corrosion potentials and current densities of all B specimens [25-mm (#8) bars].

Average current densities versus average corrosion potentials for all specimens are plotted in Figure 3.11. All specimens with potentials between -200 and -300 mV vs. SCE had average current densities smaller than 0.015 μA/cm^2. Bars with corrosion potentials between -300 and -400 mV vs. SCE had average current densities between 0.025 μA/cm^2 and 0.194 μA/cm^2. Corrosion potentials in the range of -400 to -500 mV vs. SCE correlated with average current densities of 0.115 μA/cm^2 and 0.315 μA/cm^2. Finally,

control specimens, which had corrosion potentials between -500 to -550 mV vs. SCE, experienced average current densities between 0.418 μA/cm^2 and 1.02 μA/cm^2. With this limited data, corrosion potentials between -200 and -300 mV vs. SCE correlated with negligible corrosion, potentials from -300 to -500 mV vs. SCE related to low to moderate corrosion, and potentials more negative than -500 mV vs. SCE correlated with severe corrosion.

Other researchers have measured similar corrosion potentials. Wheat and Eliezer found that loss of passivity and general corrosion of uncoated bars occurred at a potential range of -450 to -600 mV SCE.[28] Sagüés measured potentials in the range of -350 to -475 mV SCE on coated bars in uncracked columns after 300 days of exposure.[10] Zayed et al. observed potentials in the order of -400 mV SCE in damaged epoxy-coated bars in uncracked specimens.[3]

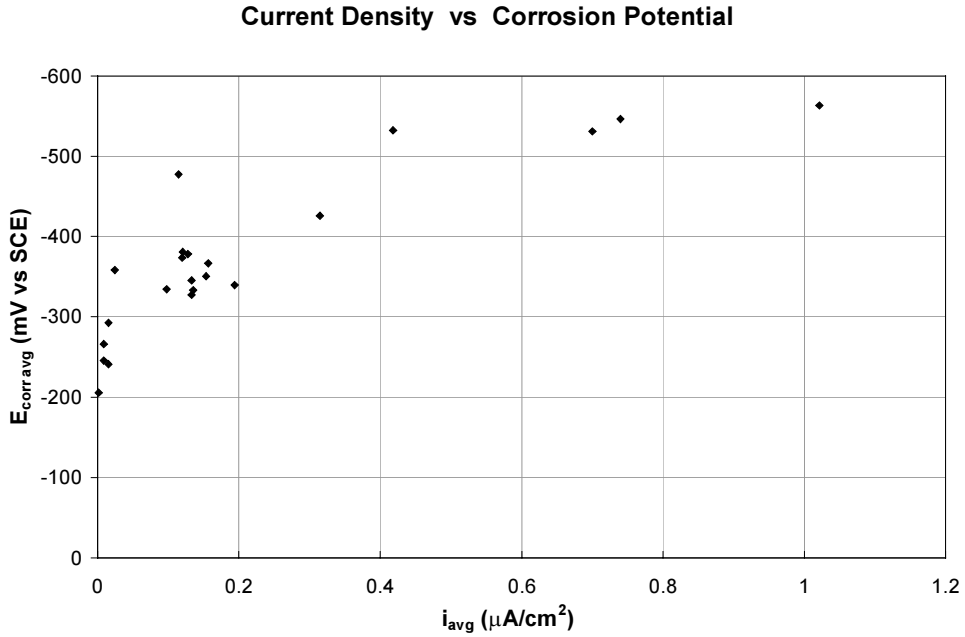

Figure 3.11 Average current densities vs average corrosion potentials for all specimens.

3.3.3 Weighted Average Current

The weighted average corrosion current I_{wa} for any specimen was evaluated by the following expression,

$$I_{wa} = \frac{\sum I_{ai}\, T_i}{\sum T_i} \qquad i = 1, n$$

where

I_{ai} = average current in time interval i,

T_i = time interval i,

n = total number of time periods of measurements.

The magnitude of the weighted average current reflects the severity of corrosion activity over the increment of time under test. The weighted average current provides a measure of the net electrons released by the corrosion process and flowing through the external link. The calculated values of weighted average current at one, two, and 4.5 years are listed in Table 3.1. These values were calculated using currents from the last triplicate specimen only. Currents from companion specimens were not used to calculate weighted averages at 1 and 2 years. The weighted average currents were very similar to the average currents because the time intervals for measuring currents were practically the same throughout the test.

Table 3.1 Weighted average corrosion current for macrocell specimens (μAmp).

Group No.	Damage Category and Condition	Series A (13 mm)			Series B (25 mm)		
		1 Yr	2 Yr	4.5 Yr	1 Yr	2 Yr	4.5 Yr
1	Control (Uncoated Bars)	32	40	55	82	134	255
2	Spots > 6x6 mm, Patched	0.16	0.19	3.21	1.37	19	46
3	Spots > 6x6 mm, Exposed	1.11	1.08	1.18	29	62	67
4	Spots > 2%, Patched	0.27	0.21	0.21	1.67	16	42
5	Spots > 2%, Exposed	1.24	11.3	17.7	56	74	108
6	Cracks < 1%, Exposed	1.16	3.90	16.8	0.29	0.28	41
7	Spots < 2%, Exposed	0.01	0.67	1.15	0.25	30	46
8	Control (Uncoated Bars)	30	71	134	76	140	241
9	Spots > 6x6 mm, Patched	0.40	1.37	2.03	7.70	15.4	34
10	Spots > 6x6 mm, Exposed	0.30	0.29	15	7.5	27	53
11	Pinholes < 1%	0.06	0.21	2.02	8.2	23	54

The table shows that the control bars exhibited much higher corrosion currents than the coated bars. The larger bars performed worse than the smaller bars. In both series, the highest corrosion currents among the coated bars were those associated with highest damage percentage (2%) followed in most cases by those with large spots of damage (6 x 6 mm). Patching the small bars was effective in suppressing the corrosion current, whereas patching the large bars merely reduced the current. The exception was the 13-mm bar with parallel ribs and damage greater than 6x6 mm, but even in this case the average current for the damaged specimen was not significant (3.21 μAmp). It should be noted that among coated specimens, the 25-mm bar with pinholes less than 1% had the third largest average current. No clear trend is discernible for different rib patterns: among series A, bars with cross ribs tended to have larger average currents, and among series B, bars with parallel ribs tended to show slightly higher average currents. Average currents tended to increase with time of exposure, suggesting that the performance of the coated bars was deteriorating. Specimens with cracks in the coating and damage less than 1% showed greater activity in the last 2.5 years of exposure: the 13-mm bar had the second largest weighted average

current among 13-mm coated bars, and the 25-mm bar had the largest increase in average current of all specimens in the last 2.5 years.

3.3.4 Corrosion Current Density

When the weighted average current is divided by the total (nominal) surface area of the anodic bar, the product is defined as the corrosion current density. From information (Reference 8, 24, and 29) on the rate of corrosion of reinforcing steel in concrete, corrosion current densities up to 0.1 $\mu A/cm^2$ denote a negligible corrosion rate, between 0.1 and 0.2 $\mu A/cm^2$ indicate a low corrosion rate and a threshold for active deterioration mechanism, and between 0.2 and 0.5 $\mu A/cm^2$ disclose a shift to a moderate corrosion rate. The average current densities obtained for the different groups are plotted in Figures 3.12 and 3.13. In each figure, a comparison can be made between the results at one, two, and 4.5 years of exposure.

Obviously, current densities showed the same trends as weighted average currents because the values are proportional. The graphical representation makes the already observed trends easier to see. For the small bar series, the uncoated bar with cross ribs had the largest current density of all specimens (including 25-mm bars). The uncoated bar with parallel ribs showed a moderate current density, the lowest among all control specimens. Generally, the corrosion rate of most coated bars was negligible. After 4.5 years, current densities in three 13-mm coated bars (damage greater than 2%, cracks with damage less than 1%, and cross ribs with damage greater than 6x6 mm) increased to the region of low corrosion rate. The rest of 13-mm coated bars still had current densities in the negligible range. Bars with patched damage performed excellently.

For the large bar series, control bars displayed current densities in the region of high corrosion rate. The coated bars clearly showed a rise in the corrosion rate from negligible to low, and tended to rise rapidly during the 4.5 years. Almost all 25-mm coated bars had current densities at least in the low corrosion rate region and one specimen (damage greater than 2%) had current density in the moderate corrosion region. The corrosion rates of 2 bars with patched damage increased from negligible to low, and that of a third bar with patched damage remained negligible but with tendency to increase. Large coated bars exhibited corrosion rates ranging from 1 (equal) to 76 times higher than those for small coated bars. Again, data from both deformation patterns were not much different.

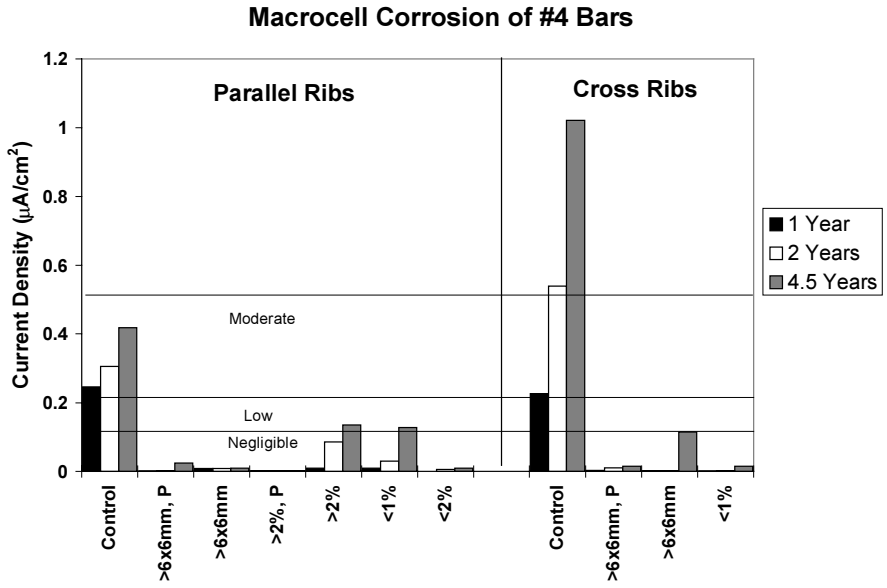

Figure 3.12 Corrosion current densities for all A specimens [13-mm (#4) bars].

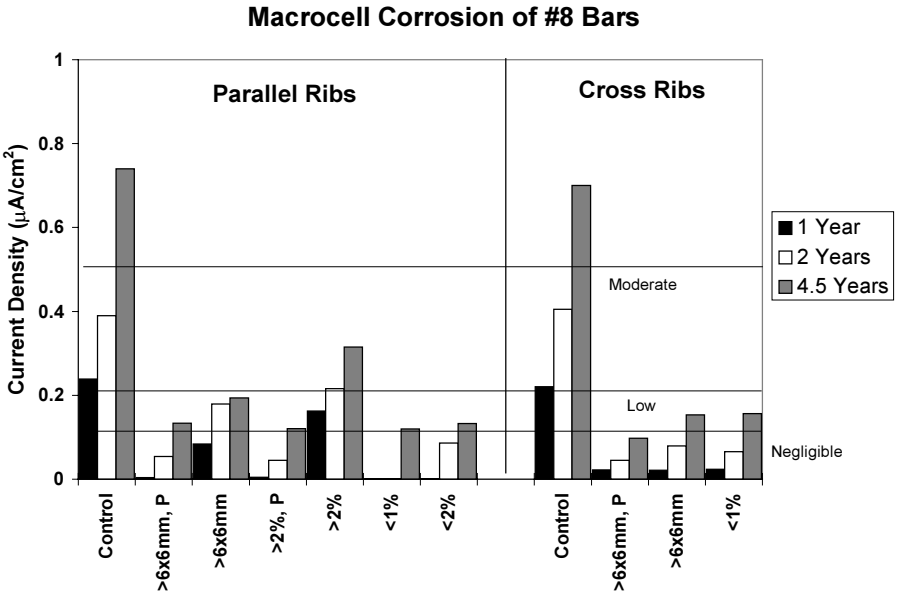

Figure 3.13 Corrosion current densities for all B specimens [25-mm (#8) bars].

3.3.5 Metal Loss

The integration of the current-time relationship gives the amount of electrical charge (flux) exchanged in a certain period of time. The amount of charge, *i.e.* number of electrons exchanged, correlates with the amount of metal consumed. Therefore, charge flux can be used as a measure of corrosion severity. The amount of charge flux passed in 4.5 years for specimens from series A and B is plotted in Figures 3.14 and 3.15. In the same figures, the amounts of charge of the coated bars are given as percentages of the uncoated bars. The plots confirm the previous discussion and show that the coated bars varied widely in their performance.

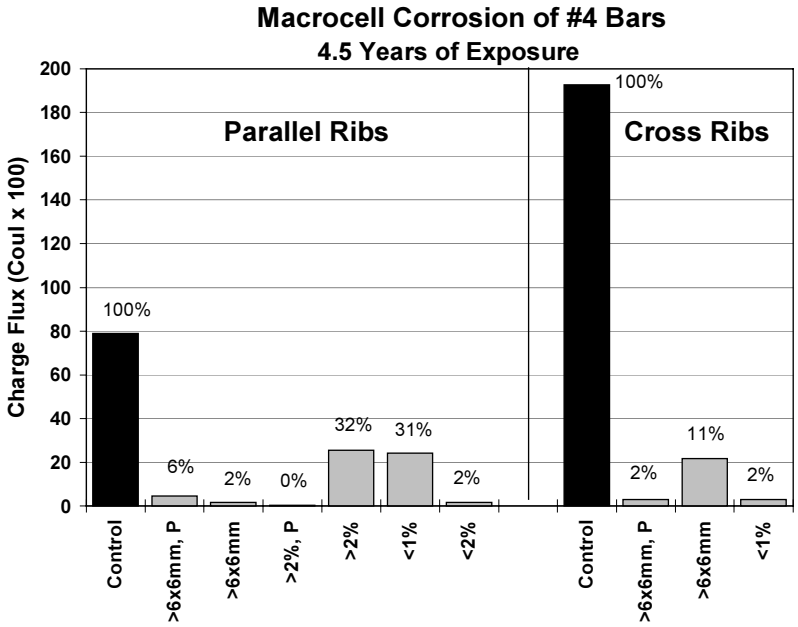

Figure 3.14 Charge flux for all A specimens (13-mm bars).

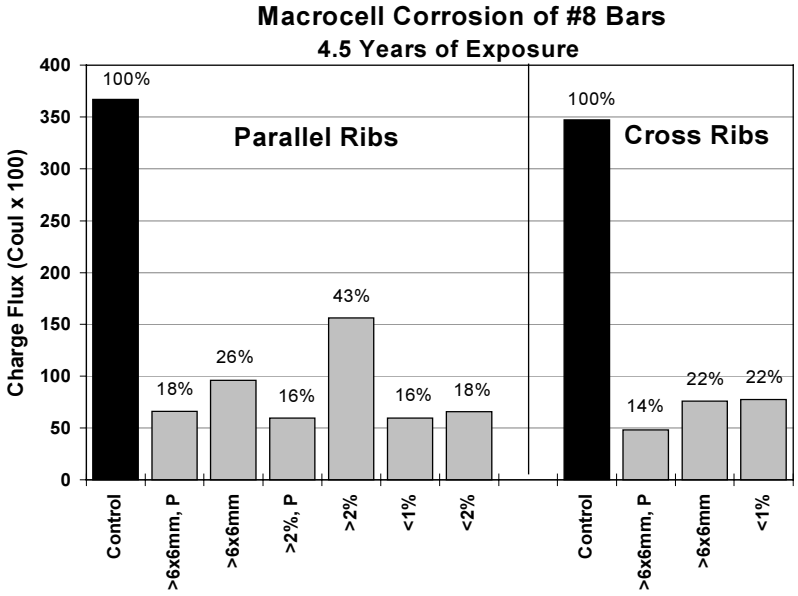

Figure 3.15 Charge flux for all B specimens (25-mm bars).

For series A, the coated bars with worst corrosion (damage > 2% and cracks with damage < 1%) passed slightly over 30% of the charge passed by the uncoated bar. The specimen with cross ribs and damage greater than 6x6 mm passed slightly less charge than the specimen with most charge passed (2164 Coulombs vs. 2548 Coulombs), but a low percentage of 11% is shown because of the excessively high amount of charge passed by the respective control specimen. Two thirds of the specimens passed 6% or less of the charge passed by their respective control specimens.

For series B, the heavily damaged bars exhibited corrosion in the range of 22–43% of the uncoated bars. Patching damage reduced corrosion to about 14%. Although the charge flux of the coated bar with worst corrosion (damage > 2%) increased from 4,677 Coulombs at 2 years to 15,614 Coulombs at 4.5 years, the percentage of charge flux passed with respect to that of the uncoated bar decreased from 55% to 43% in the same period.

Clearly, the uncoated bars deteriorated at a faster rate than some of the coated bars. Patched bar specimens passed from 14 to 18% of the charge passed by their respective control bars. Comparatively, the same patched bars passed from 11% to 14% of the charge passed by the uncoated bars after 2 years. Patched bars corroded at a slightly faster rate than damaged bars. Apparently, the effectiveness of patching diminished with time.

Virmani *et al*. used experimental data to correlate charge flux with the amount of metal consumed.[7] Based on that correlation, the amount of metal loss, in grams, from any specimen was estimated by multiplying the charge flux by 1.04. The amount of metal consumed for each group after 4.5 years of exposure is summarized in Table 3.2. All the coated bars from series B lost more than 1 gram of metal after 4.5 years. In the worst case, 4.5 grams was lost, but is still much less than the 10 grams lost by the uncoated bar. In series A, the worst coated bar lost 0.7 grams of metal compared to 2.3 grams lost by the uncoated bar.

The performance of epoxy-coated bars relative to uncoated bars is clearly better. Based on the amounts of iron lost in corrosion during the test period for the different groups, it is evident that coating reduces metal consumption. This important finding agrees with previous findings that epoxy-coated reinforcement exhibits less corrosion than uncoated reinforcement.[3,7,8,30–34]

However, the improvement of performance due to coating application needs to be quantified. The effectiveness of epoxy-coated reinforcing steel to resist corrosion relative to uncoated steel can be assessed in terms of the metal consumption ratio. The ratio is calculated by dividing the amount of metal loss of the uncoated bar by the amount of metal loss of each bar group. This ratio, called the performance ratio in Table 3.3, shows the improvement of performance of each group of coated bars relative to the control group. The performance ratio is simply the reciprocal of the charge percentage given in Figures 3.14 and 3.15. The values are tabulated for 1, 2, and 4.5 years of exposure and include group averages.

Table 3.2 Metal consumed by corrosion after 4.5 years (Amounts in grams).

Group No.	Damage Category and Condition	Series A	Series B
1	Control (Uncoated bars)	2.28	10.61
2	Spots > 6x6 mm, Patched	0.13	1.91
3	Spots > 6x6 mm, Exposed	0.05	2.78
4	Spots > 2%, Patched	0.01	1.73
5	Spots > 2%, Exposed	0.74	4.51
6	Cracks < 1%, Exposed	0.70	1.72
7	Spots < 2%, Exposed	0.05	1.91
8	Control (Uncoated bars)	5.57	10.03
9	Spots > 6x6 mm, Patched	0.08	1.40
10	Spots > 6x6 mm, Exposed	0.63	2.20
11	Pinholes < 1%, Exposed	0.08	2.24

Table 3.3 Performance ratio of epoxy-coated bars to uncoated bars based on amounts of consumed steel after 1, 2, and 4.5 years.

Group No.	Damage Category and Condition	Series A			Series B		
		1 Yr	2 Yr	4.5 Yr	1 Yr	2 Yr	4.5 Yr
1	Control (Uncoated bars)	1.0	1.0	1.0	1.0	1.0	1.0
2	Spots > 6x6 mm, Patched	739	104	17	23	8.2	5.6
3	Spots > 6x6 mm, Exposed	88	8.7	46	4.0	2.4	3.8
4	Spots > 2%, Patched	497	129	263	44	9.1	6.1
5	Spots > 2%, Exposed	7.5	4.7	3.1	2.1	1.7	2.4
6	Cracks < 1%, Exposed	112	16	3.3	16	18	6.2
7	Spots < 2%, Exposed	47	46	48	4.9	4.0	5.6
8	Control (Uncoated bars)	1.0	1.0	1.0	1.0	1.0	1.0
9	Spots > 6x6 mm, Patched	104	33	66	6.1	10	7.2
10	Spots > 6x6 mm, Exposed	14	20	8.9	3.8	3.1	4.6
11	Pinholes < 1%, Exposed	1,059	162	66	7.2	5.7	4.5

The values in Table 3.3 indicate that, after 2 years, most of the patched small bars performed about two orders of magnitude better than the uncoated bars. The corresponding improvement for the patched large bars is about one order of magnitude. After 4.5 years, most performance ratios for small coated bars were at least one order of magnitude better than uncoated bars, with improvements as high as 263 and as low as 3.1. All coated bars from group B had less than one order of magnitude improvement over the uncoated bars after 4.5 years, with performance ratios as high as 7.2 and as low as 2.4. Even in the worst conditions, where damage slightly exceeded 2% of the surface area, there was an improvement in the

performance of epoxy-coated reinforcement over uncoated reinforcement in the time frame of the test. However, performance ratios as low as 1.7 are undesirable. Results from previous testing using both epoxy-coated bars conforming and not conforming to specifications showed about an order of magnitude improvement in the performance of coated bars.[7,8]

The performance of the epoxy-coated bars in a corrosive test environment seems to deteriorate with time. The rate of increase of metal consumption of coated bars is higher than that of uncoated bars. Two thirds of all coated specimens experienced a faster rate of metal consumption than that of the uncoated bars in the last 2.5 years of exposure. For uncoated bars, the increase in metal consumption in the last 2.5 years ranged from 212% to 335%. For coated bars, the increases were widely scattered, ranging from 127% to 33,363%. Lower performance ratios are obtained after two years of exposure than at one year. Nevertheless, there was not a dramatic decrease of performance ratios after 4.5 years from those obtained after 2 years. Performance ratio decreased in about half of the specimens in a period from 2 to 4.5 years, and increased in the others. Despite the huge increases of metal consumption in some cases, the improvement in performance of coated bars was still evident because of their very low initial corrosion compared to uncoated bars.

Metal loss reflects the reduction of bar diameter or bar cross section and can be a decisive parameter for determining the deterioration rate. However, this parameter fell short of indicating whether metal loss was concentrated or distributed. Concentration of metal loss is very important from the viewpoint of structural load-carrying capacity. It has been surmised that damaged coatings could concentrate corrosion in few spots thereby intensifying localized metal loss, whereas the loss would be distributed on uncoated steel. The estimated amounts of metal loss discussed above do not necessarily support this. In fact, visual observations revealed that the uncoated bars suffered more severe pitting corrosion than damaged coated bars! Explanations for this phenomenon are given below.

3.4 CONDITION OF REINFORCING STEEL

3.4.1 Apparent Surface Corrosion

Forensic examination of bar specimens, in general, confirmed the findings of the rate of corrosion analysis. All epoxy-coated bar specimens experienced less steel corrosion than control specimens. Figures 3.16 and 3.17 show close ups of surface corrosion of an uncoated bar and a damaged coated bar specimens, respectively. The figures illustrate severe surface degradation of the uncoated bar relative to superficial corrosion on the exposed steel of the coated bar.

Figure 3.16 Surface corrosion of uncoated bar after one year of exposure.

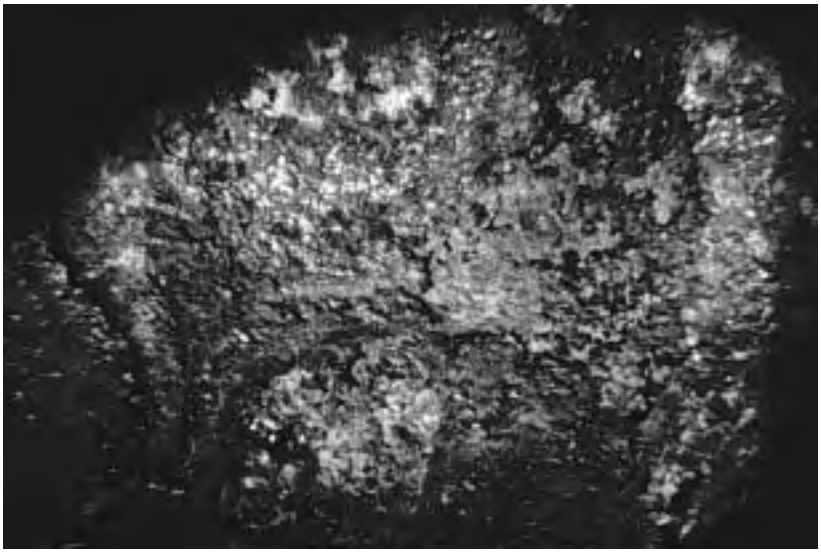

Figure 3.17 Surface corrosion of coated bar after one year of exposure.

Patched bars did not always perform better than damaged bars and corrosion did occur in patched bars. Larger bars corroded more extensively and severely than smaller bars. Most of the surface of several of the small bars remained in good metallic condition (although not completely free of corrosion) despite a very high chloride content and presence of coating damage. There was limited undercutting even though the coating was debonded around the bend. This observation agrees with some field studies which demonstrated that epoxy-coated bars extracted from deck slabs were also in excellent condition despite a chloride content between 2 and 7 kg/m^3 (3.3 and 11.7 lb./yd^3).[35] These results indicate that epoxy coating can provide full protection to reinforcing steel from chloride-induced corrosion. Nevertheless, certain conditions should be met regarding coating quality, level of damage, and quality of surrounding concrete.

Based on visible degradation of steel, the coated bar specimens can be ranked in an order of increasing degree of corrosion damage. That ranking can be compared to the order of increasing macrocell activity or amount of steel consumed, thus allowing an assessment of the corrosion monitoring techniques. For instance, Tables 3.4 and 3.5 include a ranking of small and large bars according to their observed surface condition after 4.5 years of exposure. Bars were rated from best to worst and were listed from top to bottom in that order. The rank number given by the column "visual examination" indicates the relative performance of that bar compared to the rest. For comparison, the rank number given by the column "charge flux" indicates the relative performance according to the measured charge flux.

Table 3.4 Relative performance of 13-mm bar specimens (series A) after 4.5 years of exposure. Assessment by visual examination and measured charge flux.

Group No.	Damage Category and Condition	Visual examination	Charge Flux
3	Spots > 6x6 mm, Exposed	1	3
7	Spots < 2%, Exposed	2	2
4	Spots > 2%, Patched	3	1
2	Spots > 6x6 mm, Patched	4	6
11*	Pinholes < 1%, Exposed	5	4
9*	Spots > 6x6 mm, Patched	6	5
6	Cracks < 1%, Exposed	7	8
10*	Spots > 6x6 mm, Exposed	8	7
5	Spots > 2%, Exposed	9	9
8*	Control (Uncoated bars)	10	11
1	Control (Uncoated bars)	11	10

1: Best 11: Worst
* Cross Ribs

Table 3.5 Relative performance of 25-mm bar specimens (series B) after 4.5 years of exposure. Assessment by visual examination and measured charge flux.

Group No.	Damage Category and Condition	Visual examination	Charge Flux
6	Cracks < 1%, Exposed	1	1
7	Spots < 2%, Exposed	2	3
3	Spots > 6x6 mm, Exposed	3	5
2	Spots > 6x6 mm, Patched	4	4
4	Spots > 2%, Patched	5	2
5	Spots > 2%, Exposed	6	6
1	Control (Uncoated bars)	7	7

1: Best 7: Worst

The test technique was effective in determining the magnitude and severity of corrosion of the embedded reinforcing bars. Although the correlation was not exact, there was good agreement in general between monitored currents and observed corrosion attack, with little difference in the rank order given to each specimen. There was a large discrepancy in the rank order of only one specimen, 3B.4 (damage > 2%, patched), where observed corrosion was worse than predicted by monitored currents. Another important discrepancy was that in large bars with damaged spots greater than 6x6 mm, monitored currents predicted less corrosion on the patched than on the non-repaired specimen. Visual examination revealed that although corrosion was more severe at damaged areas than at patched areas, corrosion spread much more on the metal surface beyond the patched area.

3.4.2 Coating Adhesion to Steel

There are indications that coating bond strength to steel is weakened by fabrication. Bending coated bars causes stretching of the coating at the rib bases (rib-bar intersections) on the outer surface of bend. The regions at the rib bases of the test bars seemed slightly discolored which indicated thinning of the coating and a tendency for debonding. A study has demonstrated that coating films are consistently thinner at deformation edges than in the areas between the deformations.[36] The difference in coating thickness averaged about 23 μm (0.9 mils) for straight bars, and about 55 μm (2.2 mils) for bent bars.

The initiation of corrosion activity in thin film regions is a consequence of holidays. This is a common observation in corrosion studies.[36] A thin film spot is a point of weakness where holiday formation is most likely to occur. The indicators to debonding are the micro-tears in the coating and the more noticeable cracking. Cracks in the coating on specimens from groups A.6 and B.6 were produced during fabrication. Even if the film remained unbroken, it probably allowed oxygen and water to cross the film. With debonding, the condition became worse; moisture and oxygen were retained beneath the coating and corrosion was more likely to initiate. Fabricated bars became more vulnerable and susceptible to corrosion at the bent zones. Figure 3.18 illustrates stretching and debonding in the rib base region on the outside of bend.

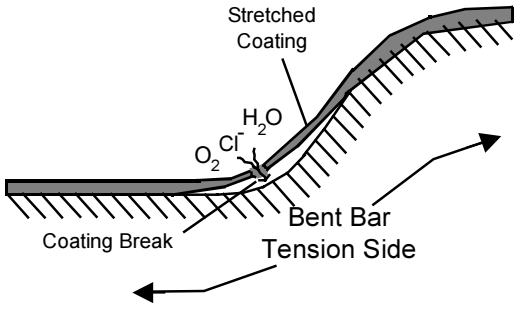

Figure 3.18 Coating thinning and debonding at rib/bar interface.

Damage on the inside of bend is usually neglected mainly because the region is compressed instead of stretched. However, coating debonding may still occur. Bending a coated bar generates high shear stresses at the steel/coating interface on both sides of the bend. The stresses may break the adhesion creating paths for oxygen and water migration to the debonded region. Figure 3.19 shows the microscopic ripples that form on a compressed coated surface. Localized compressive residual stresses at the metal surface have been recognized as a factor to initiate corrosion at the inside of bends.[37] Such a phenomenon explains why sheet steel often rusts first at bent edges.

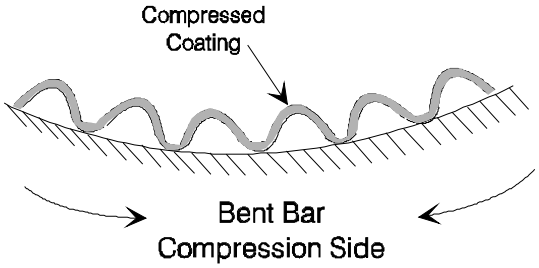

(a) Schematic drawing

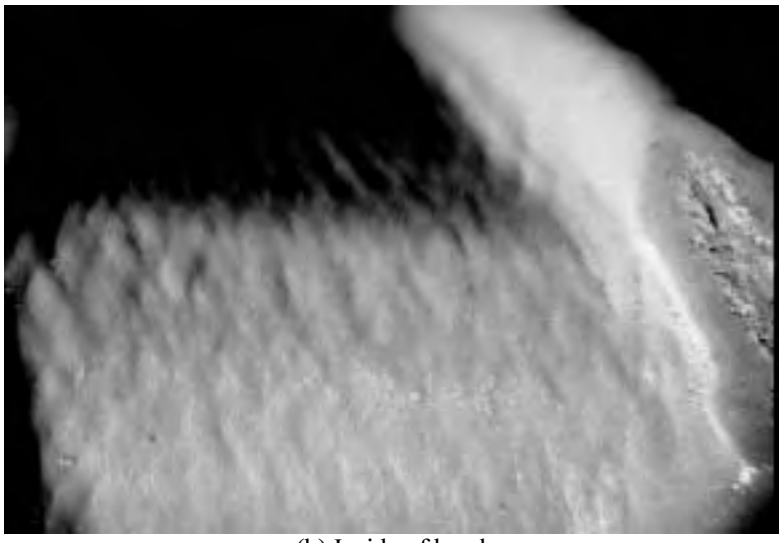

(b) Inside of bend

Figure 3.19 Compressed coating surface.

Exposure of the coated bars to the corrosive test environment seriously impaired coating adhesion to steel. The epoxy coating flaked away from exposed bars more readily than from similar unexposed bars. During the 4.5 years of cyclic exposure to salt solution, enough water permeated through the concrete and created a moist environment. This factor contributed to accelerate the loss of the already marginal adhesion at the bent zones. Loss of adhesion at the straight portions of many bars (all 25-mm bars and four 13-mm bars) confirmed this observation. Coating softening and debonding after exposure to a chloride-contaminated concrete was also reported by Clear,[8] and Sagüés *et al*.[38,39] Further,

coating debonding was observed by others in "perfect" condition bars that had passed the standard bend test.[40] It was suggested that an alteration to the epoxy/steel interface boundary occurs in the concrete environment. Another contributing factor to the observed adhesion loss may have been the possible occurrence of cathodic disbondment around damaged areas. Reference 41 refers to Romano's suggestion that "cathodic disbondment of epoxy coatings can occur adjacent to damaged areas because of the galvanic process occurring between the cathodic and anodic sites on the steel." Mechanisms of adhesion loss will be discussed in the following sections.

The straight portions of the embedded test bars initially had very strong coating adhesion relative to coating on the bent portions. These straight ends exhibited significant debonding after 2 and 4.5 years of exposure, compared to limited debonding after the first year. All 25-mm bars and four 13-mm bars suffered adhesion loss at the straight portions after 4.5 years of exposure. Underfilm corrosion on the debonded straight portions was negligible after 2 years but was substantial after 4.5 years, predominantly on large bars. It appeared that well-adhered, damage-free coatings delayed but did not prevent corrosion after prolonged periods of exposure. Nevertheless, defective areas with initially weakened adhesion (the bent portions) suffered more widespread and severe corrosion. Differences in initial adhesion and damage were a crucial factor in the relative performance between straight and bent portions.

Two possible mechanisms may have accounted for the loss of adhesion of the epoxy coating: Cathodic disbondment and adhesion loss by water action. These mechanisms are discussed in the following paragraphs.

CATHODIC DISBONDMENT

Any corrosion process requires the anodic and cathodic reactions. Active corrosion occurs at anodic areas while no corrosion takes place at cathodic areas. Anodic and cathodic areas usually coexist together on the same surface, with the cathode usually surrounding the anode. Cathodic disbondment has been reported to occur at areas with cathodic reaction.[42] It is possible then that portions of the bar with debonded coating and mottled surface underneath (as described in Section 2.6.6) may represent areas with cathodic activity. The debonded coating may have been the result of cathodic disbondment. The change of appearance to a mottled surface may have been the result of the alkalinity produced by cathodic reactions at the metallic surface. The steel surface was preserved in relatively good condition, as would be expected in a cathodic area.

The phenomenon of cathodic disbondment at a defect in a coating is illustrated in Figure 3.20.[4,43] Concrete porosity and voids, and coating defects allow access of deleterious substances to the substrate metal. The anodic reaction

$$Fe \rightarrow Fe^{2+} + 2e^{-} \qquad (8.1)$$

occurs at a coating defect that is coupled to the nearby cathode beneath the coating. Oxygen must migrate through the coating along with water in order to support the cathodic reaction

$$O_2 + 2H_2O + 4e^- \rightarrow 4OH^- \qquad (8.2)$$

This is possible because epoxy coatings are not impermeable to oxygen, water, nor ions.[43] Cathodically generated alkalinity can react with the organic polymer to disbond the coating at the interface between coating and metal at a defect, as shown in Figure 3.20. Such reaction is termed saponification. It has also been theorized that cathodic disbondment may proceed by an oxide dissolution mechanism rather than by alkaline degradation of the coating itself (based on the good stability of epoxy coatings in alkaline environments).[14] Cathodic disbondment may also occur at microscopic or smaller flaws in the coating to produce blisters, which do not require a physically obvious defect for initiation.[4]

The macrocells had a bottom layer with black bars which was intended to act as a cathode. Since the top and bottom layers were linked, any anodic reaction at the top bar would be supported by cathodic reactions at the bottom bars. However, the occurrence of cathodic disbondment at anodic bars would mean that cathodic and anodic reactions also occurred on the same bar surface. It may be possible that at low levels of corrosion activity, cathodic reactions at the bottom bars could not be well established and the initial cathodic reactions would take place on the same top bar. As undercutting progressed at the top bar, the bottom bars would eventually take over to support the necessary cathodic reactions. Schieβl states that the corrosion initiation process is not affected by electrically coupling uncoated bars to coated bars, and that coupling to uncoated bars may only slightly accelerate cathodic disbondment in the initiation stage and increases the corrosion of the exposed areas. The bottom uncoated bars play a greater roll at an advanced stage of deterioration of the coating, accelerating the corrosion rate.[43]

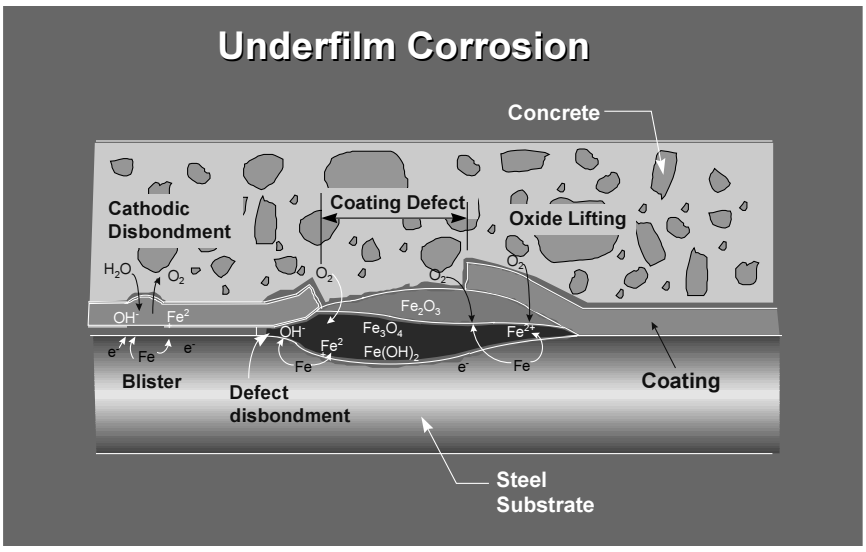

Figure 3.20 Process of cathodic disbondment and oxide lifting in coatings.

DISBONDMENT BY WATER

During the 4.5 years of cyclic exposure to salt solution, enough water permeated through the concrete and created a moist environment. It has been theorized and observed that coatings lose adhesion when subject to moist environments.[14,42,44] The coating is displaced from the substrate by a thin layer of water. The mechanism under which this phenomenon occurs is still unclear. Some of the theories are discussed in Research Report 1265-6.[45] The principle of wet adhesion loss was used for the hot water tests discussed in that report. It should be emphasized that the condition of the steel surface of samples immersed in hot water was generally bright, preserving its original appearance. This appearance was different from the mottled surfaces in bars from macrocells, indicating that "something" happened at the steel surface. Of course, the exposure conditions of the two experiments were drastically different.

3.4.3 Undercutting

Although large parts of the coating seemed unaffected when visually examined, the subsurface conditions indicated corrosion activity at various stages. Corrosion which may have started at defects and exposed metal areas spread beneath the epoxy coating. Underfilm corrosion, or undercutting, progressed with time. For some coated bar specimens, after the first year of testing, undercutting was confined to the vicinity of exposed steel areas, and coating defects and breaks documented before testing. The majority of bars inspected after two years showed either widespread underfilm corrosion or localized corrosion around pinholes not detected prior to exposure. Most bars experienced widespread corrosion activity beneath the coating after 4.5 years. In contrast, undercutting for companion specimens after 1 and 2 years was less extensive.

Underfilm corrosion (further from exposed steel areas) was, generally, in the form of light surface rusting with no significant loss in bar section. Coating protected the steel surface from direct attack by chloride ions. Similar observations were reported by Sagüés, Powers, and Zayed,[2,3,14] Mckenzie,[34] Sohanghpurwala and Clear,[41] and Kobayashi and Takewaka.[30] It has been suggested that corrosion results in the formation of flat cavities under the coating where there is little oxygen and therefore the corrosion process is slow.[46]

The corrosion morphology of steel substrate was in many aspects similar to that described by Zayed and Sagüés, in a corrosion study of epoxy-coated bars. The bars with cross deformations showed corrosion spots at holidays at the crossing of deformations. Corrosion spread on both the inside and outside bent portions. The coating could be easily peeled around the bend with a sharp blade. The corrosion products building up on the exposed steel were dark red-brown; however, the metal under the coating was covered with a greenish-black product. Away from the corroded spots, the metal was usually bright.

Undercutting occurred in the following forms: a) A change of appearance of the steel surface to a mottled, glittering golden-brown with no significant attack, such as pitting or loss of metal

[Figure 3.21(a)], and b) uniform black or dark surface rusting with random reddish-brown (or other tones of brown) rust spots and some degree of attack at several portions, such as slight pitting, rust buildup, and loss of metal [Figure 3.21(b)].

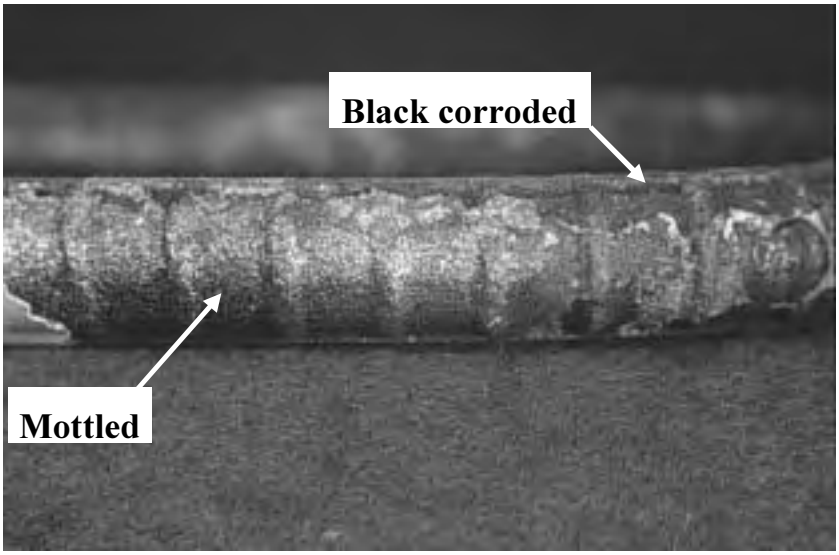

(a) Mottled, glittering golden-brown steel surface under the coating.

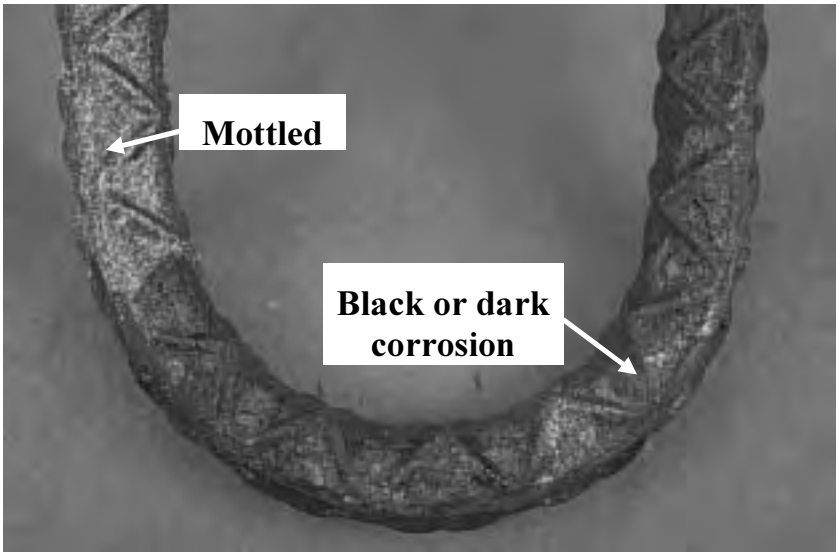

(b) Black or dark corroded surface.

Figure 3.21 Forms of undercutting of epoxy-coated bars.

At portions of bars where coating adhesion was preserved (straight portions close to front face of specimens), the steel surface maintained its originally shiny, bright aspect. Bars with little corrosion activity (small bars) showed large portions with debonded coating and a mottled, glittering golden-brown

surface underneath with very little, almost negligible corrosion attack. Bars with the greatest corrosion (large bars) showed large portions with debonded coating an a uniformly black or dark rusted surface. Clearly, portions of the bar with adhered coating and unchanged appearance of the steel surface underneath represented areas of no corrosion. Portions of the bar with debonded coating and uniformly black or dark rusted surface underneath represented areas of corrosion. Portions of the bar with debonded coating and unattacked, mottled surface underneath were though to undergo cathodic disbondment, as was explained in the previous section.

Epoxy coating looked more distressed and much thinner at more heavily corroded areas than at areas with little or no corrosion, and corrosion products adhered well to the backside of the coating. For this reason, the coating was slightly more difficult to peel with a knife at the more corroded areas. The blade usually cut through the rust layer instead of the metal/coating interface and the coating tore or broke in large and small pieces during the peeling operation. In contrast, coating integrity was maintained at uncorroded, debonded areas and could be lifted as a unit, without tearing, during peeling.

Two possible mechanisms of underfilm corrosion may have taken place: Crevice corrosion and oxide lifting. These mechanism are discussed in the following paragraphs.

CREVICE CORROSION[4,10]

Corrosion initiated at either exposed areas or coating defects. Corrosion spread at the small crevices under the coating at the edges of exposed areas or discontinuities. Coating at adjacent areas started to lose adhesion by means of cathodic disbondment or water action (or perhaps a combination of both). Adjacent debonded coating formed very thin crevices and corrosion propagated under the coating in a mechanism similar to that of crevice corrosion. Dissolved oxygen was depleted by corrosion in the small volume of the crevice by the reduction reaction (8.2), impairing passivity and increasing the concentration of metal cations by the oxidation reaction (8.1), which attracted negatively charged chloride ions Cl^- from the bulk solution (hydroxide ions also migrated from adjacent areas, but they are less mobile than chloride and migrated more slowly). This resulted in an increased concentration of metal chloride within the coating crevice. The metal chloride hydrolyzes in water by

$$Fe^{2+} + 2H_2O + 2Cl^- \rightarrow Fe(OH)_2 + 2HCl \qquad (8.3)$$

where the aqueous solution of the metal chloride dissociated into an insoluble hydroxide and a free acid.

For reasons not yet understood, both chloride and hydrogen ions accelerate the dissolution rates [equation(8.1)] of most metals and alloys. Underfilm corrosion grew autocatalytically as more chloride was attracted to the coating crevice, promoting further hydrolysis and consequent acidity. As the corrosion within the crevice increased, the rate of oxygen reduction on adjacent surfaces also increases.

This created a localized anode coupled to a cathode of larger area on the surrounding surfaces. Such surfaces are obviously cathodically protected but experienced further cathodic disbondment, which creates additional crevices under the coating and allows corrosion to progress under the film.

The presence of an acidic, clear brown solution at the interface between the substrate and the coating in the most corroded bars was evidenced by the observed solution spillage at the front face of specimens at the protruding bar ends and by the observed drops of solution at the bar surfaces during post-mortem examination. This solution was also observed in specimens examined after two years of exposure, and by other investigators, and has been described as acid moisture accumulation or "local acidification."[2,3,14] Chemical analysis of small samples collected revealed the presence of hydrochloric acid HCl in the solution. HCl, which was produced by hydrolysis of the chloride solution [equation (8.3)] as explained above, is a strong acid that accounts for the low pH measured (between 3 and 4).[4] The fluid acid has been observed to contain 3 to 10 times as much chloride as the bulk solution. Many of the observed corrosion products had the appearance of stains, seeming to indicate that the chloride solution may have partially dissolved and transported some of those products.

OXIDE LIFTING

Oxide lifting occurs when anodic corrosion products accumulate under the coating, as illustrated in Figure 3.20.[4] The lifting action of compacted oxides and resultant undercutting occurs during alternate wet and dry cycles. Flocculent oxide corrosion products in water are compacted by drying. Corrosion products form an inner layer of dissolved ferrous ions, Fe^{2+} and precipitated $Fe(OH)_2$, which partially oxidizes to form magnetite, Fe_3O_4, a black product. An outer hydrated layer of fully oxidized FeOOH completes the deposits of corrosion products. The cathodic reaction during anodic lifting again may be represented by equation (8.2) at the metal surface in the defect or possibly

$$8FeOOH + Fe^{2+} + 2e^{-} \rightarrow 3Fe_3O_4 + 4H_2O \qquad (8.4)$$

at the outer magnetite interface. Magnetite is sufficiently conductive to act as an electrode for cathodic reaction and Fe_3O_4 is reoxidized to FeOOH by dissolved oxygen. In general, oxide lifting involves electrochemical corrosion in the condensed aqueous phase during wet cycles. Colloidal corrosion products deposit during subsequent dry periods and cannot be easily redissolved or dispersed on rewetting. This results in a buildup of compact corrosion products in constricted crevices or at the interface between coating and metal, lifting or debonding the coating from the substrate.[4]

3.4.4 Corrosion Products

MAGNETITE

Corrosion spreading underneath the epoxy coating, as noted above, was characterized by the formation of a thin black (greenish-black) corrosion layer. Dark-greenish or greenish-black products were visible at several spots in the concrete surrounding the bars. The black corrosion product has been identified by others as magnetite Fe_3O_4.[31,32] Swamy *et al.*,[33] Treadaway and Davis,[32] Rasheeduzzafar *et al.*,[26] Clear and Virmani,[25] and Erdo_du and Bremner[31] made the same observation.

The black magnetite is converted to a green hydrated magnetite ($Fe_3O_4 \bullet H_2O$).[44] The black product is indicative of corrosion in a restricted oxygen environment of crevices that form under the coating. Such a corrosion product is in a low state of oxidation generated from ferrous ions Fe^{+2} present in $Fe(OH)_2$ or $FeCl_2$ or $FeCl_2.H_2O$.[26,32] Upon exposure to open air, the complex ferrous chloride ion converts instantly to a black granular product Fe_3O_4. The role of magnetite in supporting cathodic reactions during undercutting and oxide lifting was already explained. Further oxidation to ferric ions Fe^{+3} after some time of exposure to air produces the more usual and stable red-brown corrosion product Fe_2O_3.

Because of its low state of oxidation, the ratio of the volume of black corrosion product to the volume of the parent iron is small compared to that of developed red rust. The volume of rust product Fe_3O_4 is about twice as much as the original steel as shown in Figure 3.22. In saturated concrete, the increase in rust volume is only 20–50%.[47] In comparison, the reddish rust $Fe(OH)_3.3H_2O$ has a volume 6–7 times greater than the original steel. When concrete is very wet, the volume increase of black corrosion product may either reside under the coating or diffuse through the pore network of concrete. Consequently, less internal pressure is exerted on concrete in the case of the black product than higher iron oxidation products.

It follows that the corroded epoxy-coated bars produced smaller amounts of corrosion products than uncoated bars (which agrees with visual observations made on opened concrete specimens). The associated volume increase with the black product was not substantial and was insufficient to develop high enough stresses in concrete to cause cracking at early stages. This explains why some of the coated bar specimens reached higher levels of steel consumption than those associated with control bar cracking and yet did not crack. Another supplementary explanation for this phenomenon is related to the configuration of the corrosion system and is given in Section 3.7.1.

It is suspected that the formation of the greenish-black corrosion product was a result of two factors, the restricted oxygen diffusion to anodic sites and the possible high corrosion rate. Oxygen diffusion to the anodic sites (developed in the crevices underneath the coating) was limited by the coating barrier. Therefore, more ferrous ions were produced than could be oxidized to ferric ions. As a result, the

corrosion products remained in the lower state of oxidation. This was especially true for bars inspected after one and two years of exposure. Bars inspected after 4.5 years contained additional products with varying degrees of oxidation.

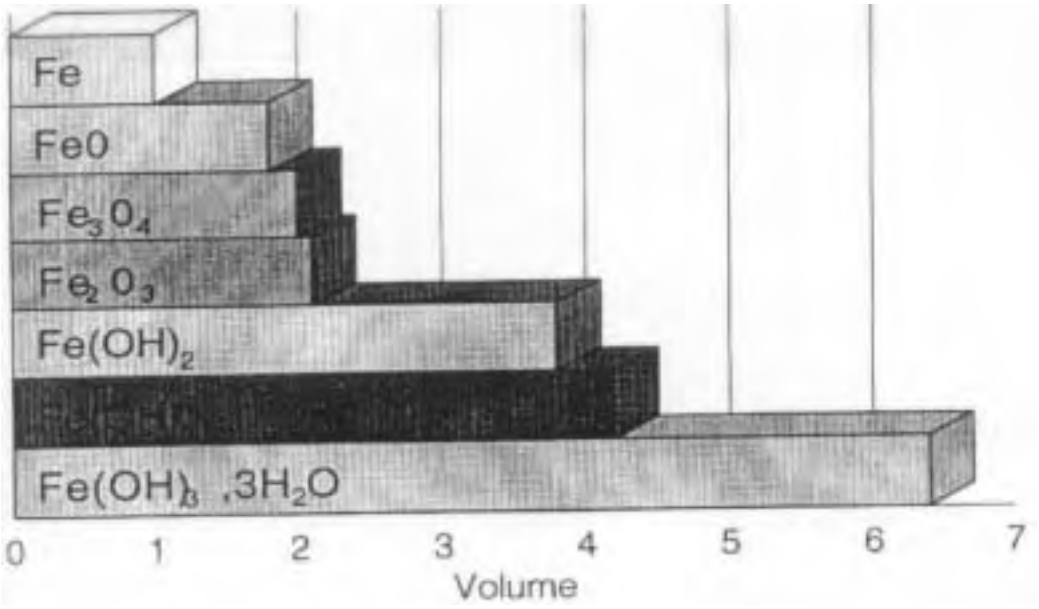

Figure 3.22 Volume ratio of corrosion products.[47]

FERROUS HYDROXIDE

Another common product found during autopsy consisted of spots with a pasty, whitish matter deposited at several portions of bar surfaces. Usually, the whitish matter turned yellowish-brown, dull-brown, and orange-brown. The white pasty deposits have been identified in the literature as ferrous hydroxide $Fe(OH)_2$, which converts to magnetite.[44] These deposits were seen in specimens examined after 2 and 4.5 years of exposure. In several cases, the whitish matter (usually combined with light-brown or yellowish-brown corrosion products) was deposited along a strip, giving the appearance of a solution trace. In other cases, whitish spots consisted of thinner films occupying large areas, having the appearance of a stain, perhaps remains of a solution. It would seem that such products traveled in a liquid solution through the bar-coating interface in an undercutting action.

OTHER PRODUCTS

Other corrosion products were deposited at random spots over the black corroded surface on specimens examined after 4.5 years. Such products had varied colors; reddish-brown, light-brown, yellowish-brown, and orange-brown. These corrosion products have a higher state of oxidation than darker corrosion products. Oxidation of rust products require availability of oxygen, which was supposed to be limited beneath the coating. Two explanations are possible:

a) As undercutting progressed, the coating was debonded by deposition of rust products beneath the coating (oxide lifting). In addition to disbonding the coating, the buildup of rust may have eventually distressed the coating, resulting in pinholes, cracks, or thinning of the coating. Examination of bars after autopsy revealed that the coating at the most corroded areas was thinner than at less corroded portions. Some cracks in the coating were also observed at the most corroded areas. As more discontinuities developed in the coating, larger quantities of dissolved oxygen became available at the substrate, oxidizing portions of the black magnetite.

b) Coating on the bars was not immediately peeled after removal from the concrete, but about 24 hours later. Although the coating was not altered after bar retrieval from the concrete, the thinner coating was possibly more permeable to air and the bars may have been exposed to larger quantities of oxygen as compared to a more restricted oxygen environment inside the concrete. It is questionable how much oxygen could reach the substrate in a very short time.

A combination of cases (a) and (b) would seem more feasible. In any case, the presence of corrosion products with higher state of oxidation revealed a more advanced corrosion stage as compared to specimens examined after one and two years, where such products were not found.

3.4.5 Coating Blistering

Blisters are local regions where the coating has lost adhesion from the substrate and where water may accumulate and corrosion may begin. Most blisters may be formed by osmotic pressures from chloride solution. As water penetrates the coating to the interface, a concentrated solution is developed with sufficient osmotic force to drive water from the coating surface to the interface and a blister is formed.[42] A blister furnishes all the necessary elements for electrochemical corrosion: It provides a location for water accumulation, oxygen penetrates through the coating, and ionic materials leach from the interface or from the coating. The rate of corrosion appears to be controlled by the oxygen permeability of the coating.[42] The cathodic region is at the periphery of the blister and the anodic region is in the center of the blister where the oxygen concentration is low.[42]

In bars examined after 2 years, blisters spread on the coating surface and indicated pitting corrosion. The pits were generally very slight (shallow depth) covered with black and brown brittle corrosion products. Figure 3.23 shows a blister under microscopic examination. At some locations, the buildup of corrosion products breached the epoxy film. At other locations, the blisters were soft and full of liquid. Blisters had varying sizes and small blisters (up to 5 mm) were more abundant than large blisters (greater than 5 mm). A concrete void was always present adjacent to a blister in the coating (Figure 3.24). Concrete voids provided an ideal environment for the formation of blisters, because chlorides, water and oxygen could

be stored in those voids. Consequently, corrosion was particularly intense at bar locations facing concrete voids where corrosion products accumulated and increased in volume under the coating, eventually bulging or blistering the coating. The greater quantity of concrete voids at the lower half of the bar surfaces explains the prevalence of more blisters at those regions.

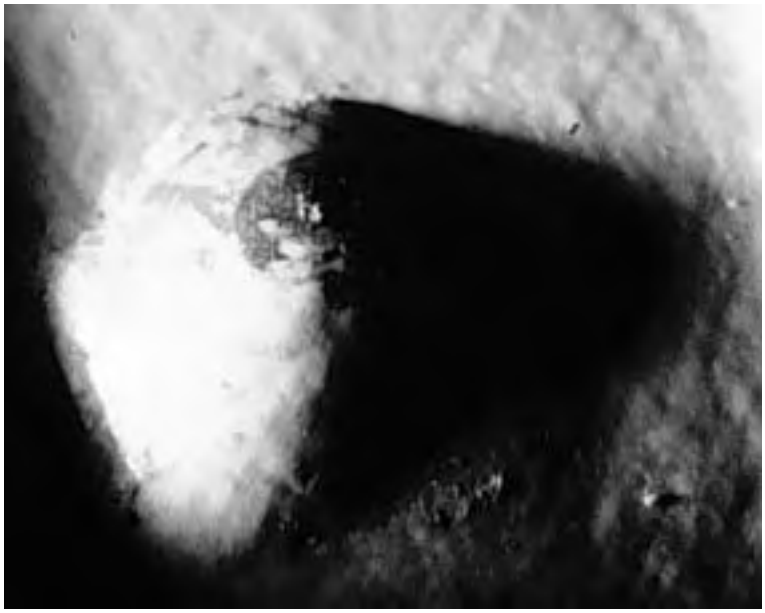

(a) Blister on Coating Surface

(b) Corrosion product buildup in blister

(c) Pitting Inside Blister

Figure 3.23 Blister under microscopic examination.

Figure 3.24 Blisters always formed adjacent to concrete voids.

Blisters were formed because of the increase in volume of the corrosion products in the vicinity of coating defects. Sohanghpurwala and Clear,[41] and Treadaway and Davie[32] reported similar observations. Pfeifer *et al.*[36] also observed blistering and cracking of the coating over a corroded bar which exhibited a high macrocell corrosion current during their experiment. Clear noticed rust stains exiting from the edges where the bars protruded from concrete similar to the swelling spots observed in this study.

After 1 and 2 years of exposure, a clear or pasty (whitish) liquid was frequently found trapped under freshly chipped epoxy coating and inside blisters. The surrounding concrete was relatively dry indicating the ability of the coated bar to retain the solution between the epoxy film and steel surface. This solution was also observed by other researchers such as Sagüés[2,3,14,39] who described it as acid moisture accumulation or "local acidification". He also noticed that blisters formed at locations facing air voids in concrete. Treadaway and Davies[32] indicated that the green product was always found in concrete with high chloride concentration and in association with very localized regions of lower pH (*i.e.* acid solution).

Unlike blisters observed after one and two years, most blistered areas had a very hard, solid consistency after 4.5 years of exposure. Several of the blisters observed after two years were soft and full of liquid and others were filled with black and brown brittle corrosion products.[23] Many blisters were associated with pitting. It may be possible that at very prolonged periods of exposure, the initially dissolved and brittle products solidified and hardened. As more corrosion products built up in the blister during wet periods, corrosion products were compacted during dry periods. As previously noted, examination of bar surfaces was conducted at least 24 hours after bars were retrieved from the concrete, and blisters may

have dried during that period. However, 24 hours may not be long enough to turn a soft, brittle blister into such a hard solid mound.

3.5 CONCRETE CONSOLIDATION AROUND REINFORCING BARS

3.5.1 General

The effects of concrete placement and consolidation on corrosion performance of embedded steel has not been strongly emphasized in literature. In this study, it was found that the condition of the concrete region surrounding the coated bars played a significant role in the corrosion process. The following discussion will expose the factors that had profound effects on corrosion initiation and coating degradation observed in the macrocell test.

3.5.2 Differences in Concrete Consolidation

During concrete consolidation and setting, water migrates towards the top concrete surface. Some of the bleed water is trapped under the horizontal epoxy-coated bars. As fresh concrete settles, small gaps are formed under the coated bar. Gap formation is enhanced by lack of interlock and cohesion between cement mortar and coated bar surface. Free water may then accumulate in that zone underlying the bar. When water eventually evaporates, it leaves voids or air pockets adjacent to bar surface. These voids will not be filled during hydration similar to the voids forming around the aggregates due to bleeding and inefficient packing of the cement mortar. As a result, a weak porous zone, with possible interconnected cavities, forms underneath the bar. This zone is characterized by a dull, light gray appearance as shown in Figure 3.25.

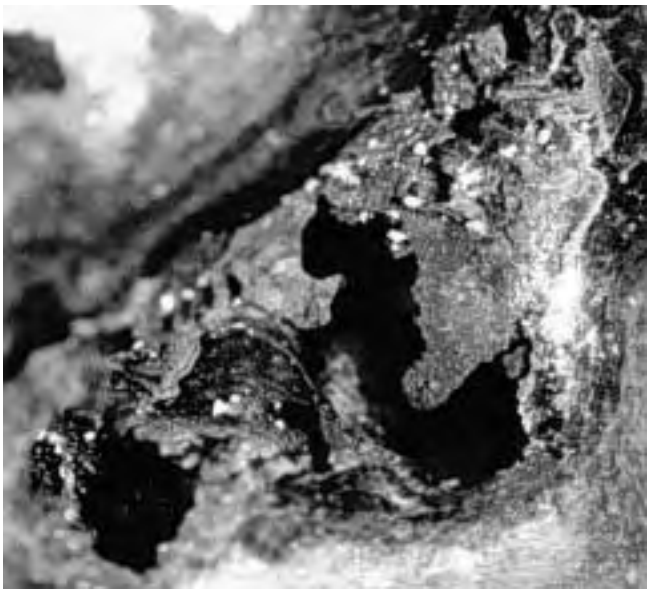

Figure 3.25 Concrete below coated bar.

Based on observations from the opened macrocell specimens, initial efforts were made in this study to investigate the possibility of gap formation beneath the coated bars. One concrete prism of similar dimensions to the macrocell specimens was cast with an individual coated bent bar typical of those bars used in series B. Concrete was vibrated as in a normal casting procedure. The prism was sawcut after few days in a plane perpendicular to the bar axis. The condition of concrete above and below the bar was microscopically inspected. Although concrete was compacted well above the bar, a gap was found underneath the bar. A view of the gap is shown in Figure 3.26.

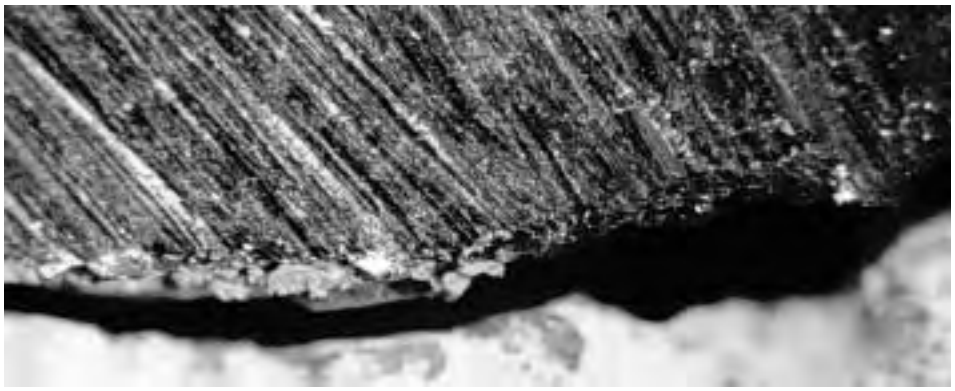

Figure 3.26 Gap formation below coated bar.

The zone under the bar may trap relatively large amounts of harmful substances very close to the bar surface. Moisture, oxygen, and chlorides are the specific agents necessary for corrosion. With time, these agents penetrate to the metal surface mainly through damaged spots, coating defects, and holidays. Salt solution may also accumulate under the bar and beneath the coating bridging between concrete and the corroded sites. Corrosion commences and progresses causing widespread undercutting.

In contrast, concrete resting on top of the coated bar will be more dense and closely-packed than that below the bar. Concrete consolidates as it builds up on top of the bar. The smoothness of the coated surface facilitates displacement of concrete to the sides of the bar. With vibration, more cement paste concentrates at the bar/concrete interface. As a result, the condensed fine mortar on top of the bar will generally have a smooth and continuous interface layer. This layer appears glossy and relatively dark gray when cover is removed as shown in Figure 3.27.

Figure 3.27 Concrete above coated bar.

3.5.3 Influence of Concrete Consolidation on Corrosion

MAIN FACTORS

The differences in concrete environment above and below the coated bar are expected to influence the corrosion performance negatively. First, any steel exposed (at holidays or damaged areas) facing the gaps may be more prone to corrode upon exposure to salt than steel covered by alkaline concrete. Second, differences in the concrete surrounding the bar (the electrolyte), even if slight, may promote concentration cell development. Variations in concrete above and below the bar, related to moisture distribution, oxygen supply, and chloride concentration, are most likely to occur. Therefore, steel areas exposed on the top and bottom of the bar have a potential for macrocell activity.

Chloride ions, for example, have restricted movement in dense mortars.[48] This suggests that the amount of chloride in the zone immediately above the bar may be limited. However, the porous zone below the bar, as stated earlier, can retain deleterious materials such as chlorides. Fraczek[49] also indicated that high localized concentrations of chlorides occur primarily in voids in concrete that are in direct contact with steel. Hence, there is probably less chloride concentration at the top side of bar than at the bottom, even though chlorides are penetrating from the top concrete surface!

There is evidence that corrosion activity takes place in voids in concrete facing embedded steel. Escalante and Ito[16] illustrated the process as it might occur adjacent to a steel surface in concrete. They showed that moisture saturated concrete will have solution-filled voids containing low concentrations of

chlorides and oxygen. However, as the concrete dries, salts concentrate and precipitate on the walls of the voids as shown in Figure 3.28. Oxygen diffuses into the concrete and concentrates in these voids. Thus, both wetting and drying, and concentration of chlorides and oxygen in voids, promote corrosion. In addition, concrete voids facing bar surfaces provide a physical space for the buildup and expansion of corrosion products, facilitating the formation of blisters. Figure 3.29 shows corrosion products found in voids in contact with exposed steel on a coated bar specimen.

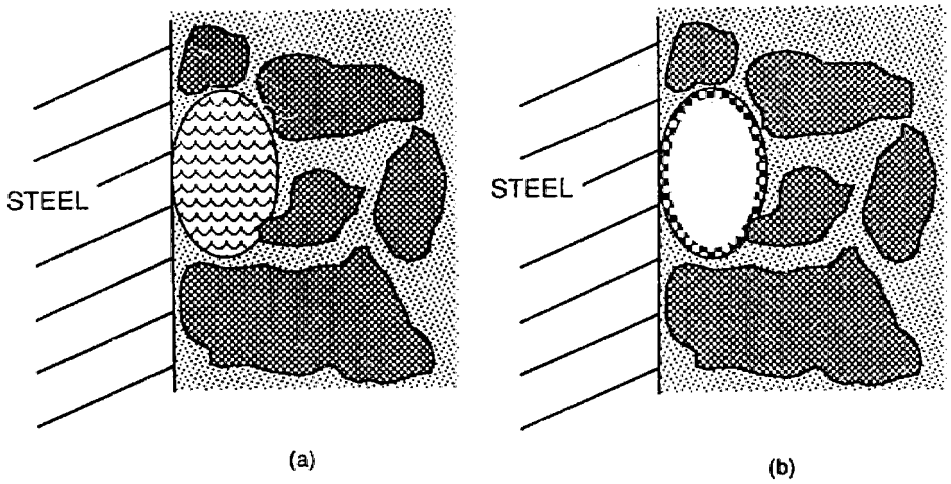

(a) Void adjacent to steel containing a solution of low concentration of salts and oxygen;

(b) concentration of salts on walls of void during drying cycle.

Figure 3.28 Voids promoting steel corrosion in concrete.

Figure 3.29 Corrosion products found in voids at coated bar surface.

Based on the concept of corrosion protection by a steel passivation film, steel will not be passivated at the spot where a void exists. Hime and Erlin[50] illustrated the formation of the oxide film over a steel surface fully embedded in a high pH concrete as shown in Figure 3.30. In their illustration, a void at the steel surface which interrupted the formation of the oxide film is shown. Hence, discontinuity of the protective layer is attributed to the void formation. Hime[27] also suggested that a possible cause of localized corrosion on a steel bar in concrete is an attached air bubble that does not allow penetration of the alkaline paste.

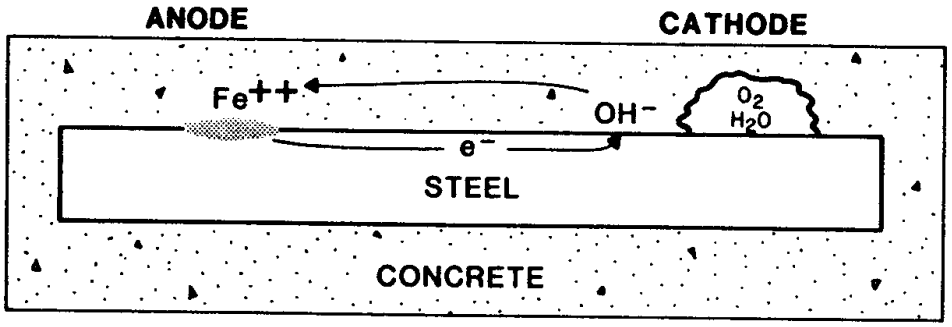

Figure 3.30 Steel depassivation at void formation in concrete.[50]

The discussion above agrees fully with the observations of autopsied bar specimens presented in Sections 2.4.4, 2.4.6, and 2.4.7, and the discussion in Section 3.4.1. Corrosion was worse on the lower half of the coated bars than on the upper half. Concrete surfaces below the bars had more extensive rust staining and greater amounts of corrosion products than concrete surfaces above the bars (previous Figure 2.50). Blisters formed in voids in contact with the bar surface, particularly at the bottom side. A trapped solution was detected beneath the coating with different precipitates along the bottom surface of the bar. More voids existed at the bar/concrete interface below the bar than above it. Laitence and some whitish deposits were observed underneath the coated bars. The presence of laitence along the bottom bar trace in concrete was very probably the result of chemical reactions between the concrete and the acidic solution.

In addition, photographs of the exposed steel areas on bar specimens retrieved after one year of testing were re-examined. The purpose was to confirm that corrosion initiated generally at the edges of the open areas, *i.e.* around the perimeter of the cut in coating (as shown in the example in Figure 3.31). It is possible that while casting concrete, the cement paste filled these open areas but bridged over the sharply cut edges. If so, both the gaps that were formed and the crevice effect at the coating edges encourage corrosion initiation as shown in Figure 3.32.

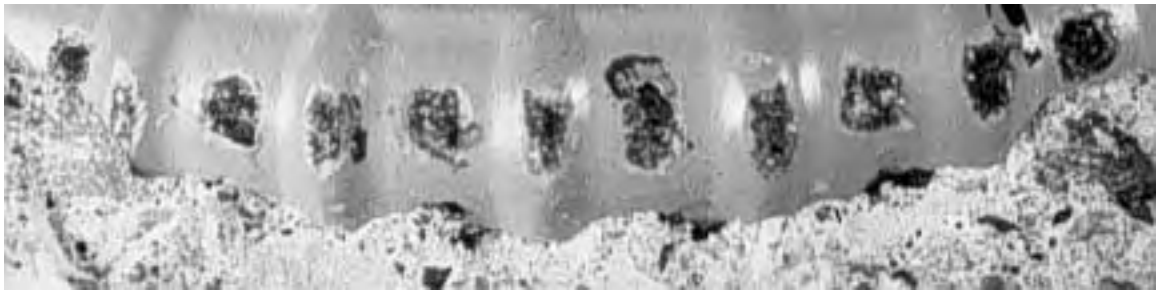

Figure 3.31 Corrosion initiation around exposed steel areas on damaged coated bars embedded in concrete.

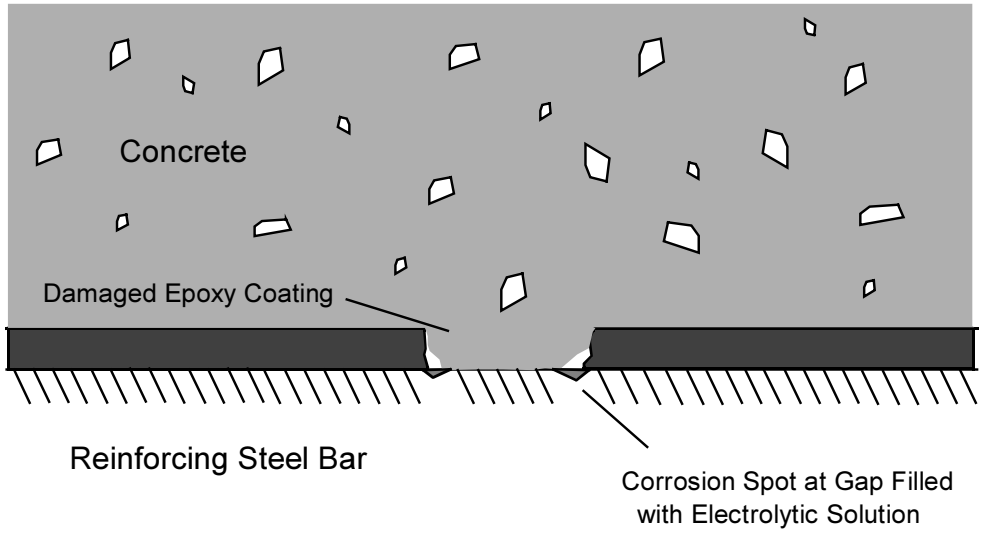

Figure 3.32 Schematic diagram of corrosion initiation around exposed steel areas on damaged coated bars embedded in concrete.

The discussion above may also explain why pitting corrosion was observed primarily on large damaged spots. The larger the damaged area of coating, the more it is exposed to the electrolyte. Then, chances are higher for chloride solution to accumulate excessively in the pores or voids in contact with steel. As soon as an anodic potential develops, corrosion starts and accelerates under the catalytic action of chlorides. Hence, the size of the defect or damaged area is a physical constraint that governs the severity of chloride attack. Both the frequency and size of the damaged areas need to be controlled to reduce probability of corrosion.

PARTICULAR CASES

The influence of the concrete environment may help to explain why corrosion did not occur at the large exposed areas of bars 3A.3 (13-mm bar, parallel ribs, damage > 6x6 mm) and 3A.7 (13-mm bar, parallel ribs, damage < 2%) after 4.5 years of exposure. As was already shown, the steel surface at such damaged spots preserved its original shiny and bright condition, without the slightest evidence of corrosion. The neighboring steel surface beneath the coating presented a mottled, glittery appearance with no evidence of corrosion attack or metal loss. Chloride content in the concrete at the level of the bars was 0.29% and

0.26% by weight of concrete for specimens 3A.3 and 3A.7, respectively. Although these values were below the average content of 0.34% by weight of concrete for all small bar specimens, they were still high enough to promote corrosion.

Concrete adjacent to damaged locations was examined and no evidence of concrete voids was found and the concrete was well consolidated. Apparently, dense concrete in close contact with the exposed areas effectively prevented the accumulation of chloride ions in great concentrations and severely restricted the access of water and oxygen, all necessary agents for corrosion initiation. In addition, the alkalinity of the cement paste maintained the protective oxide layer stable.

Observed corrosion in both bars occurred at zones away from exposed areas. In bar 3A.3, corrosion occurred at the outer side of the right bar leg close to the front face of the specimen. Coating was damaged at that location during fabrication (that spot was a point of restraint during bend fabrication). In specimen 3A.7, corrosion was observed at the lower portion of the inner bend. Coating was damaged at the transverse ribs during fabrication. In both cases, voids and porosity in the concrete were visible next to the corroded sites. Therefore, corrosion started at spots or sites that offered the most favorable conditions for corrosion initiation. In addition, the exposed areas at the outer bends may have been cathodically protected during the corrosion process. As previously discussed, mottled surfaces beneath debonded coating were very probably cathodic areas.

3.6 INFLUENCE OF INITIAL CONCRETE CRACKING ON CORROSION

3.6.1 General

Cracks which follow the line of reinforcing bar, for example plastic shrinkage cracks and plastic settlement cracks, are very damaging in a corrosive environment.[6] These cracks are frequently wide, and allow corrosion to spread appreciably along the bar. They also reduce concrete resistance to spalling. The relation between these types of cracks and the susceptibility of epoxy-coated bars to corrosion need to be examined.

3.6.2 Crack Formation and Consequences

Excessive amounts of deep cracking have been observed on bridge decks constructed with epoxy-coated bars.[46] The cracks were developed during the early stages of curing. This may indicate a serious problem involving plastic settlement cracks. In addition, research conducted on bond characteristics of coated bars in beams indicated that flexural cracking occurred at every section containing a coated stirrup.[51] In effect, the coated transverse reinforcement, tie or stirrup, tends to act as a crack inducer. Additionally, the crack widths were larger than those associated with uncoated bars.

In the macrocell study, relatively wide plastic settlement cracks were observed on the top concrete surfaces of some specimens (see Appendix A). The width of the cracks varied considerably but were as large as 0.4 mm (0.015 in.). This observation and the preceding ones above suggest that coated bars are more prone to develop wide plastic settlement cracks and flexural cracks in the same planes of the bars. This tendency has a negative influence on the corrosion performance of coated bars. For instance, the plastic settlement cracks that were observed on the top concrete surfaces of three specimens propagated after about 2.5 years of exposure. In addition to facilitating the ingress of chlorides, pre-existent cracks became weak links through which corrosion-induced deterioration further propagated. When plastic settlement cracks are present, chloride contamination is virtually instantaneous. Cady and Weyer[52] predicted that, due to plastic settlement cracking, a bridge deck with 25 mm (1 in.) average cover will be critically contaminated with chloride over more than 50% of the deck from the very first season of deicer application. Excessive levels of chloride contamination at bar surface can be reached within a very short time of service.

3.6.3 Crack Development

In addition to the three specimens where plastic settlement cracks propagated, seven other specimens experienced cracking at different times of exposure, generally during the last 2.5 years of exposure. In total, eight specimens with larger bars and two specimens with smaller bars experienced cracking. Most cracks had a "U" shape following the line of the reinforcement and were located almost directly above the top bar. Crack widths were in the range of 0.08 mm to 0.20 mm. In comparison, none of the specimens examined after one and two years developed cracks during the course of the exposure, and in a few specimens, only the initial cracks due to plastic settlement with no further growth were observed.

Coated bars inside cracked specimens were among the most corroded. The only notable exception was specimen 1A.5, which suffered the worst corrosion among the specimens with small bars and yet did not experience concrete cracking. The good correlation between cracked concrete and corrosion damage seemed to indicate that cracks were caused by corrosion. Corrosion was more extensive in coated bars after 4.5 years than after 2 years. Most cracks were very narrow or hairline (about 0.08 mm wide) and no rust deposits or stains were observed inside the cracks. Corrosion-induced cracking in coated bar specimens was in an incipient stage at the end of 4.5 years of exposure. It would be expected that with longer periods of exposure, those cracks will allow a faster penetration of chlorides, water, and oxygen to the bar surface, further propagating the corrosion process.

3.7 ASPECTS OF CORROSION OF EPOXY-COATED BARS

3.7.1 Conceptual Behavior

From the preceding sections, it seems that many unfavorable conditions may combine where epoxy-coated bars are used. Wide plastic settlement cracks may form, there may be frequent gaps beneath the bar, adhesion to concrete may be lacking and, as a result, there is instantaneous contamination by intruding chlorides. From the standpoint of preparing for the worst case, epoxy-coated steel used as top reinforcement in slabs, may develop the conditions depicted in Figure 3.33 (with exaggeration for clarity).

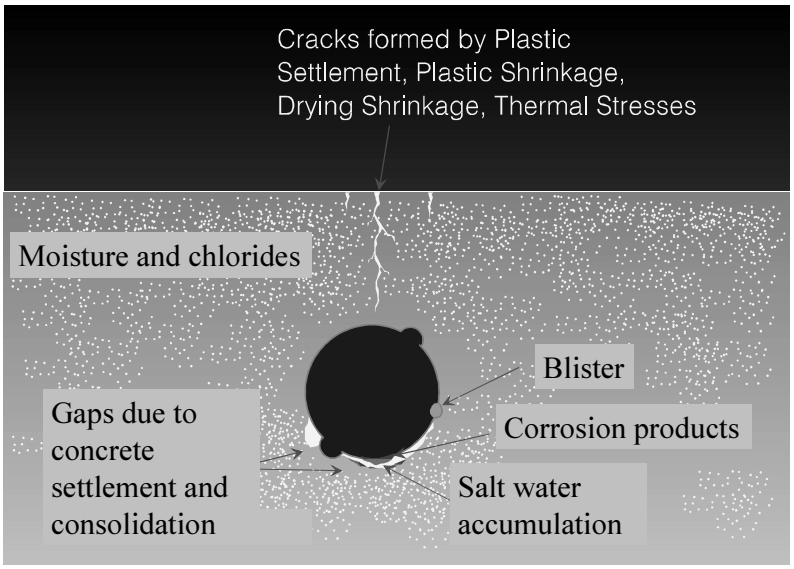

Figure 3.33 Conditions conducive to corrosion for coated bars embedded in concrete.

A few interesting key points emerge from the preceding diagram. First, corrosion products that develop on the lower half of the coated bar may turn brownish if moisture and oxygen were available in the voids to further oxidize the initial black corrosion products. In addition, the availability of *space* in these voids allows friable corrosion products to build up. Conversely, the steel substrate at the upper half of the bar, where concrete is well consolidated, remains in an air-tight zone suffering from oxygen starvation. As a result, a very thin black layer forms underneath the coating. Moisture may also reach to the upper surface by means of capillary action or "web effect," or simply permeation through the coating.

Second, a fundamental difference in corrosion behavior between epoxy-coated bars and uncoated bars can be deduced. With all other variables being equal, the uncoated bars tended to suffer more corrosion at the upper half of the bar after one and two years of exposure, where intruding chlorides attack first. Corrosion builds up voluminous solid products that exert radial pressure against concrete cover causing early cracking (as illustrated in Figure 3.34. However, with prolonged periods of exposure, corrosion eventually spread more on the bottom side than on the top side, as evidenced by the bars inspected after 4.5 years.

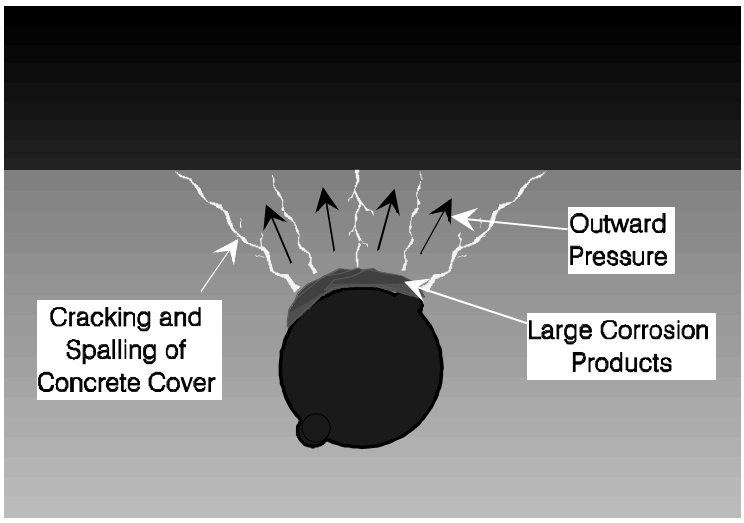

(a) Uncoated bar

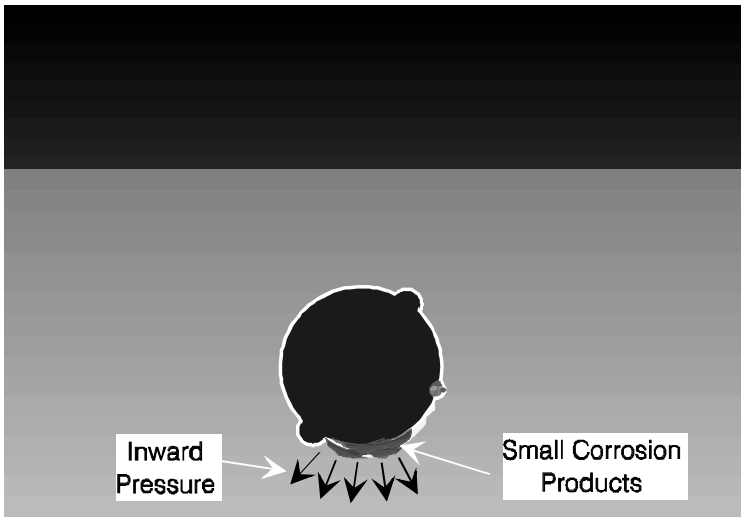

(b) Coated bar

Figure 3.34 Differences of corrosion behavior between uncoated and coated bars in concrete.

The opposite is true for the epoxy-coated bars placed near the top concrete surface. Unless the coated bars are heavily damaged at random, corrosion tends to commence at the lower half of the bar. Corrosion remained worse on the bottom side at all periods of exposure, although the difference in condition between top and bottom sides became less significant with time. The corrosion products remain in a low state of oxidation and may diffuse through concrete pores; the volume of the corrosion products is nearly always small. Consequently, the generated internal pressure is low and in an inward direction (as illustrated in Figure 3.34). Therefore, the risk of developing corrosion-induced cracking and deterioration is lower for coated bars than uncoated bars. This explains again why concrete specimens containing coated bars with large amounts of lost steel underwent limited cracking during the macrocell test.

Based on the foregoing discussion, concrete cracking should not be construed as a principal criterion of comparison between the corrosion performance of coated and uncoated bars. Cracking simply does not indicate the true level of corrosion activity of coated bars. The amount of metal lost is a more reliable indicator of the severity of corrosion, although it does not correlate with the intensity of corrosion at the exposed metal surface.

This consideration has a significant impact on the evaluation of bridge decks based on surface condition surveys only. The absence of cracking, despite being a positive sign of good performance, may actually be a deceptive sign! This should not be interpreted, however, to devalue the benefit of using coated bars, as they still show improved performance over uncoated bars. Until this time, there has been no better alternative to detect the condition of coated bars in the field than visual inspection at some check points.

3.8 ANALYSIS OF VARIABLES

3.8.1 Uncoated vs. Coated Steel

Clearly, uncoated bars performed much worse than coated bars, as evidenced by monitored currents and potentials, and the observed condition of concrete and bars (Figure 3.35). This is a very important fact that has to be kept in mind when evaluating epoxy-coated bars. Research by others[32,53,54] and results from this research clearly show that the epoxy-coating will not completely prevent corrosion of steel reinforcement. In fact, if chloride levels at the rebar level are high enough, corrosion of coated bars will be almost unavoidable. However, it is important to consider how extensive the corrosion damage would be if uncoated bars were used. None of the specimens with coated bars experienced extensive cracking, rust staining, delamination, and scaling of the concrete surface. The main purpose for using epoxy-coated bars is to improve performance of reinforced concrete infrastructure. Results from this study support the use of epoxy-coated bars over uncoated bars for concrete structures subjected to aggressive environments.

The coated specimen with largest metal loss as measured by charge flux experienced 43% of the charge flux of the respective uncoated bar after 4.5 years. This would mean that the worst performing coated bar was about 2.3 times better than the uncoated bar. The ratio for the worst performing coated bar after 2 years was 1.7. Comparison of performance ratios of all specimens after 2 and 4.5 years showed that almost half of the specimens performed better in a 4.5 year period than in 2 years. Although corrosion of coated bars increased from 2 to 4.5 years, uncoated bars experienced an even larger increase of corrosion activity and deterioration in the same period. From the experimental program alone, it is difficult to predict the probable service life of structures with epoxy-coated bars. Specimen design did not accurately reflect real field conditions. Some of the parameters were selected to accelerate corrosion. Concrete with high water/cement ratio and low concrete cover are not desirable characteristics. Finally, the performance

reported herein corresponds to a coating formulation produced in the early 1990's and may not necessarily indicate how the most recent coatings would perform in similar conditions. Coatings produced in the late 1990's would be expected to have a better corrosion performance.

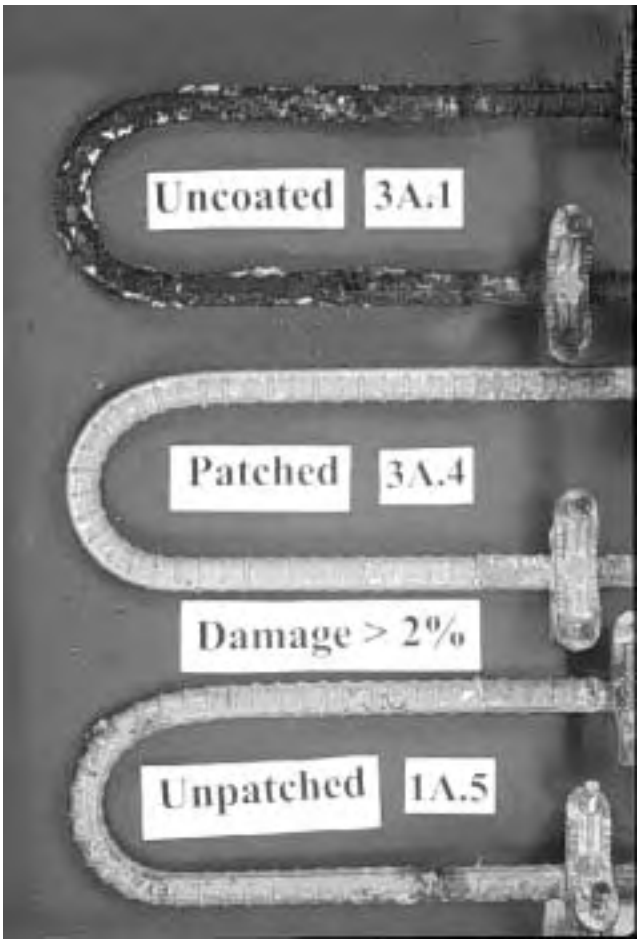

Figure 3.35 Comparative performance of uncoated and coated bars after 4.5 years of exposure.

3.8.2 Effect of Coating Damage and Repair

Bars with damaged spots greater than 2% of the bar surface suffered the worst corrosion among coated specimens. With the remarkable exception of bar 3A.3, bars with damaged spots greater than 6x6 mm experienced similar levels of corrosion after 4.5 years of exposure. In comparison, bars with patched damage experienced lower amounts of current, with the exception of bar 3A.4 (spots > 6x6 mm, patched), that exhibited higher corrosion currents than the respective unpatched bar 3A.3. Despite displaying slightly lower currents, the steel surface of most bars with patched coating showed levels of corrosion similar to bars with exposed, damaged areas (Figure 3.36). Corrosion products built up at exposed sites while only a very light rusting developed at patched areas. However, corrosion spread on the steel surface

far beyond patched areas and was not dissimilar from the corrosion observed at bar surfaces beyond exposed areas. These observations were in good agreement with measured macrocell currents.

In general, corrosion in bars with exposed areas tended to be slightly more severe and corrosion in bars with repaired areas tended to be more widespread. Patching damaged areas on the outside of the bend only was not sufficient. Corrosion also propagated from mandrel indentations at the inside of the bend and at the outside of one straight leg (at point of support for bending operation). The only case where a bar with patched coating presented a substantially improved steel surface condition relative to a bar with exposed areas after 4.5 years was provided by the small bars with parallel ribs and damaged spots greater than 2% of the bar surface.

(a) Patched bar 3B.2, outside bend.

(b) Bar 2B.3 with unpatched damage at outside bend.

Figure 3.36 Comparative steel corrosion under the coating at outside bend of bars with damaged coating, with and without repair.

The presence of cracks in the coating may reduce performance of coated bars in the long term. The amount of metal consumption (charge flux) was very low for specimens examined after one and two

years. Even for the specimens examined after 4.5 years, the amount of charge flux was very low during the first two years of exposure. However, a large increase in metal consumption occurred during the last 2.5 years of exposure. This suggests a slightly different corrosion mechanism than that observed for bars with larger exposed areas. A hypothesis for corrosion mechanism of bars with cracked coating will be formulated in a subsequent section.

3.8.3 Effect of Bar Size and Deformation Pattern

Both measured corrosion currents and examination of specimen conditions at the end of exposure clearly indicated that larger bars experienced more extensive and severe corrosion than smaller bars. Several factors may have contributed to the observed differences in behavior. One significant factor for the discrepancy is that the concrete environments surrounding the two different bar volumes were different. Concrete consolidation around the top reinforcement is affected by the bar size. Variations in consolidation will, in turn, affect the formation of plastic settlement cracks and the void structure in contact with the reinforcing bar. From the forensic examination, there were smaller and fewer voids around the 13-mm (#4) bars than the 25-mm (#8) bars.

Another factor that has been identified in the literature to greatly affect corrosion performance is the ratio of concrete cover to bar diameter. Smaller ratios lead to worse performance. This ratio takes into account the importance of large concrete covers for adequate corrosion protection. The ratio to the bar diameter is intended to account for the scale factor. Specimens of both series A and B had the same concrete cover of 25 mm. The ratio of cover to bar diameter was therefore smaller for bars of larger size. In other words, for the same size of concrete cover, larger bars have greater chances of becoming more contaminated and more likely to be attacked by chlorides. Other contributing factors for the difference in behavior between the two bar sizes may be their different metallurgy and the dissimilar concrete electrical resistivity in the two different concrete mediums.

No clear trend was found in the performance of bars with different corrugation patterns. Among series A, bars with cross ribs tended to have larger average currents than bars with parallel ribs. Visual examination of autopsied specimens confirmed this trend. Among series B, though, bars with parallel ribs tended to show slightly higher average currents than bars with cross ribs. This trend could not be confirmed because the specimens with cross ribs were not autopsied for examination.

3.9 CORROSION MECHANISM

3.9.1 General

The following sections will describe a hypothesis of macrocell action on the test bars (both uncoated and coated) and of cathodic bars. The scenario reconstructs the most likely sequence of steps that lead to the

observed behavior. The first part of the hypothesis is based on published research findings on the causes of rapid concrete distress in bridge decks presented by Clear and Virmani more than a decade ago.

The proposed corrosion mechanism takes into account the condition observed in bars after 1, 2, and 4.5 years of exposure. The mechanism for corrosion initiation and progression during the first half of the exposure is similar to that proposed in Reference 23. Additional events that occurred during the period from 2 to 4.5 years of exposure were incorporated in the mechanism proposed here.

3.9.2 Macrocell Action on Uncoated Bars

Uncoated bars corroded more severely than the coated bars, *i.e.* showed deeper pits and worse surface degradation. The surface area of rust on the uncoated bars was not significantly larger than that of the coated bars extending beneath the coating. A likely mechanism for this behavior is presented below:

When sufficient amounts of chloride ions penetrated the concrete cover and reached the top uncoated reinforcement, the pH of concrete at several locations lowered and the protective oxide film was broken. Corrosion micro-cells were thus initiated on the bar surface. Such cells were primarily located at the straight portions of the bar, close to the front face of the specimen where bars project to the outside, possibly because of the availability of oxygen at those regions. Cathodic reactions were possibly supported at the bar surface adjacent to the concrete front face. As the pH of the local anodes dropped (as evidenced by the presence of acidic solution) due to hydrogen ion H^+ generation by the corrosion reaction, the remaining steel area on the top bar maintained a relatively high pH value because of the alkalinity provided by the concrete. This created an initial macrocell on the top bar which intensified metal dissociation at the anodes. Anodic areas were located mainly at straight portions and cathodic areas were located mainly at the bend.

The potentials of the micro-anodes decreased rapidly and reached very negative values, possibly more negative than -350 mV CSE. Consequently, there was a large potential difference between the anodic sites and the large volume of cathodic steel at the bottom of the specimen. A macrocell corrosion current flowed between the two reinforcing layers. Availability of both water and oxygen is necessary to support the cathodic reactions and to provide the electrolyte needed for developing a corrosion cell. Therefore, the large macrocell between top and bottom bar layers was possibly not triggered until after a few wet and dry cycles, when enough moisture penetrated inside the specimen and reached the bottom bars. The periodic wetting and drying promoted further corrosion activity. In the end, the corroded areas covered only a fraction of the total surface area of the top bar before concrete cracking occurred.

Initially and during about the first 2 years, corrosion was more extensive at the top side of the bar because more chlorides reached and accumulated on the top sides earlier. Availability of oxygen made it possible for corrosion products to reach a higher state of oxidation, with the consequent volume increase

that exerted a radial pressure against the concrete cover, causing early cracking. After cracking, excessive amounts of chlorides and oxygen reached the top steel to accelerate the corrosion process and convert the corrosion products to higher oxides. Perhaps, as concrete further disintegrated and separated from the metal surface, new anode sites developed and corrosion propagation continued on the surface. The presence of a gap, along with the greater porosity and void structure of the concrete under the top bar allowed a much greater accumulation of chlorides and corrosion progressed more extensively at the bottom surface, extending to the bent zone.

Between 2 and 4.5 years, chlorides continued to diffuse inside the concrete until they eventually reached the cathodic bars at the bottom of the specimen. When chloride concentration was large enough, corrosion started at the cathodic bars. Corrosion of "cathodic" bars occurred primarily on their side and bottom surfaces. When this happened, the original, simple macrocell became more complex. The bars at the bottom were no longer purely cathodic and the measured current between top and bottom layers became inaccurate and should explain why the current readings in all control specimens became more erratic between 2.5 and 3.5 years of exposure.

To complicate matters, a macrocell effect among the bottom bars was observed: Usually, one of the bottom bars corroded much more than the others (in one specimen, one of the bottom bars did not show any corrosion). A complex system of corrosion cells remained, with anodic areas consisting of the straight portions and bent zone (lower side) of the top bar, plus the surface of a bottom bar with most corrosion. Cathodic areas were confined to the bent zone (top side) of the top bar, plus most of the surface (generally the upper half) of bottom bars with less or no corrosion.

Several observations strongly support the above hypothesized mechanism. First, the surface of the top bar after one and two years was virtually free of rust away from corroded sites. This indicated that steel next to the pits was cathodically protected. Second, darker colored concrete around the unaffected steel (similar to that observed around the cathodic bars at the bottom) provided further evidence of the macrocell formation on the top bar. Third, there was a pattern of relatively clean surfaces on the top side of bent portions and corrosion of the remaining bar surface after 4.5 years of exposure. Also, it has been established by test results that the pH at the bar/rust interface reaches 3.0 or lower, while the pH of the neighboring concrete remains at 12 or more.[55]

Interestingly, a 13-mm bar with parallel ribs (3A.1) showed somewhat more severe and widespread corrosion than a 13-mm bar with cross ribs (3A.8) after 4.5 years of exposure. The opposite situation was expected because of the much higher average current density measured for the 13-mm bar with cross ribs. When the bottom cathodic bars were examined, the corrosion in specimen 3A.8 was more extensive and

severe than on the bar in specimen 3A.1. Undoubtedly, corrosion of bottom cathodic bars effected the macrocell currents measured.

A parallel but interrelated mechanism of deterioration was observed in control specimens. When corrosion-induced cracking propagated, chloride solution penetrated more easily and deeper towards the bottom parts of the specimen. Salt was deposited in capillary pores when water evaporated during the dry cycles. This created a concentration gradient because the remaining water close to crack surfaces had higher concentration of salt than water at the interior of the specimen. This gradient drove the salts in the water near crack surfaces towards the zones of lower concentration deeper inside. This transport process is called diffusion.[56] Upon re-wetting, additional chlorides penetrated capillary pores and diffused further in the next dry cycle.

Diffusion of chlorides in control specimens was greatly facilitated by the propagation and opening of cracks. The salt driven to the bottom parts of the specimen created another type of physical attack in the concrete. Salts in the form of crystals were left in the capillary pores when water evaporated during the dry cycles. Upon subsequent wetting, the crystals re-hydrated and grew, exerting an expanding force on the surrounding cement paste. The crystallization of salt in a zone having a free evaporation surface or to which the solution is raised by capillary forces results in destructive internal pressures that may crack and deteriorate the concrete.[5,56,57] It has been reported that moisture effects and salt crystallization are believed to be the two most damaging factors in the decay of historic stone monuments.[5]

The effect of disruptive forces by expansive hydrated crystals was visible in the lateral surfaces of the specimens in the form of concrete scaling. At scaled areas, the hardened cement paste and embedded fine aggregate particles were removed, leaving behind protruding coarse aggregate particles (Figure 3.37). Large deposits of salt crystals were visible at scaled surfaces. The lateral surfaces with more extensively scaling were near the concrete cracks on the top surface, reinforcing the notion that cracks facilitated percolation of salts towards the inside. Both processes of salt weathering and corrosion-induced cracks interacted with each other to further propagate deterioration. Specimens with coated bars also experienced concrete scaling on their lateral surfaces, but the scaling was much less extensive and not severe. Undoubtedly, the lack of extensive concrete cracking greatly reduced the amount of salt weathering in specimens with coated bars.

Figure 3.37 Severe concrete scaling on specimen 3A.8 with uncoated bars.

3.9.3 Macrocell Action on Coated Bars

MECHANISM

A corrosion mechanism of coated bars was construed by analyzing and comparing the corrosion progression of bars with varying degrees of corrosion. The initiation of corrosion on the exposed metal areas of the epoxy-coated bars followed the same sequence described for the uncoated bars. Corrosion started when enough chloride ions penetrated the concrete cover and reached the exposed areas (sites with damage or flaws in the coating) on the top coated bar to depassivate the steel. A porous concrete adjacent to or near exposed areas allowed for the accumulation of chlorides, oxygen, and water, all necessary agents for corrosion initiation. In contrast, exposed areas surrounded by very dense, well consolidated concrete (such as in bars 3A.3 and 3A.7) were free of corrosion. A probable distinction from corrosion of uncoated bars relates to the chloride concentration associated with the onset of corrosion. The limited areas available for reaction on the coated bars necessitated higher levels of chlorides to accumulate sufficiently in the vicinity of these exposed areas to depassivate the steel.

INITIATION

The mechanism for corrosion initiation at local exposed areas or defects in the coating is illustrated in Figure 3.38. Corrosion started at exposed areas, with anodes and cathodes developing locally, in a process similar to the Evans water drop experiment. As corrosion progressed locally and the exposed area was covered by corrosion products, a self-polarization of the exposed area occurred. This induced a polarization in the opposite direction in the adjacent areas covered by the coating, and a cathodic reaction (with consequent cathodic disbondment) may take place at such areas.[43] Corrosion spread at the small crevices under the coating at the edges of exposed areas or discontinuities. Adjacent debonded coating (by cathodic disbondment, water action, or a combination of both) formed very thin crevices and corrosion propagated under the coating in a mechanism similar to that of crevice corrosion.

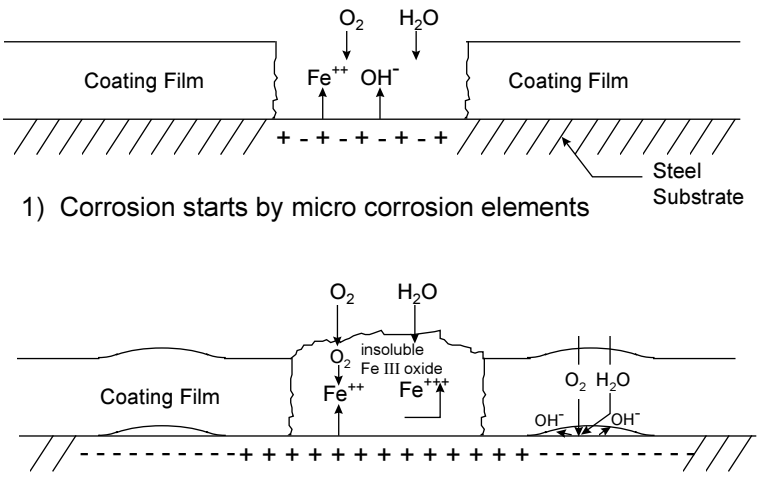

Figure 3.38 Corrosion initiation mechanism in coated bars.[43]

Because of the presence of greater quantities of exposed or defective areas and weakened coating adhesion, corrosion generally started and was more extensive at the bent portion than at straight legs, as opposed to uncoated bars. The portions adjacent to the exposed sites (generally at the outer bends) were initially cathodic with respect to the primarily anodic exposed sites. The already marginally adhered coating at the bends was cathodically disbonded because of saponification of the coating produced by the alkalinity generated during the cathodic reaction. Cathodic disbondment extended beyond the bends into the straight portions of the bar. Coating adhesion may have also been lost by the moist environment and water action at the coating/substrate interface. Sometimes anode formation with cathodic disbondment started at a weaker spot in the straight portion, like in bar 3A.3, but the overall mechanism was the same. This hypothesis is based on experimental and field evidence that the substances causing coating disbondment migrate to the coating-substrate interface through coating defects rather than through the bulk of the coating (Report 1265-6[45], references 53 and 58).

As already mentioned, the occurrence of cathodic disbondment at top bars indicated that cathodic and anodic reactions occurred on the same bar surface, forming a local corrosion cell. This seemed to indicate that the initiation process was characterized by self-polarization and occurred independently of any electrical coupling between coated and uncoated bars.[43] Cathodic reactions at the bottom bars would not be established until enough moisture reached the bottom bars (to provide the water necessary for oxygen reduction) and a large potential difference developed between the anodic sites at the top bar and the cathodic steel at the bottom of the specimen. Moisture also helped to reduce concrete resistivity, facilitating ionic flow between bar layers, thus causing the concrete to act as the electrolyte of the electrochemical macrocell. At this point, macrocell action came almost exclusively from the potential difference developed between the corroding anodes and the bottom macro-cathodes. The steel surface

remained isolated from the alkaline pore solution of concrete. Thus no large macrocells were formed on the top bar due to variation of pH along the bar surface.

CORROSION CURRENT

Once a larger macrocell corrosion current between the two bar layers was set up, underfilm corrosion accelerated on the coated bar and oxide lifting took place. As already explained, oxide lifting occurs when anodic corrosion products accumulate under the coating. The lifting action of compacted oxides and resultant undercutting occurred during alternate wet and dry cycles. In addition, disbonded coating facilitated migration of chloride ions, and other species in the electrolyte, to new locations under the coating. The pH at the anodic sites and their vicinities dropped to acidic levels due to ferrous ion hydrolysis in chloride solution. The acid chloride solution promoted further anodic growth and dissolution. As acidification continued, the oxygen supply became deficient in flat crevices under the coating and created a self-perpetuating corrosion environment. As the acid solution travelled freely along the steel surface, an additional cathodic reaction involving hydrogen reduction might have occurred. Undercutting progressed more extensively at the lower portion of the bars. The gap and void structure in the surrounding concrete allowed for better travel, distribution, and accumulation of chloride solution and dissolved oxygen under the bars. Concrete voids provided the physical space for the expansion of corrosion products to form blisters. Corrosion in most bars spread from the outer and lower bends towards the inner bend and straight bar legs.

CORROSION PRODUCTS

Typical corrosion products consisted of dissolved ferrous ion, Fe^{2+}, precipitated $Fe(OH)_2$, which partially oxidized to magnetite, Fe_3O_4, and perhaps an outer hydrated layer of fully oxidized FeOOH, which is common rust. Limited availability of oxygen beneath the coating caused most corrosion products to be in a low oxidation state. This accounted for the predominance of magnetite, which is the uniformly black corrosion product observed at the corroded surfaces, and for the smaller amounts of reddish-brown and other brownish corrosion products. Black corrosion products spread thinly and accumulation of low pH, chloride rich liquid under the epoxy coating has also been found by other researchers.[32,53] Corrosion products either diffused in concrete at coating breaks, or deposited at the bottom cavities alongside the continuous rib. The slight volume increase and rust accumulation in some bars caused incipient concrete cracking (very fine, narrow cracks) in several specimens, or the opening and growth of plastic settlement cracks. Nevertheless, severity of concrete deterioration and width of cracks was much lower for coated bar specimens than for control specimens. Likewise, measured and observed corrosion activity on coated bars was below the level found on uncoated steel. Both oxygen starvation at the anodic end (beneath the

coating), and the high electrical resistivity of the path between anodes and macro-cathode (due to dielectric properties of the coating) lessened the severity of corrosion action.

OBSERVATIONS

There are three observations that support the mechanism described above. First, the ferrous hydroxide corrosion product was seen under the loosely-adhered coating as indicated by some white pasty deposits. Second, an acidic solution was found trapped beneath the coating and blisters. Third, chloride ions were also traced in the same trapped solution by other researchers.

An irony and a dilemma coexist in the preceding description of the corrosion mechanism of coated bars. The irony is that the same coating which is used to protect steel from corrosion becomes the cause of undercutting due to expansion of the anodic area in the debonded regions. The epoxy film deprives the steel from the natural protection afforded by concrete and this allows the creation of a self-propagating corrosion mechanism in the flat crevices beneath the coating.

The dilemma arises in that the reason why epoxy-coated bars performed better than uncoated bars is that corrosion was distributed behind the coating rather than concentrated in limited steel areas. This means that debonding may actually help the coated bar to perform better than to be detrimental to performance! Further illustration of this point is given below.

The anodic area increased in the debonded region due to migration of low pH solution. The acid solution nucleated new pits so large in number and closely spaced that a general corrosion state rather than localized pitting was approached. This condition was exactly opposite to that occurring on the uncoated bar that developed a relatively large macrocell on its surface. In effect, macrocell action between different regions of the same bar (as opposed to the primary macrocell between the layers) was significantly reduced on the coated bar and corrosion was distributed. Figure 3.39 shows a bend on a control bar free of rust (because localized severe pitting occurred at the straight ends), and a corroded bend after stripping the damaged coating.

It must not be forgotten that the overall performance was better for the coated bars. Even when a large anodic area was formed, the restricted oxygen supply forced most corrosion products to remain in a low state of oxidation. These products were soluble when moisture was available, so corrosion occurred without exerting high enough pressure to cause extensive cracking or spalling of the concrete. Bars with less coating damage performed better than those heavily damaged which emphasized the fact that a better initial product results in better corrosion resistance.

(a) Uncoated bar free of rust at bend

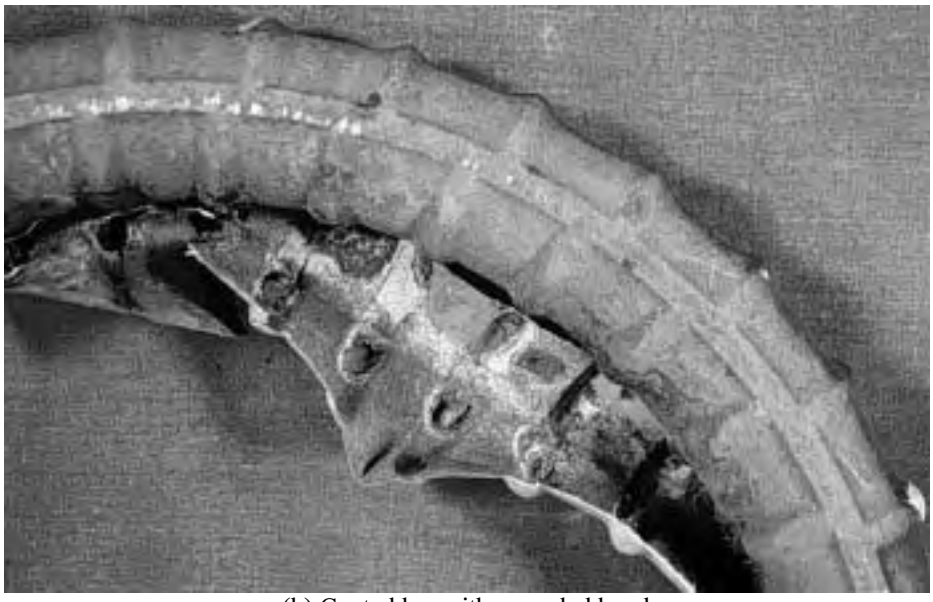

(b) Coated bar with corroded bend

Figure 3.39 Comparison of corrosion distribution along bends of uncoated and coated bars after 2 years of exposure.

3.9.4 Corrosion Mechanism in Bars with Cracked Coating

As already noted, specimens with cracked coating showed very little activity during the first two years but much larger corrosion currents during the last 2.5 years of exposure. Examination of companion triplicates after 2 years showed either very minor (25-mm bar) or no apparent corrosion (13-mm bar). The last triplicates showed more extensive and uniform corrosion after 4.5 years of exposure. The presence of narrow cracks seemed to delay corrosion initiation and the corrosion rate remained low

during the first two years compared to other types of damaged and exposed areas. These observations may suggest that a slightly different corrosion mechanism takes place for bars with cracked coating.

The following mechanism may have occurred: Coating cracks are very narrow and expose limited areas that required a longer time to develop a high enough chloride concentration for corrosion initiation. Corrosion started at about 1.5 years for bar 2A.6 and at about 2 years for bar 2B.6, with chloride concentrations at the level of the steel of about 0.15% and 0.19% by weight of concrete, respectively, as measured at companion concrete prisms. During this "incubation" time, chloride solution may have penetrated under the coating through the cracks and other damaged areas (such as mandrel indentations at the inner bends) as easily as through the larger exposed areas at other bars, as evidenced by the presence of trapped acidic solution in the bars after 4.5 years. Considering that the cracks indicated failure of the coating to pass the bend test, coating adhesion was presumably so weak that the process of solution penetration under the coating was greatly facilitated. Water penetration caused further loss of adhesion, which was as extensive as in other bars.

Corrosion activity was limited during the first 1.5 to 2 years of exposure because of the very small anodic surfaces. Corrosion progressed slowly under the coating crevices formed at the edges of the cracks, in a mechanism similar to that explained above. No macrocell action was yet established, and anodes and cathodes were formed on the same bar. At some point between 1.5 and 2 years, polarization at anodic areas on the top bar was sufficiently large to develop a larger macrocell action with the bottom bars. Corrosion accelerated rapidly thereafter aided by the macrocell action and the availability of chloride solution at the metal/coating interface.

3.9.5 Corrosion of Cathodic Bars

The bottom cathodic bars of a few specimens with top coated bars were mostly free of corrosion, as opposed to bottom cathodic bars from specimens with top uncoated bars. This finding was somewhat puzzling because it implied that the type of bar in the top layer affected the behavior of the bar at the bottom layer. Chloride contents at the level of the bottom bar were not directly measured. Chloride contents measured at the deepest levels (3.25 in) were similar for these specimens, so it is very likely that chloride contents at the level of the bottom bars were also similar for specimens with both coated and uncoated top bars. No explanation of this phenomenon was found in the literature but some hypotheses can be formulated:

1. When both top and bottom bars are uncoated and enough chlorides reach the bottom bars, the electrically continuous top and bottom layers may become a complex corrosion system. Macrocell currents may reverse and start to flow from bottom to top, making the bottom bars more anodic than the top bars. If enough chlorides reached the bottom bars in specimens with

coated bars at the top layer, a possible reversal of macrocell current would be severely limited by the dielectric properties of the coating, presenting a path of high electrical resistivity for the top bars to become an effective cathode. This phenomenon could not be verified, though, because no reversal or change in sign was observed in the measured currents of control specimens.

2. The concrete in the specimens with uncoated bars experienced much greater deterioration than concrete in specimens with coated bars. The combined action of cracking and salt crystallization created a general state of distress that allowed greater percolation of chloride solution, which in turn worsened concrete deterioration. In contrast, concrete in specimens with coated bars was much less distressed and cracked. As a result, the concrete was dryer and maintained higher resistivity compared with concrete in specimens with uncoated bars.

Although the mechanism is uncertain, it seems that a twofold advantage was gained with the use of coated bars. Both top and bottom bars underwent less corrosion, even if only the top bar was coated. However, it would not be recommended to rely on top coated bars for corrosion protection of uncoated bottom bars in the field. Macrocell specimens did not accurately resemble real field conditions. The top and bottom bars in the specimens were electrically continuous, a condition that may not be present or certain in the field.

CHAPTER 4

SUMMARY, CONCLUSIONS AND RECOMMENDATIONS

4.1 SUMMARY

To study the performance of bent epoxy-coated bars damaged to various levels, a macrocell corrosion experimental program was conducted. Triplicate concrete prisms were built and each specimen had a fabricated coated bar in the top layer which was electrically connected to uncoated bars in the bottom layer. Chlorides intruded from the top surfaces in cyclic exposures up to a 4.5 year period. Time development of corrosion and corrosion currents were monitored and specimens were opened for examination of the bar condition after 1, 2, and 4.5 years. The main conclusions of this study pertaining to bent coated bars are given in the following sections.

4.2 CONCLUSIONS

4.2.1 Onset of Corrosion

Corrosion of damaged epoxy-coated steel in concrete was delayed and started at chloride concentrations around twice the levels associated with the onset of corrosion of uncoated steel.

4.2.2 Effectiveness of Epoxy-Coated Steel

The epoxy coating, even if damaged, was effective in reducing the severity of reinforcement corrosion under macrocell action in chloride-contaminated concrete over a 4.5 year period. Regardless of coating condition, coated bars performed much better than uncoated bars. Based on the measured charge flux, the worst coated bar performed about 2.3 times better than an uncoated bar (Figure 3.15). None of the specimens with coated bars experienced extensive cracking, rust staining, delamination, and scaling of the concrete surface, as control specimens did. Although corrosion of coated bars increased between 2 and 4.5 years of exposure, uncoated bars experienced an even larger increase of corrosion activity and deterioration in the same period. Corrosion currents in most specimens with coated bars were not increasing and seemed to have reached a steady-state after 4.5 years of accelerated exposure. The test results do not permit prediction of the probable service life of structures with epoxy-coated bars.

The performance of coated bars deteriorated with longer periods of exposure. The rate of increase of metal consumption of coated bars was higher than that of uncoated bars. However, despite the huge increases of metal consumption in some cases, the improvement in performance of coated bars was still evident because of their very low initial corrosion. Moreover, it is the state of oxidation, rather than the amount of corrosion products that induces corrosion deterioration.

Several factors contributed to the improved performance of epoxy-coated bars. The coating delayed the initiation of corrosion and corrosion started at higher levels of chlorides compared with uncoated steel. The number of anodic areas was initially reduced by the presence of the coating. The dielectric properties of the coating offered a path of high electrical resistivity between the anode and the bottom cathode, thereby reducing the rate of corrosion. The coating limited the availability of dissolved oxygen and kept a large portion of the corrosion products in a low state of oxidation, thus reducing the severity of corrosion. The lower distress in the concrete in specimens with uncoated bars slowed chloride penetration and diffusion, and preserved a denser and drier concrete with high electrical resistivity.

4.2.3 Effect of Coating Damage and Repair

Corrosion resistance was governed by the degree of damage to coating. Both the frequency and size of damage were dominant factors for performance. Bars with greater damage tended to perform worse. Patching coating damage reduced but did not prevent corrosion in most specimens. The effectiveness of patching was reduced with time. The common practice of patching only the damage on the outside of the bend did not prove to be sufficient; corrosion spread from damage on the outside and the inside of bend. The results encourage the practice of patching all visible damage to further improve performance. Bars with coating cracks and exposed areas less than 1% experienced increasingly higher corrosion currents at the end of 4.5 years while other damaged bars seemed to have reached steady-state behavior.

The above conclusions are valid for the type of patching material tested. However, as was demonstrated in Research Report 1265-5,[59] different patching materials perform differently. The patching material used for the macrocell study had a very thin consistency and in fact, its production has been discontinued since the study started. The conclusions may have been different if other repair materials had been used.

The limits on allowable damage to coating in earlier and some current specifications are not strict enough. Damage close to these limits, if concentrated at critical locations such as on bent bars near the concrete surface, provides access to deleterious substances that can cause breakdown of the coating adhesion and widespread underfilm corrosion. To improve corrosion resistance of coated bars, both stringent specification limits and better field practice are required.

4.2.4 Effects of Bar Size and Deformation Pattern

Coated reinforcing bars with smaller diameters exhibited less corrosion than bars with larger diameters. The influence of bar size on corrosion severity was significant. Possible factors included differences in the concrete environment caused by the bar size, influence of concrete cover to bar diameter ratio, and discrepancies in the metallurgy between the two bar sizes. Test data on the relative performance of bars with parallel and cross deformations did not show a consistent trend.

4.2.5 Effects of Concrete Environment

Quality and consolidation of the surrounding concrete was an important factor in the corrosion processes of epoxy-coated bars. More corrosion was observed at the bottom side of coated bars than at the top sides because the adjacent concrete was more porous with more and larger voids, was not well adhered (there was a gap below coated bars), and was less dense than concrete above the bars. Consequently, chlorides, water, and oxygen were more easily accessible to the bottom surfaces of the bars, even though chlorides were penetrating from the top concrete surface. The epoxy coating tended to develop blisters and to break down at air pockets facing bar surface. The more the likelihood of void formation around the bar (particularly in the vicinity of a damaged spot), the higher the chances of developing a corrosion cell. On the contrary, exposed areas in contact with dense concrete did not corrode at all.

The coated bars consistently showed high propensity for plastic settlement cracking, most probably due to lack of adherence between the epoxy coating and concrete. Cracks produced by shrinkage and plastic settlement have the adverse effect of allowing chloride penetration directly to the bar surface. Incipient corrosion-induced cracks in coated bar specimens generally propagated from shrinkage and plastic settlement cracks. Coated bars inside cracked specimens were among the most corroded.

4.2.6 Coating Debonding

The exposure conditions of the test caused debonding of the epoxy coating. Adhesion was first weakened by fabrication, then further reduced by exposure. Surface defects and mechanical damage to coating permitted the corrosive substances to penetrate the coating, initiate underfilm corrosion, and increase coating delamination. Debonding did not correlate with the level of coating damage or extent of undercutting, nor was it a consistent indicator of poor performance.

4.2.7 Corrosion Mechanism

Corrosion started when enough chlorides penetrated the concrete cover and reached the exposed areas on the top coated bar to depassivate the steel. Corrosion spread at the small crevices under the coating at the edges of exposed areas or discontinuities. Adjacent debonded coating (by cathodic disbondment, water action, or a combination of both) formed very thin crevices and corrosion propagated under the coating in a mechanism similar to that of crevice corrosion. The corrosion initiation process was characterized by self-polarization and occurred independently of any electrical coupling between coated and uncoated bars. A macrocell effect was established at more advanced stages of corrosion, when a large potential difference developed between top and bottom bar layers, and enough moisture penetrated the specimen to sustain cathodic reactions at the bottom layer and to reduce concrete resistivity. When the macrocell current between the two bar layers was sufficiently large, corrosion products built up at exposed areas, underfilm corrosion accelerated on the coated bar, and oxide lifting took place. Corrosion became more

distributed on the coated bar than on the uncoated bar. Concentration of corrosion on smaller parts of the uncoated bar resulted in severe pitting corrosion and early cracking of concrete.

Regardless of the level of corrosion, the epoxy coating extensively debonded from the steel substrate. Black corrosion products (magnetite) uniformly spread over the bar surface along with other corrosion products in lower amounts, and accumulation of low pH, chloride rich liquid were typically found under the epoxy coating and in blisters. Limited availability of oxygen beneath the coating caused most corrosion products to be in a low oxidation state. In addition, corrosion concentrated more on the lower part of the bar than on the top. Hence, corrosion proceeded without early signs of cover cracking. With longer exposure, the slight volume increase and rust accumulation in some bars caused incipient concrete cracking (very fine, narrow cracks) in several specimens.

4.3 RECOMMENDATIONS

4.3.1 Quality Of Coating

Protective materials, such as high density plastic sleeves, should be used at contact points between the coated bar and bending equipment when bars are fabricated. Coating bars after fabrication should be considered. The benefits of coating after bending are expected to outweigh the extra cost in terms of added years of service.

If significant improvement of adhesion of coating to substrate is needed, pretreatment of steel is recommended. Pretreatment is a chemical process that enhances adhesion and corrosion resistance. Another option is to clean the steel bars twice.

4.3.2 Specifications

Stricter specification requirements regarding coating damage should be considered such as: limiting the number of accepted holidays to 3/m (1/ft.) during coating; patching all visible damage at all stages (at fabrication plant, after arrival to construction site, and before concrete placement); and limiting the percentage of patched damage to a total of 1% of the bar surface area per unit length of coated bar.

4.3.3 Design Recommendations

Bending epoxy-coated bars to the minimum radii allowed in design may cause damage and weakening of coating adhesion on the outside of bend. Tight bending radii should be avoided unless required for structural purposes. Use of smaller diameter bars is encouraged; however, spacing between bars should be sufficient to avoid excessive damage caused by vibration. Mixing coated and uncoated bars should be avoided. The cost for using coated bars exclusively in construction would not be prohibitive.

4.3.4 Field Recommendations

Damage to coating must be kept to a minimum throughout construction. The use of padded materials to protect the bars during handling and transportation is one example to improve field practice.

To improve concrete consolidation around bars, and to reduce plastic settlement and gap formation underneath the bars, both concrete slump and depth of lifts should be reduced. Careful operation of internal vibrators is required to reduce damage during concrete placement. Vibrators with “soft” heads reduce the amount and severity of coating damage but require longer times of insertion to achieve the same degree of consolidation.

4.3.5 Inspection

A comprehensive quality control plan should be developed to ensure proper production, installation, inspection, and repair of coated reinforcement. All parties involved should be well educated about the necessity of obtaining a quality product.

APPENDIX A

DETAILS OF MACROCELL CORROSION TEST

A.1 SPECIMEN DESIGN

A.1.1 General

One of the requirements of this test was to simulate the conditions of concrete bridge deck slabs exposed to chloride-based deicing salts. The primary destructive mechanism of such bridge slabs is the corrosion-induced deterioration related to macrocell action. Corrosion develops as a result of the anodic activity on the top reinforcing layer being intercepted by the intruding chlorides, and the cathodic activity on the bottom layer resting in chloride-free concrete.

To simulate such conditions, concrete prisms were designed with two reinforcing layers. The test bars were placed at the top (anode) of the macrocell model. The bottom bars were all uncoated and served as the cathode. A direct electrical link was provided between the two reinforcing layers to allow the corrosion cell to operate. To accelerate corrosion, a wet-dry cyclic exposure regime was selected. The top concrete surface was ponded, intermittently, with chloride solution to supply the chloride ions necessary for accelerated corrosion initiation.

Series A. The details of Series A test specimen are shown in Figure A.1. The outer dimensions of the concrete prism were 200 x 200 x 180 (height) mm (8 x 8 x 7 in.). The top reinforcing layer consisted of a single 13-mm (#4) bar with a 180^{o} bend (after rebound on a mandrel diameter of 50 mm (2 in.)). Bending was done in accordance with ACI 318-89[60] and AASHTO M31[61] requirements for minimum bend diameters for stirrups and ties.

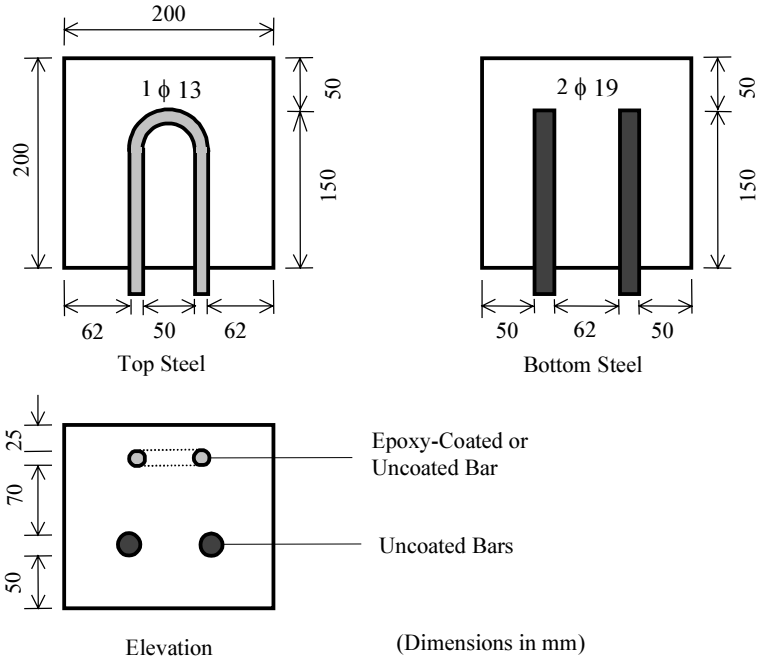

Figure A.1 Details of Series A macrocell specimens.

The bottom reinforcing layer consisted of two straight uncoated 19-mm (#6) bars. The choice of the size and number of these bars was based on a calculated surface area ratio of bottom to top steel of approximately 1.4. Only the embedded portions of these bars and their nominal surface areas were considered in the calculations. The ratio provided a theoretical index of the corrosion driving force assuming the total steel surface area beneath the coating to be the anode.

The clear concrete cover over the top bar was only 25 mm (1 in.) to accelerate the onset of corrosion. The distance between the two reinforcing layers was 70 mm (2.75 in.). The concrete cover on all sides and under the bottom bars was 50 mm (2 in.).

Series B. The details of Series B test specimen are shown in Figure A.2. The outer dimensions of the concrete prism, in this case, were 300 x 230 x 200 (height) mm (12 x 9 x 8 in.). The reinforcement details were similar to those of Series A except for the following: the top reinforcement was a 25-mm (#8) bar bent on a mandrel diameter of 150 mm (6 in.) (a standard in ACI 318-89 and AASHTO M31); the bottom straight reinforcement consisted of three-28-mm (#9) bars; and the clear distance between the two reinforcing layers was 73 mm (2.88 in.).

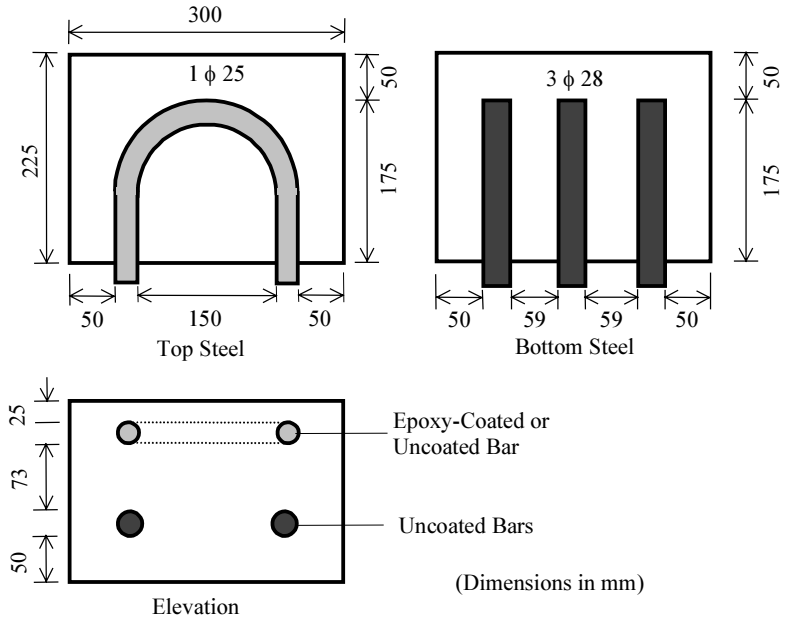

Figure A.2 Details of Series B macrocell specimens.

The ratio of the surface area of bottom steel to top steel embedded in concrete was also 1.4. The ratio was kept a constant for specimens with both bar diameters to provide the same theoretical corrosion driving force. In addition, the distance between the reinforcing layers was roughly equal in both cases in an attempt to maintain similar ionic flow through concrete between layers.

Series C. The determination of chloride content in concrete, particularly at the steel level, is an important consideration in any corrosion study. The chloride concentration was measured periodically to relate changes in the corrosion behavior to variations in chloride level around the steel. Chloride determination requires extracting

concrete powder by drilling holes in the specimen. Since this operation is destructive, the test specimens themselves could not be sampled because the salt solution used for contaminating the concrete would accumulate in the hole and disturb the uniformity of exposure.

Another series of unreinforced concrete prisms was constructed to enable chloride determination without disturbing the macrocell specimens. The prisms were cast from the same concrete as Series A and B. The dimensions of the prisms were 180 x 170 x 150 (height) mm (7 x 6.75 x 6 in.). The specimens in three series were subjected to the same exposure conditions so that chloride concentrations in the concrete were expected to be nearly the same.

A.2 EPOXY-COATED REINFORCING STEEL

A.2.1 Steel Procurement

The epoxy-coated reinforcing bars (12 m (40 ft.) length) used in this test were plant-coated and selected from a normal production run. The coating plant is a major supplier of coated bars to the TxDOT projects. The bars were coated with a commercially available and widely used coating material in the US approved for use by the TxDOT. The coating material was certified as conforming to ASTM A775/A775 M-90, ASTM D3963-86, ASTM A884-88, AASHTO M284-86, and AASHTO M254-77. All bars were Grade 60 meeting ASTM A615-87a.[62]

Uncoated bars from the same heat of steel (for each bar size and rib pattern) were also obtained to be used as control specimens. The chemical analysis of the steel according to certified test reports available at the coating plant is shown in Table A.1. There were no significant differences in steel composition among the different bar groups.

Table A.1 Chemical analysis of steel for macrocell study (mill test report: percent by weight).

Composition	13-mm Bars Parallel	13-mm Bars Cross	25-mm Bars Parallel	25-mm Bars Cross
C	0.37	0.42	0.43	0.38
Mn	0.85	0.95	0.98	0.89
P	0.017	0.023	0.011	0.031
S	0.037	0.027	0.033	0.054
Si	0.29	0.23	0.29	?
Cu	0.5	0.36	0.48	?
Cr	0.17	0.13	0.14	?
Ni	0.16	0.12	0.19	?
Mo	0.029	0.04	0.05	?
Other	0.007	0.015	0.024	?

The bars were cut in 3 m (10 ft.) lengths by the coating applicator. The bars were bundled and firmly wrapped with protective polyethylene layers to avoid damaging the coating during handling and transportation. At the laboratory, the bars were cut to the required lengths and the coating thickness was measured. Afterwards, the bars were wrapped again and shipped back to the coating plant for fabrication.

At the coating plant, a bar bender equipped with high density plastic sleeves over steel mandrels was used to fabricate the bars into the required "U" shape. During bending, some coating damage was inadvertently introduced, especially on the inside of bends, where ribs were pressed against the mandrels. Damage was in the form of some mashed coating spots on the ribs. The bars were carefully shipped back to the laboratory to avoid further damage to the coating.

A.2.2 Bar Identification

Series A and B each had 11 groups of three replicate specimens distinguished by the test variables summarized in Table A.2. The specimens are identified by a three character label: the order within the group (1-3); series type (A or B), and group number (1-11). For example, specimen 1 A.1 is the first specimen in group 1 of Series A, the 13-mm (#4) bar series, and it is a control specimen. Specimen 3 A.2 is the third replicate in group 2 of Series A and contains an epoxy-coated bar with damaged spots slightly greater than 6 x 6 mm (1/4 x 1/4 in.) patched before concrete placement. Specimen 3 B.2 is similar to 3 A.2 except for the bar size.

Table A.2 Macrocell test group summary.

Group Number		Deformation	Coating	Damage
Series A[a]	Series B[b]	Pattern	Damage[c]	Condition
A.1	B.1	Parallel	"Control" Uncoated Bars	
A.2	B.2	Parallel	Spots > 6 x 6 mm	Patched
A.3	B.3	Parallel	Spots > 6 x 6 mm	Not Patched
A.4	B.4	Parallel	Spots > 2%	Patched
A.5	B.5	Parallel	Spots > 2%	Not Patched
A.6	B.6	Parallel	Cracks < 1%	Not Patched
A.7	B.7	Parallel	Spots < 2%	Not Patched
A.8	B.8	Cross	"Control" Uncoated Bars	
A.9	B.9	Cross	Spots > 6 x 6 mm	Patched
A.10	B.10	Cross	Spots > 6 x 6 mm	Not Patched
A.11	B.11	Cross	As Received < 1%	Not Patched

a 13-mm (#4) bar series.

b 25-mm (#8) bar series.

c Refer to either the size of damaged spots or percentage of damaged area to bar surface area embedded in concrete.

Two more isolated specimens were added to the list of test specimens. The first was a 13-mm (#4) epoxy-coated bar with parallel rib deformations. The bar was bent conventionally on an unprotected metallic mandrel and no additional damage was introduced. The specimen is designated 1 A.* and had no replicates. The other added specimen was a 25-mm (#8) epoxy-coated bar with cross rib deformations. The coating of the bar was so thin that the dark steel substrate was partially visible. This specimen was designated 1 B.* and also had no replicates.

A.2.3 Steel Tensile Strength

Two coated steel samples of each bar size and deformation pattern were tested to obtain the tensile yield strength, yield strain, and ultimate strength. No significant differences existed between the results of the replicate test samples. Therefore, the average test values were used to construct the stress-strain curves shown in Figures A.3 and A.4. The measured strengths conformed to the requirements of ASTM A615-87a,[62] as all yield strengths exceeded 414 MPa (60 ksi) and all ultimate strengths exceeded 621 MPa (90 ksi). The average yield strength of the small and large size bars were 486 and 439 MPa (70.4 and 63.6 ksi), respectively.

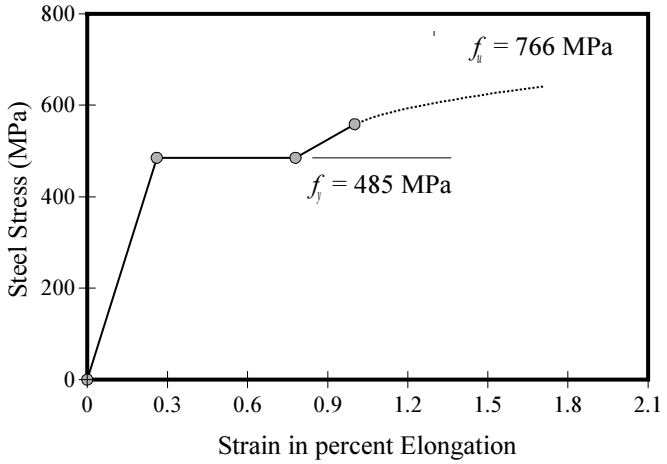

(a) Parallel Deformation Pattern

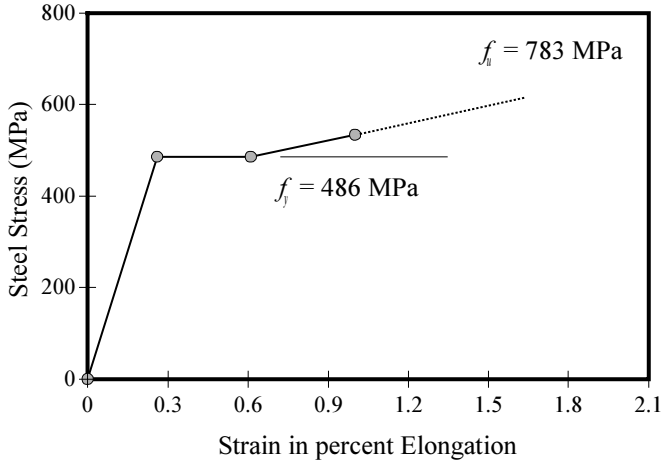

(b) Cross Deformation Pattern

Figure A.3 Stress-strain curves for 13-mm (#4) bars.

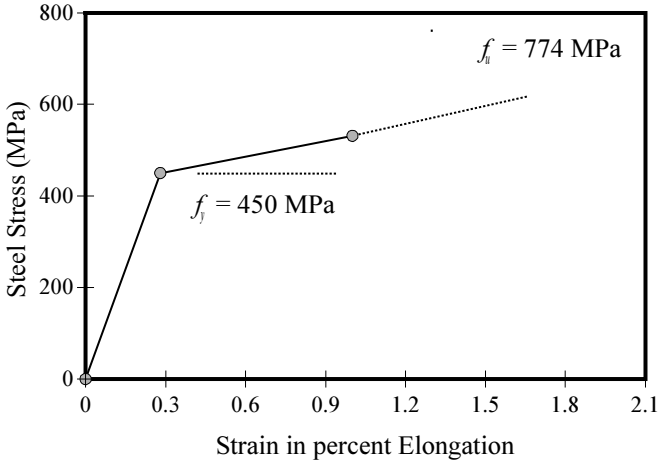

(a) Parallel Deformation Pattern

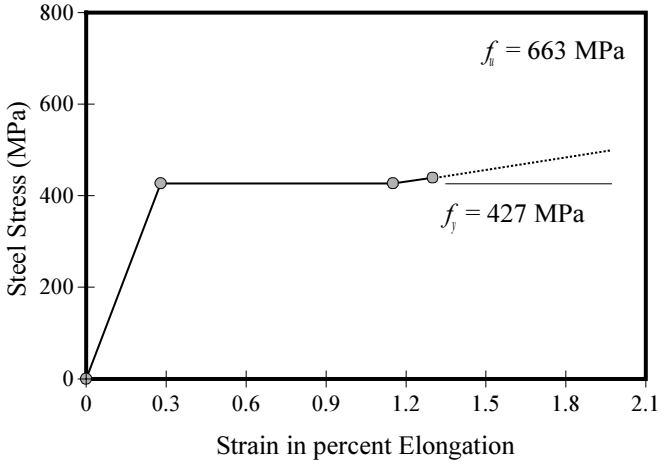

(b) Cross Deformation Pattern

Figure A.4 Stress-strain curves for 25-mm (#8) bars.

A.2.4 Epoxy-Coating Thickness

A thumbwheel pull-off magnetic gage was used to measure the coating thickness of the epoxy-coated bars before bending (as shown in Figure A.5). Coating thickness was measured at three locations on each side of the bar; a side being considered the bar surface between longitudinal ribs. The procedure described in ASTM G12-83[63] was followed. Coating thickness was obtained only on areas between the deformations in accordance with ASTM A77[17] and ASTM D3963.[18] For each bar specimen, the average coating thickness of six measurements and the maximum deviation in thickness from the average are reported in Tables A.3 and A.4.

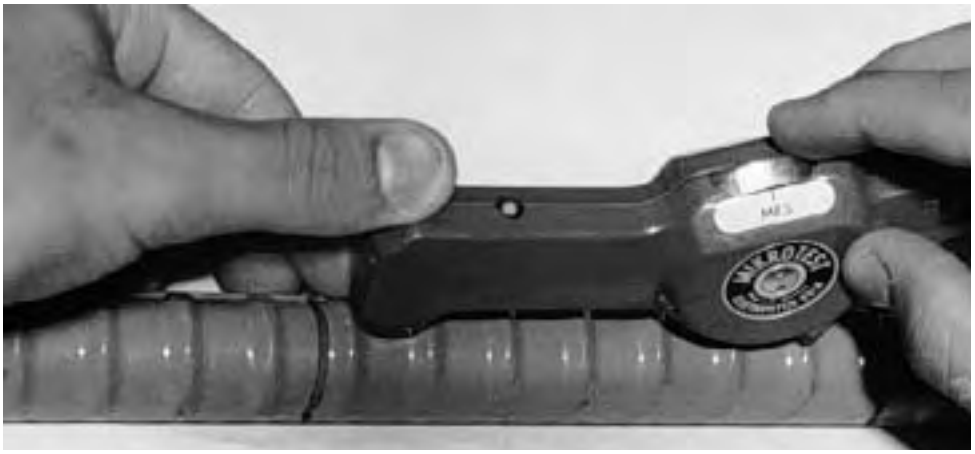

Figure A.5 Coating thickness measurement using a magnetic gage.

Table A.3 Coating thickness measurements, Series A (130 μm = 5 mils, 300 μm = 12 mils).

Specimen	Average Coating Thickness (μm)	Maximum Deviation from Average	
		(μm)	(%)
1 A.2	250	**+85**	**34**
2 A.2	220	**+68**	30
3 A.2	290	+38	13
1 A.3	280	**+55**	20
2 A.3	220	**+59**	27
3 A.3	240	+38	16
1 A.4	240	+42	18
2 A.4	**310**	+25	8
3 A.4	250	**+81**	**32**
1 A.5	230	+46	20
2 A.5	240	+36	15
3 A.5	240	+13	5
1 A.6	270	+40	15
2 A.6	220	**+55**	25
3 A.6	290	+38	13
1 A.7	240	-40	16
2 A.7	220	+21	10
3 A.7	290	**+68**	24
1 A.9	270	**+85**	**31**
2 A.9	280	**-97**	**35**
3 A.9	280	**+55**	20
1 A.10	260	**-55**	21
2 A.10	280	+46	16
3 A.10	230	+27	12
1 A.11	250	**+85**	**34**
2 A.11	240	**+51**	21
3 A.11	280	**+81**	29
1 A.*	280	**+55**	20

Table A.4 Coating thickness measurements, Series B (130 μm = 5 mils, 300 μm = 12 mils).

Specimen	Average Coating Thickness (μm)	Maximum Deviation from Average (μm)	Maximum Deviation from Average (%)
1 B.2	290	**+66**	23
2 B.2	220	-29	13
3 B.2	250	**+59**	24
1 B.3	270	**-61**	23
2 B.3	230	-40	17
3 B.3	220	**+89**	**41**
1 B.4	260	-27	11
2 B.4	230	**-72**	**31**
3 B.4	220	-46	21
1 B.5	250	**+53**	21
2 B.5	250	-49	19
3 B.5	240	-40	16
1 B.6	240	**+68**	29
2 B.6	260	+44	17
3 B.6	220	+38	18
1 B.7	280	**-51**	18
2 B.7	220	**+59**	27
3 B.7	250	**+57**	23
1 B.9	260	+42	16
2 B.9	240	+49	20
3 B.9	240	**+66**	27
1 B.10	240	-27	11
2 B.10	260	+42	16
3 B.10	180	**-53**	29
1 B.11	230	**+51**	22
2 B.11	250	+30	12
3 B.11	200	-42	17
1 B.*	170	**+64**	**38**

Both ASTM A775 and ASTM D3963 require that at least 90% of all recorded film thickness measurements be between 130 and 300 μm (5-12 mils). The first specification further requires that the deviation in coating thickness not exceed ±50 μm (±2 mils) or ±30% from the average thickness, whichever is less. All coating thickness measurements were equal to or greater than 130 μm (5 mils). However, 22 readings, or 18% of all measurements, exceeded 300 μm (12 mils). The maximum thickness was 350 μm (14 mils). In addition, the deviation in coating thickness of almost half of all steel specimens fell beyond the allowable limits. Thus, there was a lack of uniformity in the coating thickness and the specifications were not strictly met.

In general, the 13-mm (#4) bar specimens had slightly thicker coatings than the 25-mm (#8) bar specimens. The average coating thickness of the smaller size bars with parallel and cross deformations were 250 and 270 μm (9.9 and 10.5 mils), respectively. The corresponding average coating thickness of all the larger size bars were 240 μm

(9.5 mils). The differences in average coating thickness between bars with different deformation patterns were insignificant, although bars with cross deformations tended to be slightly thicker than those with parallel deformations. The overall average coating thickness was approximately 250 μm (10 mils).

The uniformity of coating thickness did not relate to bar size or deformation pattern. This was concluded from calculations of the difference between the highest and lowest measured coating thickness on each individual bar. The difference was expressed as a percentage of the bar average coating thickness. The results of these calculations were compared between the bars of different sizes and different deformation patterns and no consistent trend was apparent.

The bars in each group of Series A and B were carefully selected in order to minimize the effect of coating thickness variability on the corrosion performance. The criterion of selection was that the average thickness of coating of bars in a group was not significantly different from group to group. Hence, any difference in the corrosion behavior among the groups would be related to the study variables discussed earlier. For example, a difference between the average corrosion rate of bars in A.2 group and that of A.3 group would be due solely to patching the damaged spots on group A.3 bars. The average coating thickness for each group in Series A and B are shown in Table A.5.

Table A.5 Group average coating thickness for macrocell steel specimens.

Series A		Series B	
Group Number	**Average Coating Thickness (μm)**	**Group Number**	**Average Coating Thickness (μm)**
A.2	250	B.2	250
A.3	250	B.3	240
A.4	260	B.4	240
A.5	240	B.5	250
A.6	260	B.6	240
A.7	250	B.7	250
A.9	270	B.9	250
A.10	260	B.10	230
A.11	250	B.11	220

A.2.5 Coating Defects and Introduced Damage

The bars were carefully inspected before deliberately introducing further damage. As mentioned earlier, despite the protection on the mandrels used for bending, impressions on the ribs along the inside of bends were introduced. In addition, the backup barrel (a pin which holds the bar straight during bending) generally caused one or two relatively large damaged spots on the outside surface near the beginning of bend. These damage areas, and any others, were included in the calculations of the required additional exposed steel areas to reach the levels of damage set for testing.

The condition of each bar was carefully documented. The documentation included the coating appearance, and the number, approximate size, and location of existing damage. A commercially available holiday detector (SPY Model 67) was used to determine the number and location of holidays. The majority of bars had the same uniform, glossy

appearance. Only a few bars had either slightly discolored coating, or very thin films through which the dark substrate was visible. Except for this last group of thinly-coated bars, coating coverage was fair and the deformations were well-defined.

Some bars, particularly the 13-mm (#4) bars with parallel deformations, disclosed hairline cracking along the transverse ribs on the outside of bends. The cracks extended between approximately 6 to 12 mm (1/4 to 1/2 in.). Sometimes, these cracks appeared at almost every transverse lug in the bend area. Cracks on bars with cross deformations were generally in the form of very fine intermittent tears (pinholes) concentrated along the rib bases. In all cases, no discernable debonding was detected.

Where additional surface damage was desired, damage was purposely introduced on the outside of bends. File marks were made at the transverse lugs and in between the lugs in small rectangular shapes using a sharp blade. Coating prying was easier on the bar surface than on the lugs, and even easier on the bent portion compared to the straight ends. Generally, the coating on the straight ends was tough and difficult to pry. Some of the coating flakes removed showed dark spotting on the backside.

The introduced damage was documented and each bar was photographed for a record of initial conditions. Tables A.6 to A.9 list descriptions of the introduced damage, the total steel surface area damaged, and the total damage percentage for each bar. Figures A.6 to A.12 show examples of the damaged bars included in the macrocell test.

Table A.6 Description of coating damage of steel specimens, Series A, parallel deformations.

Specimen	Introduced Damaged Area		Total Steel Area Damaged[a]	Total Damage Percentage (%)	
	No. and Size (mm)	Condition	(mm^2)	Patched[b]	Exposed
1 A.2	1 Spot 10 x 7	Patched	160	0.56	0.64
2 A.2	1 Spot 10 x 9	Patched	160	0.64	0.57
3 A.2	1 Spot 10 x 8	Patched	160	0.58	0.61
1 A.3	1 Spot 10 x 8	Exposed	160	-	1.23
2 A.3	1 Spot 11 x 8	Exposed	160	-	1.22
3 A.3	1 Spot 11 x 8	Exposed	160	-	1.21
1 A.4	7 Spots 5 x 2 8 Spots 5 x 4	Patched	280	1.57	0.54
2 A.4	7 Spots 5 x 2 8 Spots 5 x 4	Patched	280	1.60	0.56
3 A.4	7 Spots 5 x 2 8 Spots 5 x 4	Patched	280	1.56	0.56
1 A.5	7 Spots 5 x 2 8 Spots 5 x 4	Exposed	270	-	2.09
2 A.5	7 Spots 5 x 2 8 Spots 5 x 4	Exposed	270	-	2.08
3 A.5	7 Spots 5 x 2 8 Spots 5 x 4	Exposed	270	-	2.08
1 A.6	(Existing Cracks)	Exposed	80	-	0.65
2 A.6	(Existing Cracks)	Exposed	80	-	0.62
3 A.6	(Existing Cracks)	Exposed	80	-	0.65
1 A.7	3 Spots 5 x 5 5 Spots 2 x 2	Exposed	160	-	1.23
2 A.7	5 Spots 5 x 4	Exposed	160	-	1.22
3 A.7	5 Spots 5 x 4	Exposed	160	-	1.22

a Area includes damage on both the inside and outside of bend.
b Only introduced damaged area on the outside surface of bend was patched.

Table A.7 Description of coating damage of steel specimens, Series A, cross deformations.

Specimen	Introduced Damaged Area		Total Steel Area Damaged[a]	Total Damage Percentage (%)	
	No. and Size (mm)	Condition	(mm^2)	Patched[b]	Exposed
1 A.9	1 Spot 11 x 10	Patched	160	0.81	0.43
2 A.9	1 Spot 11 x 10	Patched	160	0.81	0.41
3 A.9	1 Spot 11 x 10	Patched	160	0.81	0.46
1 A.10	1 Spot 10 x 10	Exposed	160	-	1.20
2 A.10	1 Spot 11 x 10	Exposed	160	-	1.23
3 A.10	1 Spot 11 x 10	Exposed	160	-	1.20
1 A.11	(Existing Pinholes)	Exposed	90	-	0.68
2 A.11	(Existing Pinholes)	Exposed	80	-	0.57
3 A.11	(Existing Pinholes)	Exposed	80	-	0.64

a Area includes damage on both the inside and outside of bend.
b Only introduced damaged area on the outside surface of bend was patched.

Table A.8 Description of coating damage of steel specimens, Series B, parallel deformations.

Specimen	Introduced Damaged Area		Total Steel Area Damaged[a]	Total Damage Percentage (%)	
	No. and Size (mm)	Condition	(mm^2)	Patched[b]	Exposed
1 B.2	2(9 x 7) + 2(13 x 4)	Patched	520	0.66	0.85
2 B.2	2(10 x 6) + 2(13 x 5)	Patched	510	0.70	0.79
3 B.2	2(10 x 6) + 2(13 x 6)	Patched	510	0.82	0.64
1 B.3	2(10 x 7) + 2(14 x 4)	Exposed	500	-	1.47
2 B.3	2(10 x 7) + 2(14 x 4)	Exposed	500	-	1.45
3 B.3	2(10 x 6) + 2(14 x 6)	Exposed	500	-	1.46
1 B.4	16(5 x 5) + 12(6 x 2)	Patched	740	1.51	0.65
2 B.4	16(5 x 4) + 12(6 x 2)	Patched	730	1.34	0.76
3 B.4	16(5 x 5) + 12(5 x 2)	Patched	740	1.45	0.70
1 B.5	16(5 x 4) + 12(5 x 2)	Exposed	770	-	2.24
2 B.5	16(5 x 5) + 12(5 x 2)	Exposed	750	-	2.19
3 B.5	16(6 x 5) + 12(5 x 2)	Exposed	740	-	2.13
1 B.6	6 Hairline Cracks	Exposed	300	-	0.89
2 B.6	6 Hairline Cracks	Exposed	300	-	0.84
3 B.6	6 Hairline Cracks	Exposed	300	-	0.86
1 B.7	5(6 x 5) + 6(6 x 2)	Exposed	410	-	1.19
2 B.7	5(5 x 5) + 4(5 x 2)	Exposed	410	-	1.19
3 B.7	5(5 x 5) + 6(6 x 2)	Exposed	390	-	1.11

a Area includes damage on both the inside and outside of bend.
b Only introduced damaged area on the outside surface of bend was patched.

Table A.9 Description of coating damage of steel specimens, Series B, cross deformations.

Specimen	Introduced Damaged Area		Total Steel Area Damaged[a] (mm^2)	Total Damage Percentage (%)	
	No. and Size (mm)	Condition		Patched[b]	Exposed
1 B.9	1 Spot 11 x 6 1 Spot 10 x 6 1 Spot 25 x 2 1 Spot 16 x 3	Patched	330	0.64	0.30
2 B.9	1 Spot 11 x 6 1 Spot 10 x 7 1 Spot 29 x 2 1 Spot 13 x 3	Patched	670	0.85	1.10
3 B.9	1 Spot 10 x 6 1 Spot 11 x 6 1 Spot 11 x 6 1 Spot 13 x 3	Patched	500	0.70	0.74
1 B.10	1 Spot 10 x 6 1 Spot 10 x 6 1 Spot 32 x 2 1 Spot 14 x 3	Exposed	580	-	1.69
2 B.10	1 Spot 10 x 6 1 Spot 11 x 6 1 Spot 22 x 2 1 Spot 13 x 3	Exposed	700	-	2.02
3 B.10	1 Spot 10 x 6 1 Spot 10 x 5 1 Spot 25 x 2 1 Spot 19 x 3	Exposed	500	-	1.42
1 B.11	(Existing Pinholes)	Exposed	180	-	0.52
2 B.11	(Existing Pinholes)	Exposed	210	-	0.62
3 B.11	(Existing Pinholes)	Exposed	210	-	0.62

a Area includes damage on both the inside and outside of bend.
b Only introduced damaged area on the outside surface of bend was patched.

(a) 13-mm (#4) bar (groups A.2, A.3)

(b) 25-mm (#8) bar (groups B.2, B.3)

Figure A.6 Damage spots > 6x6 mm, bars with parallel deformations.

(a) 13-mm (#4) bar (groups A.4, A.5)

(a) 25-mm (#8) bar (groups B.4, B.5)

Figure A.7 Damage spots > 2%, bars with parallel deformations.

(a) 13-mm (#4) bar (group A.6)

(b) 25-mm (#8) bar (group B.6)

Figure A.8 Hairline cracks, total damage < 1%, bars with parallel deformations.

(a) 13-mm (#4) bar (group A.7)

(b) 25-mm (#8) bar (group B.7)

Figure A.9 Damage spots < 2%, bars with parallel deformations.

(a) 13-mm (#4) bar (groups A.9, A.10)

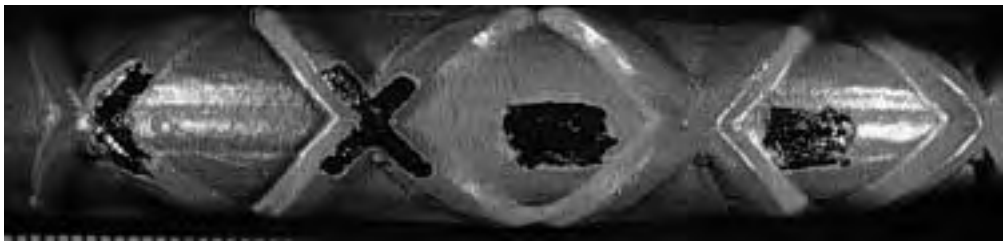

(b) 25-mm (#8) bar (groups B.9, B10)

Figure A.10 Damage spots > 6x6 mm, bars with cross deformations.

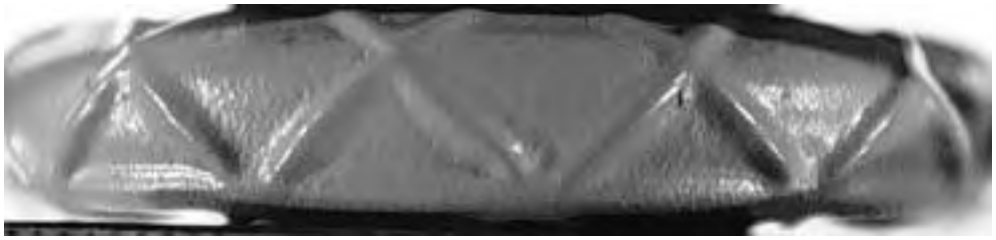

(a) 13-mm (#4) bar (group A.11)

(b) 25-mm (#8) bar (group B.11)

Figure A.11 As-received (pinholes) < 1%, bars with cross deformations.

(a) Bar with parallel deformations

(b) Bar with cross deformations

Figure A.12 Typical damage on the inside of bend.

Only the introduced damaged areas on bar specimens in groups A.2, A.9, B.2, and B.9 were patched. A two-part liquid epoxy, especially formulated for coating repair, was applied by brush. The exposed steel areas were not given any special treatment before patching. Figure A.13 shows examples of patched damaged areas on two test bars.

(a) Damage spots > 6x6 mm, bar with parallel deformations

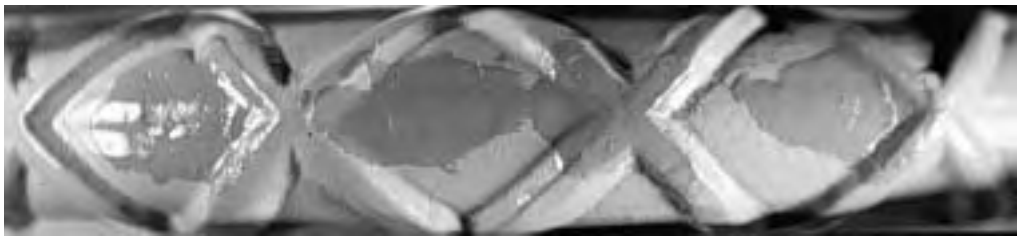

(b) Damage spots > 6x6 mm, bar with cross deformations

Figure A.13 Examples of patched coating damage.

A.3 UNCOATED REINFORCING STEEL

A.3.1 Anode Steel Bars

The uncoated bars used as control specimens were left in their "as received" condition, *i.e.* with mill scale. These bars represent, as closely as possible, bars placed in the field.

A.3.2 Cathode Steel Bars

All bars used in the bottom reinforcing layer of the specimens were grade 60 with a parallel deformation pattern. The bars of each size, the 19- and 28-mm diameters (#6 and #9), were obtained from the same heat of steel so that they would have the same chemical composition and mechanical properties. This selection ensured that the rates of corrosion of the anodes were not influenced by differences in the electrical properties of the cathodes.

The bars were further treated chemically by a pickling process as per ASTM G109-92[64] before placement in formwork. The process started with wire brushing and dusting the bars to remove mill scale. The bars were subsequently dipped in a 10% sulfuric acid solution for 15 to 20 minutes. Upon removal, they were rinsed in two baths of clean water for about three minutes each. Finally, the bars were spayed with rubbing alcohol and dried with paper towels.

A.4 FORMWORK AND STEEL INSTALLATION

A.4.1 Formwork

The formwork for the macrocell specimens consisted of a plywood base with plywood dividers that formed individual compartments (see Figure A.14). The front plywood panel of each compartment was predrilled to position the top and bottom bars at the proper dimensions. The formwork was completed by placing wales along the top of both sides of the forms and several braces across the forms. The wales and braces maintained the dimensions of specimens during casting.

(a) Series A

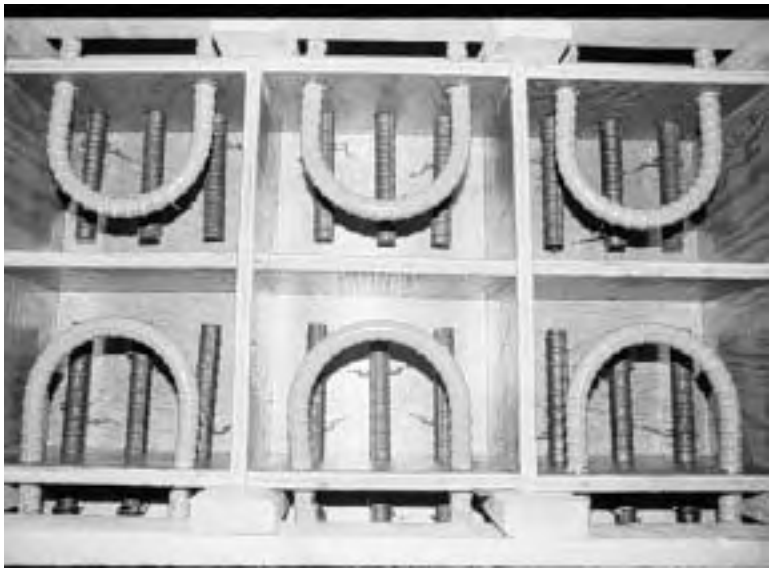

(b) Series B

Figure A.14 Formwork for macrocell specimens.

The formwork for the companion chloride specimens was constructed similarly. These specimens were small and the forms did not require bracing.

A.4.2 Steel Installation

The reinforcement was placed into the formwork by inserting the bars through the front plywood panel as shown in Figure A.14. The bottom bars were firmly fixed so that their position would not change during concrete placement. The top bars were tightly maintained in position by the front panels and the wales.

A.5 CONCRETE

A.5.1 Mixture Design

Since concrete of inferior quality will offer less protection against corrosion of the embedded steel, it is often used in corrosion testing to accelerate the corrosion process and produce results within reasonable time limits. Therefore, concrete of reduced strength and increased permeability was used to construct the test specimens. The concrete mixture contained 231 kg/m^3 (389 lb./yd^3) of total cement content, and a maximum aggregate size of 20 mm (3/4 in.). The water/cement ratio was fairly high at 0.57 which resulted in a slump of 150 mm (6 in.) without using a water reducing agent. The details of the concrete mixture are shown in Table A.10.

Table A.10 Concrete mixture details for macrocell study.

Material	Quantity	Unit
20 mm Rock, SSD	1097	kg/m^3
Sand, SSD	875	kg/m^3
Type I Portland Cement	221	kg/m^3
Pozzolana R	10	kg/m^3
Water	132	kg/m^3
Water/Cement Ratio	0.57	
Unit Weight	2278	kg/m^3
Slump	150	mm

A.5.2 Casting

Concrete was provided by a ready mix supplier. Casting was done indoors by placing concrete with shovels into the forms. The concrete was placed in one lift and consolidated using 50 mm (2 in.) head internal vibrators as shown in Figure A.15. The vibrators were inserted only at the back sides of Series A specimens to avoid shifting or damaging the steel bars.

The same concrete was used to cast all 68 macrocell specimens in Series A and B, 30 specimens in Series C, and a large number of standard cylinders. The specimens were screeded immediately after placing concrete and trowelled shortly after. The specimens were then covered with plastic sheets to reduce water evaporation.

Figure A.15 Casting macrocell specimens.

A.5.3 Curing

After two days of casting, the forms and cylinder molds were stripped and no further curing of the specimens was provided. The idea was to slow concrete strength gain which is normally considered an indicator of concrete permeability. Some cylinders were placed in a humidity chamber under standard curing conditions. The rest of the cylinders were exposed to the same atmospheric exposure conditions as the macrocell specimens.

A.5.4 Compressive Strength

Concrete strength was determined at 2, 7, 14, 28, 90, and 365 days after casting. The 28-day strength was determined from both air-cured cylinders and cylinders just removed from the curing chamber which yielded similar results (around 30 MPa (4350 psi)). The strength-gain curve is shown in Figure A.16.

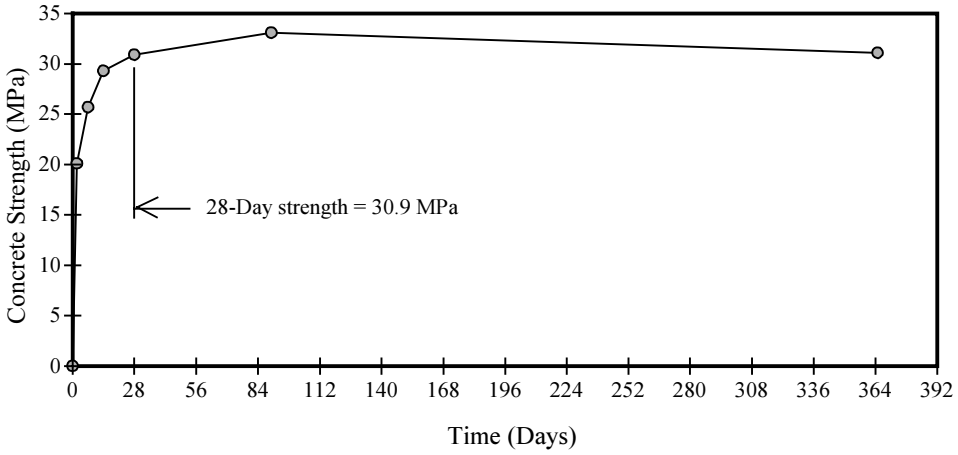

Figure A.16 Compressive strength gain of macrocell concrete.

A.5.5 Permeability

Concrete permeability was determined from 100 x 200 mm (4 x 8 in.) cylinders using a standard test procedure for Rapid Determination of the Chloride Permeability of Concrete (AASHTO T277-83).[65] The cylinders were air-cured under the same conditions as the macrocell specimens, and tested at ages of 280 and 490 days after casting. The respective permeability measurements were 9360 and 6600 coulombs which fell under the standard classification of "high" permeability.

A.6 TEST SETUP

A.6.1 Specimen Preparation

The sides of all specimens were sealed to simulate a continuous slab environment. Two coats of a clear waterproof material were applied (brush strokes) at right angles on each side for effective insulation. Plexiglass dikes 75 mm (3 in.) high were mounted with silicon around the edges of the top surfaces to contain the salt solution. The specimens were placed on shelves on narrow wooden strips to allow air circulation under the soffits.

The bottom bars were made electrically continuous by welding a short, 6-mm diameter (#2) bar across the protruding ends. Electrical leads were attached to the top and one of the bottom bars using electrical ground clamps properly secured into the steel metal. A 100 ohm resistor was connected to the two clamps to bridge between the reinforcing layers. This ohmic resistance is in the low range when compared with the internal resistance of concrete. Wires of equal length were used to connect the specimens to the electronic data acquisition equipment to avoid unequal potential drops in the wires between the specimen and the equipment. Figure A.17 shows a schematic view of one of Series B macrocell specimens.

The resistors were measured before starting the test and were found to vary by a maximum of about 10%. Therefore, the resistance reading for each specimen was recorded and checked several times at different dates. To read the resistance, one end of each resistor was disconnected from the clamp and a hand-held voltmeter was used for measurement. An average resistance for each resistor was calculated and used for determining the corrosion current passing through the particular specimen.

The attachment areas and the protruding portions of the epoxy-coated bars were coated with a patching epoxy compound. The exposed parts of the uncoated bars were frequently covered with a protective oil.

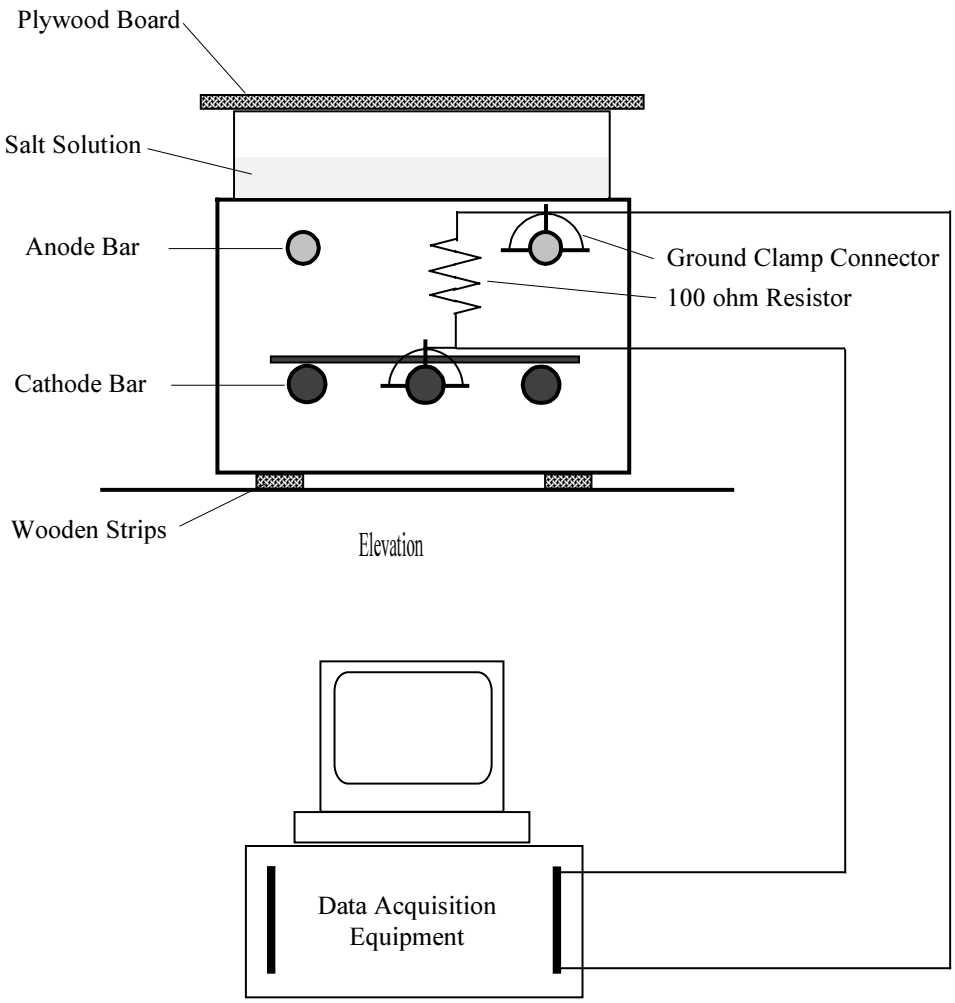

Figure A.17 Schematic view of macrocell test specimen.

A.6.2 Exposure Conditions

All macrocell specimens, and the specimens used for chloride determination, were subjected to alternate wetting and drying using a 3.5% NaCl solution. Only the top surfaces were ponded with solution to a depth of about 35 mm (1.5 in.). Evaporation of the solution was minimized by covering the dikes with plywood. The wetting period lasted two weeks, followed by removing the solution and allowing the specimens to dry at room temperature for two more weeks. The four-week exposure cycle was repeated continuously. The first ponding period was started when concrete was 42 days old.

A fresh solution was prepared at the beginning of each wet period. The solution was removed by suction and discarded at the end of the wet period. The top surfaces of the specimens were washed periodically (every 3-4 cycles) with clean water to dissolve any salt buildup or crystallization in the concrete cover.

To avoid varying temperatures, which can alter the electrical resistivity of concrete between the reinforcing layers, and therefore, the corrosion rate, the specimens were placed in a temperature-controlled room. This eliminated the need for adjusting the measured macrocell currents to a uniform base.

A.7 ROUTINE MONITORING

A.7.1 Visual Examination

The macrocell specimens were visually inspected at the beginning of the test and periodically thereafter. Any initial cracks detected on the top concrete surfaces (suspected to be due to plastic settlement), such as those shown in Figure A.18, were documented before testing. Specimens that exhibited such cracking were the following:

Series A: 1A.3, 2A.6, 1A.8, 2A.8, 2A.10.

Series B: 2B.1, 1B.3, 3B.3, 1B.4, 2B.4, 3B.4, 1B.5, 2B.5, 3B.5, 3B.6, 3B.7, 2B.9, 1B.10.

The development of surface staining and new cracks were monitored during the test.

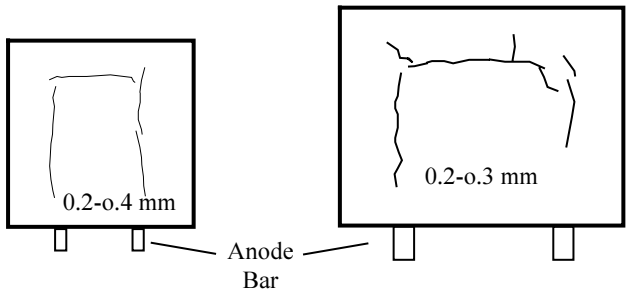

(a) 1 A.3 Specimen (b) 3 B.7 Specimen

Figure A.18 Examples of initial cracks detected on top surfaces of macrocell specimens.

A.7.2 Voltage and Current Measurements

A closed electrical circuit was maintained at all times during the test. The voltage drop across the resistor in each macrocell specimen was electronically monitored. A digital data acquisition system was used to scan the voltages periodically. Before starting the test, the initial voltage readings were obtained and stored. Subsequent voltage measurements were taken every one or two weeks (at the end of each wetting and drying period) for five months. The voltages were, thereafter, measured every week to observe any abrupt changes.

A voltage is developed when an electrical current flows through the resistor. Since the only electrical contact between the reinforcing layers was exterior to the specimen, the flowing current was the net corrosion current developed in the macrocell. The measured voltage is related to the current by Ohm's Law,

$$I = \frac{V}{R} \qquad \text{(A.1)}$$

where, I is the electrical current, V is the voltage, and R is the resistance. The voltage data were automatically converted to electrical currents. Adjustment for the initial voltage readings was done by processing the data using an electronic spreadsheet.

A.7.3 Corrosion Potential Measurement

Corrosion potentials of the top bars were monitored for the last 10 months of exposure for the last triplicates only. Corrosion potentials were measured by placing a saturated calomel electrode probe on the top surface of the specimens. The probe was located at three points: above the middle of straight bar legs and above the center of the bent portion, as indicated in Figure A.19. The probe was connected to a voltmeter and the circuit was completed by connecting the other terminal to the top bar. During initial potential measurements, the continuity between top and bottom bars was temporarily interrupted to isolate the top bar and reflect its true potentials. This practice was later abandoned because only a small difference was observed in the potentials depending on continuity between bar layers.

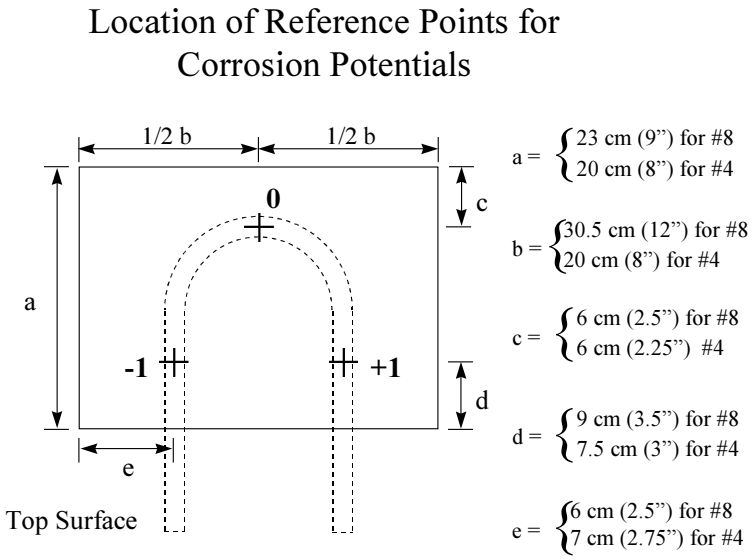

Figure A.19 Top surface of macrocell with points for corrosion potentials.

A.7.4 Temperature Measurement

The temperature inside the test room was measured every week at the time of voltage reading. Although the temperature was automatically controlled, slight variations occurred from one season to another. The yearly average temperature was 23° C (73° F). About 90% of the time the temperature remained within ±3° C (±5° F). Therefore, the effects of temperature changes on the corrosion rates during the test period can be neglected.

A.7.5 Chloride Content Determination

During the first two year of exposure, chloride levels in concrete were determined every full cycle of exposure, *i.e.* every 28 days. Because of the limited number of prisms available for the last 2.5 years of exposure, samples were obtained much less often during that period. A different specimen from Series C was used every time to extract concrete powder samples used for chloride determination. The concrete samples were collected from multiple holes. The holes were drilled to various depths, at about 6-mm (1/4-in.) intervals, to determine chloride concentrations at different levels of penetration. Two chloride samples were analyzed from each selected depth range. Figure A.20 shows the drilling procedure for concrete sampling.

Figure A.20 Extracting concrete powder sample for chloride determination.

The acid-soluble chloride content was determined using a rapid method of measuring chlorides in concrete on site. The test has the same accuracy as standard titration made in the laboratory. The chloride concentrations measured with time are shown in Table A.11. These concentrations, particularly at the steel level, were related to corrosion activity.

Table A.11 Acid-soluble chloride concentrations in concrete during macrocell exposure testing (percentage by weight of concrete).

Days of Exposure	Sampling Depth Ranges (mm)					
	6-12	19-25	32-38	45-51	57-63	70-76
28	0.25	0.09				
56	0.56	0.16				
84	0.42	0.20	0.09			
112	0.47	0.27	0.15			
140	0.43	0.20	0.08			
168	0.62	0.28	0.17	0.10		
196	0.62	0.34	0.20	0.09		
224	0.49	0.32	0.18	0.10		
252	0.53	0.34	0.20	0.11	0.07	
280	0.40	0.28	0.20	0.09	0.06	
308	0.63	0.31	0.29	0.16	0.07	0.07
336	0.40	0.28	0.21	0.07	0.00	0.00
364	0.38	0.25	0.17	0.06	0.00	0.00
392	0.40	0.25	0.20	0.17	0.07	0.00
420	0.35	0.29	0.22	0.13	0.03	0.00
448	0.28	0.18	0.10	0.04	0.00	0.00
476	0.38	0.21	0.17	0.12	0.01	0.00
504	0.33	0.18	0.15	0.12	0.00	0.00
532	0.31	0.29	0.15	0.10	0.04	0.00
560	0.34	0.29	0.18	0.10	0.02	0.00
588	0.44	0.28	0.17	0.12	0.02	0.00
616	0.41	0.38	0.19	0.20	0.13	0.05
644	0.34	0.17	0.22	0.26	0.13	0.04
672	0.37	0.25	0.18	0.12	0.07	0.02
700	0.34	0.24	0.25	0.19	0.12	0.05
728	0.38	0.22	0.18	0.16	0.15	0.06
821	0.41	0.26	0.21	0.12	0.07	0.002
869	0.44	0.27	0.26	0.23	0.12	0.09
925	0.39	0.29	0.27	0.26	0.14	0.08
981	0.35	0.25	0.32	0.26	0.12	0.06
1,037	0.56	0.44	0.33	0.27	0.32	0.31
1,653	0.63	0.46	0.45	0.41	0.44	0.43

A.8 POSTMORTEM EXAMINATION

A.8.1 General

One of the replicate specimens in each group was removed for demolition after 1, 2, and 4.5 years of exposure. Generally, the selected specimen was the one showing maximum corrosion activity indicated by the history of the corrosion current.

A.8.2 Concrete Condition

Prior to destruction, delamination of concrete was checked by hammer sounding. Concrete surfaces were struck with a hammer at several locations to detect any delaminated areas. Corrosion-induced cracks and stains on the specimens removed are illustrated in Figures A.21 though A.26.

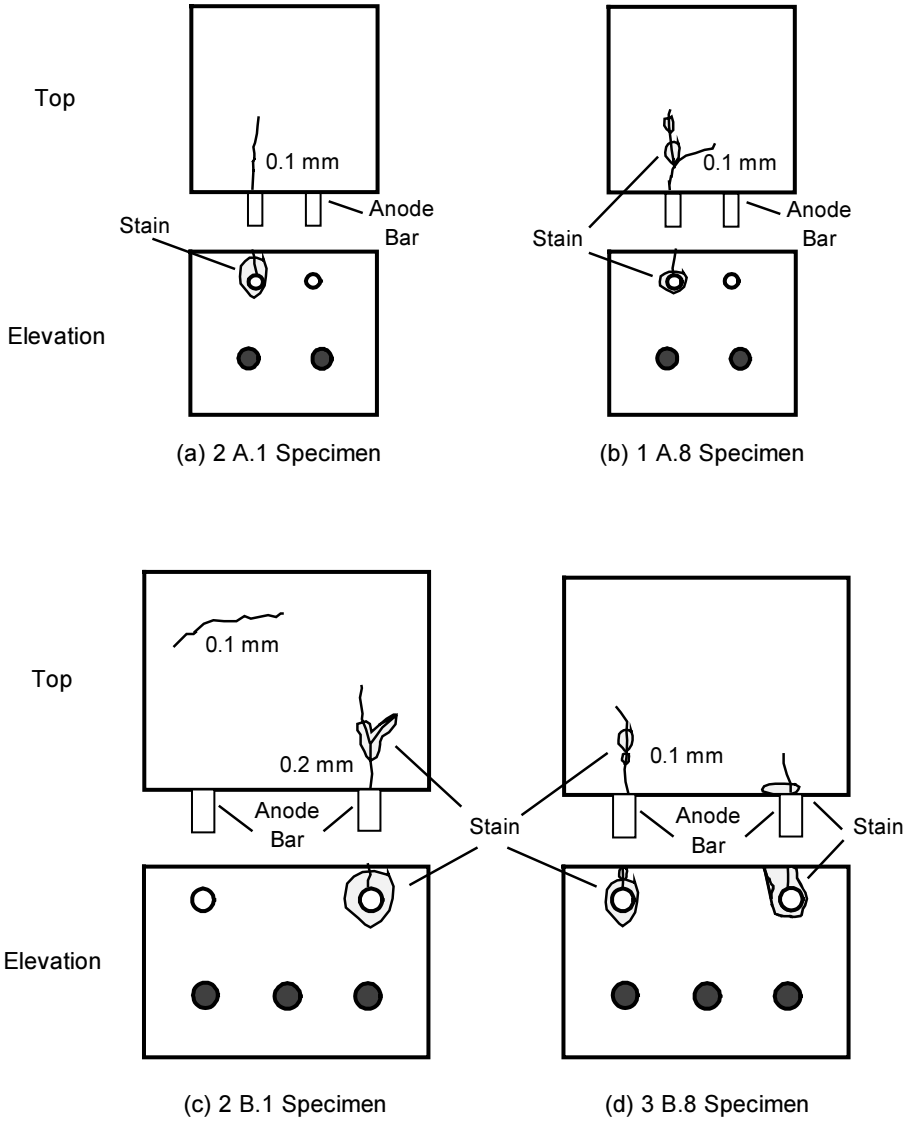

Figure A.21 Cracks and stains on macrocell specimens autopsied after one year of exposure.

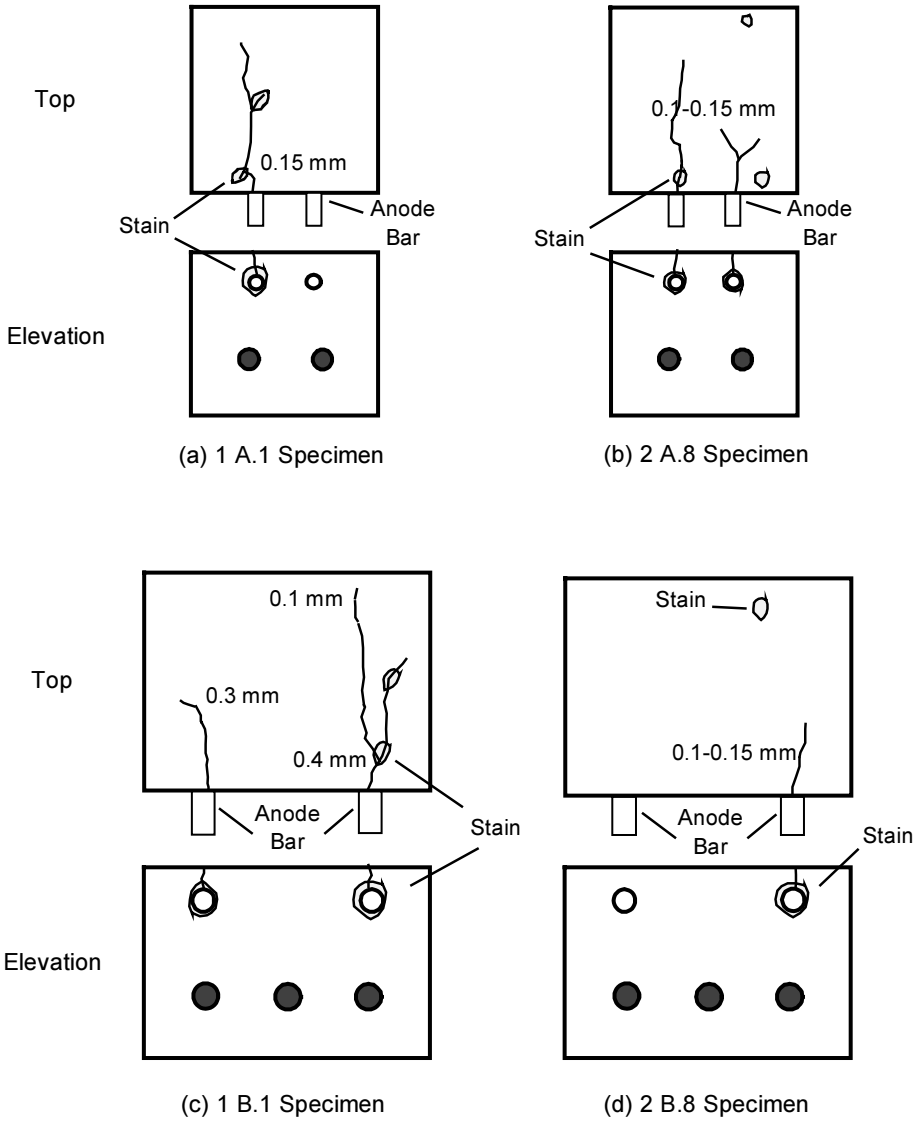

Figure A.22 Cracks and stains on macrocell specimens autopsied after two years of exposure.

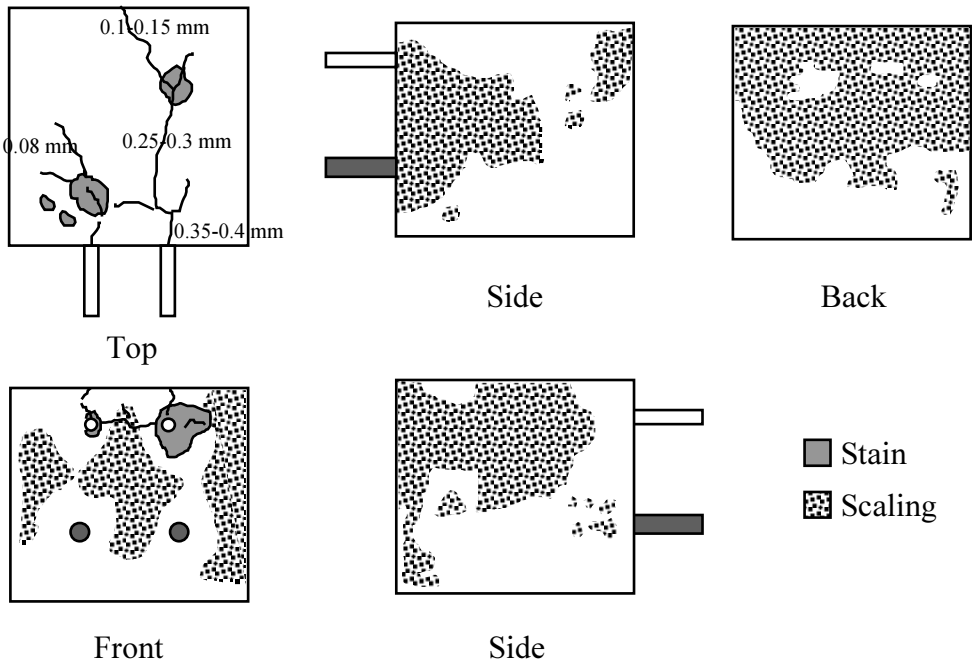

(a) 3A.1 Specimen

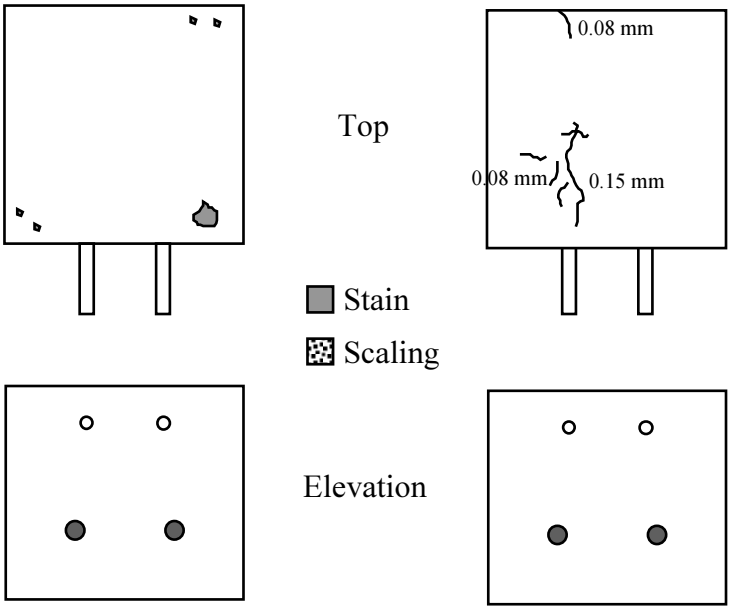

(b) 3A.4 Specimen (c) 2A.6 Specimen

Figure A.23 Cracks and stains on macrocell specimens 3A1, 3A.4, and 2A.6 inspected after 4.5 years of exposure.

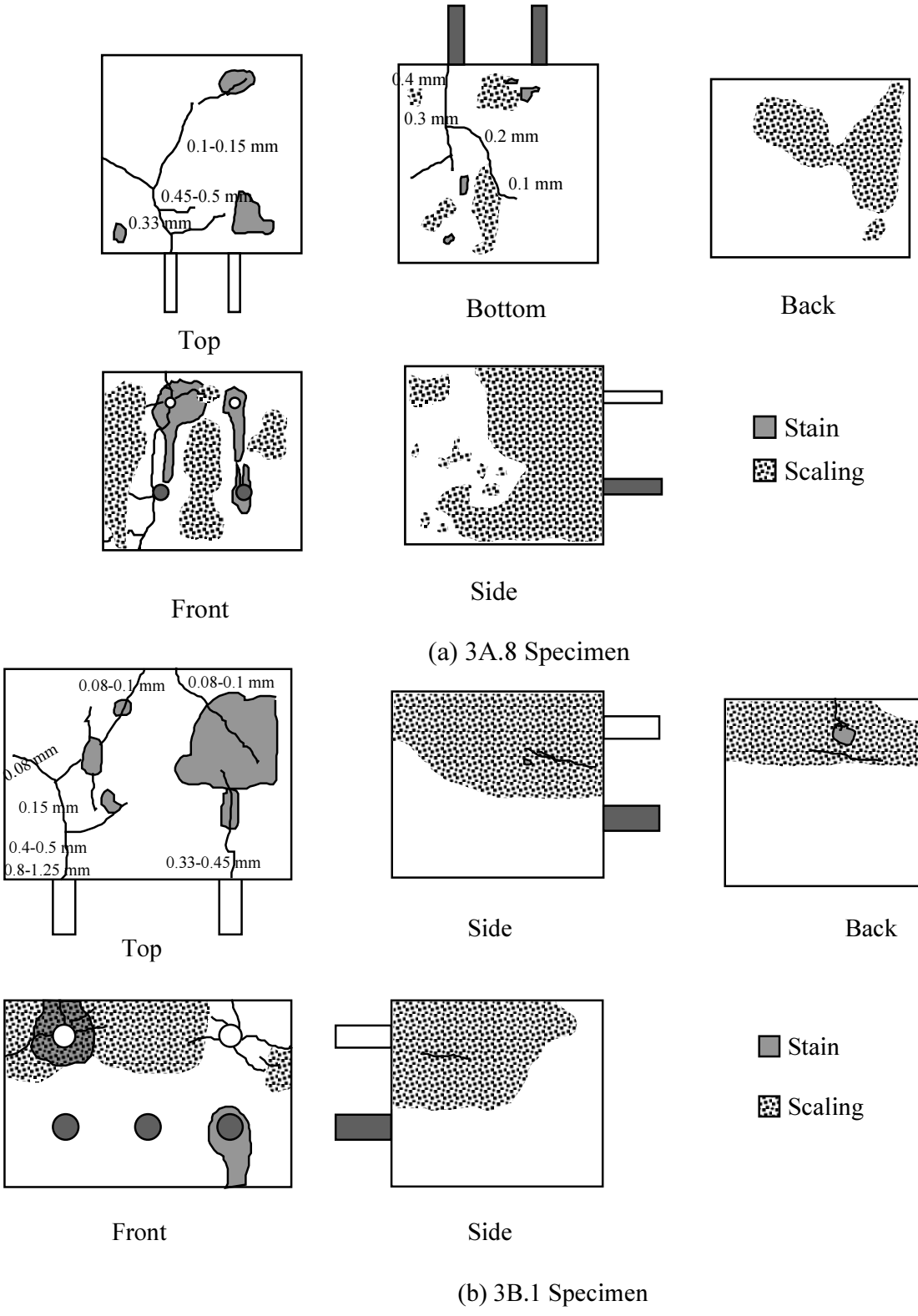

Figure A.24 Cracks and stains on macrocell specimens 3A.8 and 3B.1 inspected after 4.5 years of exposure.

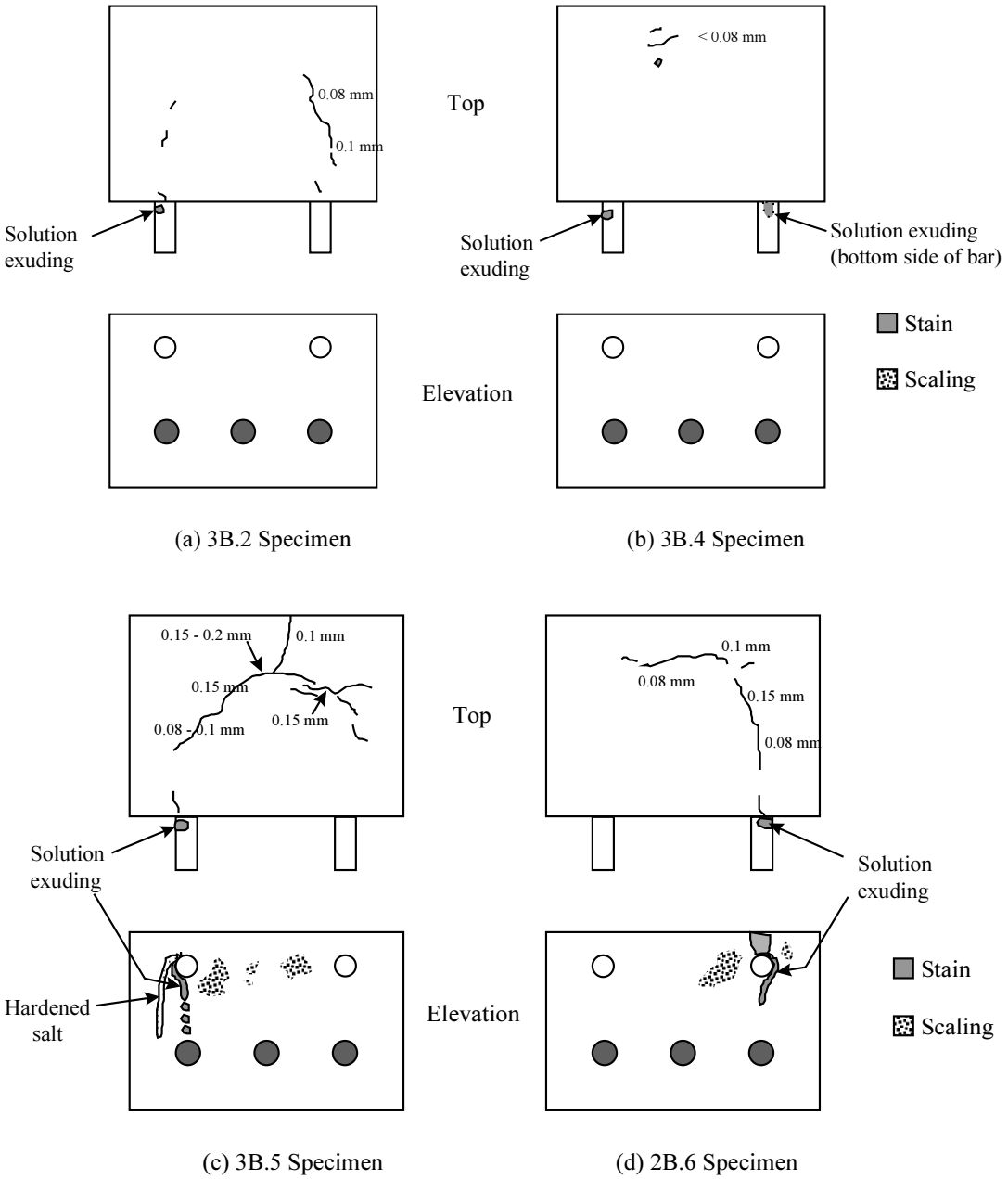

Figure A.25 Cracks and stains on macrocell specimens 3B.2, 3B.4, 3B.5, and 2B.6 inspected after 4.5 years of exposure.

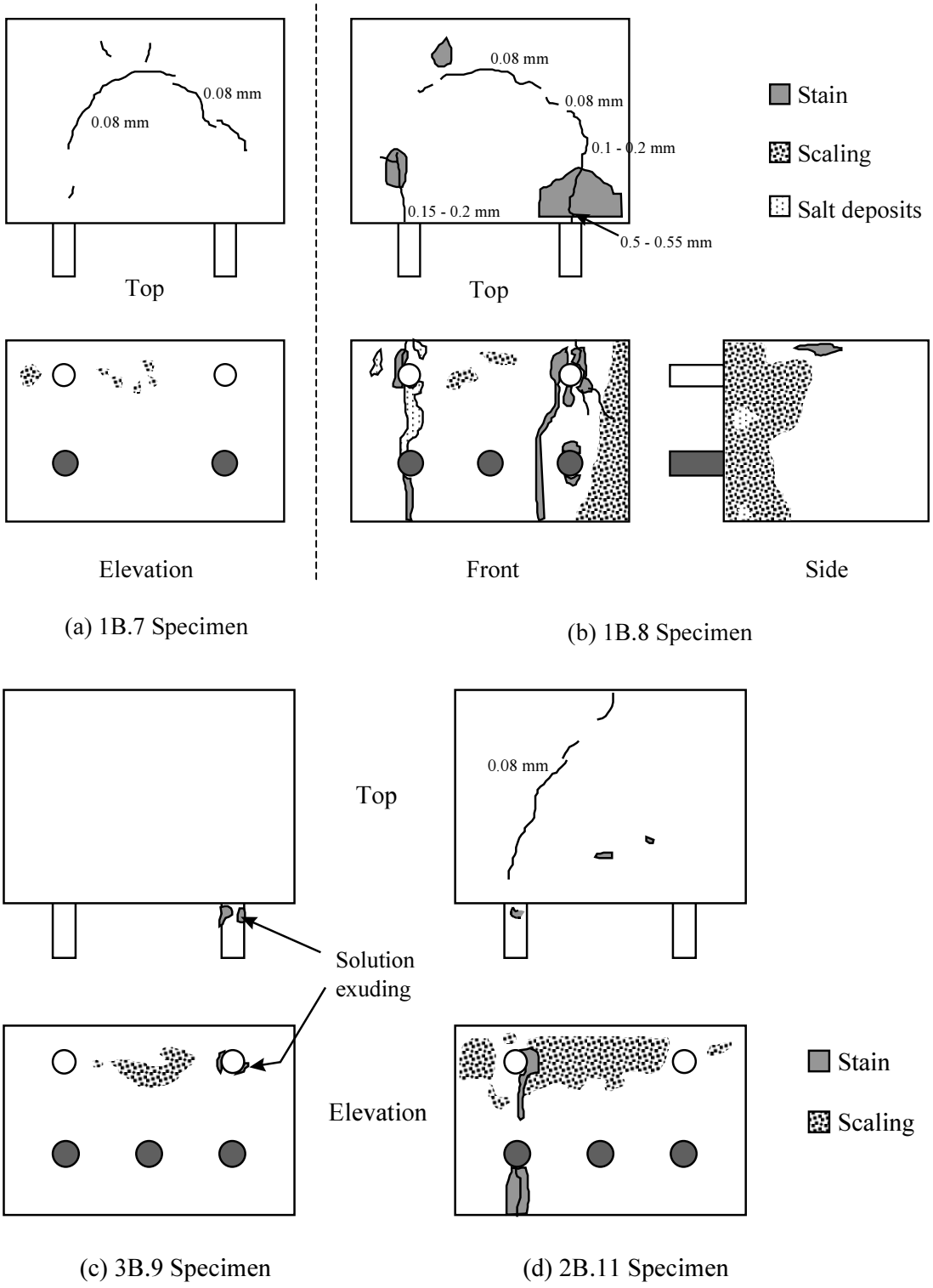

Figure A.26 Cracks and stains on macrocell specimens 1B.7, 1B.8, 3B.9, and 2B.11 inspected after 4.5 years of exposure.

A.8.3 CHLORIDE CONTENT

Chloride samples from each specimen removed were extracted and analyzed to determine the acid-soluble chloride content at various depths. The samples were obtained (before performing autopsy of the specimens) from a single hole drilled very close to the middle of the inside radius of the embedded bent bar. Two samples for each representative depth were obtained. The chloride contents of the autopsied specimens at 1, 2, and 4.5 years are shown in Tables A.12, A.13, and A.14, respectively.

Table A.12 Acid-soluble chloride concentrations in autopsied macrocell specimens after one year of exposure (percentage by weight of concrete).

Specimen	Sampling Depth Ranges (mm)				
	6-12	19-25	32-38	45-51	57-63
2 A.1	0.49	0.35	0.18	0.15	0.05
1 A.2	0.21	0.24	0.16	0.07	0.03
2 A.3	0.42	0.35	0.19	0.10	0.05
1 A.4	0.35	0.26	0.23	0.10	0.02
2 A.5	0.32	0.23	0.20	0.14	0.07
1 A.6	0.30	0.24	0.19	0.08	0.01
1 A.7	0.408	0.24	0.12	0.10	0.03
1 A.8	0.42	0.30	0.21	0.19	0.10
1 A.9	0.41	0.25	0.12	0.09	0.01
3 A.10	0.39	0.32	0.14	0.12	0.01
1 A.11	0.39	0.26	0.15	0.07	0.00
2 B.1	0.41	0.29	0.20	0.11	0.05
2 B.2	0.39	0.27	0.24	0.17	0.08
1 B.3	0.49	0.28	0.19	0.18	0.07
1 B.4	0.45	0.25	0.17	0.10	0.09
1 B.5	0.44	0.29	0.22	0.17	0.11
3 B.6	0.55	0.27	0.20	0.30	0.14
2 B.7	0.59	0.41	0.27	0.20	0.08
3 B.8	0.42	0.28	0.20	0.10	0.05
2 B.9	0.34	0.23	0.20	0.14	0.11
1 B.10	0.39	0.30	0.26	0.17	0.10
3 B.11	0.30	0.30	0.21	0.12	0.08

Table A.13 Acid-soluble chloride concentrations in autopsied macrocell specimens after two years of exposure (percentage by weight of concrete).

Specimen	Sampling Depth Ranges (mm)			
	19-32	**32-38**	**38-51**	**76-89**
1 A.1	0.24	0.30	-	0.05
2 A.2	0.22	0.19	-	0.00
1 A.3	0.17	0.17	-	0.07
2 A.4	0.22	0.14	-	0.00
3 A.5	0.23	0.23	-	0.00
3 A.6	0.25	0.27	-	0.00
2 A.7	0.22	0.20	-	0.00
2 A.8	0.34	0.31	-	0.08
2 A.9	0.19	0.17	-	0.00
2 A.10	0.33	0.24	-	0.00
2 A.11	0.37	0.22	-	0.00
1 B.1	0.26	-	0.19	0.05
1 B.2	0.27	-	0.19	0.06
3 B.3	0.20	-	0.20	0.03
2 B.4	0.23	-	0.18	0.05
2 B.5	0.19	-	0.22	0.09
1 B.6	0.25	-	0.24	0.08
3 B.7	0.28	-	0.22	0.09
2 B.8	0.19	-	0.16	0.07
1 B.9	0.33	-	0.20	0.05
3 B.10	0.14	-	0.10	0.09
1 B.11	0.28	-	0.22	0.07

Table A.14 Acid-soluble chloride concentrations in autopsied macrocell specimens after 4.5 years of exposure (percentage by weight of concrete).

Specimen	Sampling Depth Ranges (mm)			
	19-32	32-38	38-51	76-89
3A1	0.30	0.30	-	0.19
3A2	0.40	0.38	-	0.19
3A3	0.30	0.29	-	0.14
3A4	0.31	0.30	-	0.12
1A5	0.37	0.33	-	0.18
2A6	0.30	0.23	-	0.18
3A7	0.35	0.26	-	0.13
3A8	0.43	0.36	-	0.29
3A9	0.34	0.38	-	0.21
1A10	0.41	0.45	-	0.19
3A11	*	*	-	*
3B1	0.33	-	0.27	0.23
3B2	0.41	-	0.25	0.21
2B3	0.41	-	0.31	0.19
3B4	0.41	-	0.37	0.24
3B5	0.55	-	0.32	0.17
2B6	0.47	-	0.31	0.23
1B7	0.30	-	0.21	0.16
1B8	0.36	-	0.24	0.20
3B9	0.41	-	0.27	0.20
2B10	0.37	-	0.31	0.22
2B11	0.43	-	0.32	0.30

* Lost data

A.8.4 Specimen Destruction

The mechanical removal of concrete was done with great care to avoid damaging the epoxy-coated bars. In the first two triplicates (opened after 1 and 2 years of exposure), saw cuts were made along the sides of the specimen parallel to the top steel bar, and across the top surface. The concrete was then forced to break in the top bar plane by use of a jack hammer along the saw cuts (as shown in Figure A.27). Additional minor chipping allowed complete removal of the bar from the concrete. The lack of adhesion between the coated bar and concrete greatly facilitated bar retrieval. The bar debonded from the surrounding concrete readily and cleanly.

Figure A.27 Demolishing macrocell specimens.

The method used to open the last triplicate specimens (after 4.5 years of exposure) was similar to that used for the first two triplicates. The main difference was that instead of using a jackhammer, a deep slot was saw-cut around the specimens (along with other shallower cuts on the top surface) at a section below the top bar. Concrete was removed by chiseling with a hammer. In this way, larger pieces of concrete could be removed and damage to epoxy coating was minimized.

A.8.5 VISUAL INSPECTION

The bars were visually inspected for any evidence of corrosion and blistering. During removal of the coating to examine underfilm corrosion, the ease or difficulty of peeling was reported as an indicator of the degree of debonding. The extent of corrosion on the steel substrate was documented. All observations of the retrieved bars at 1, 2, and 4.5 years are given in Tables A.15 to A.20. In addition, some of the bottom reinforcing bars were exposed to examine their condition. Finally, the bar trace on concrete for all recovered bars was carefully inspected for the presence of voids, dried solution deposits, and corrosion products. The observations of the bar trace for the autopsied specimens at 1, 2, and 4.5 years are given in Table A.21.

Table A.15 Observations of macrocell 13-mm (#4) bar specimens, one year exposure.

Specimen	Bar Surface Condition	Coating Adhesion	Undercutting
2 A.1	Concentrated rib and surface degradation and pitting (0.8 mm deep). Equal corrosion on top and bottom sides.		
1 A.2	No apparent corrosion.	Poor bond on bent portion only.	Bright steel, no visible metal loss.
2 A.3	Minor surface corrosion (very shallow metal loss)	Poor bond on bent portion only.	Slight spreading (6 mm) from edges of damaged spot.
1 A.4	No apparent corrosion.	Poor bond on bent portion only.	Bright steel, no visible metal loss.
2 A.5	Minor pitting, small blisters.	Very poor bond on bent portion only.	Moderate spreading on bent portion, trapped solution.
1 A.6	No apparent corrosion.	Poor bond on bent portion only.	Bright steel, no visible metal loss.
1 A.7	Minor surface corrosion, small blisters.	Very poor bond on bent portion only.	Moderate spreading on bent portion, trapped solution.
1 A.8	Concentrated rib and surface degradation and pitting. More corrosion on top than on bottom side.		
1 A.9	No apparent corrosion.	Poor bond on bent portion only.	Slight spreading around patched area.
3 A.10	Minor surface corrosion.	Poor bond on bent portion and partly on straight ends.	Moderate spreading on bent portion.
1 A.11	No apparent corrosion.	Poor bond on bent portion only.	Bright steel, no visible metal loss.

Table A.16 Observations of macrocell 25-mm (#8) bar specimens, one year exposure.

Specimen	Bar Surface Condition	Coating Adhesion	Undercutting
2 B.1	Concentrated rib and surface degradation and moderate pitting (1–1.2 mm deep). Slightly more corrosion on top than on bottom side.		
2 B.2	Very minor surface corrosion, small blisters.	Poor bond on bent portion only.	Thin black layer, very shallow metal loss, trapped solution.
1 B.3	Minor pitting, small blisters.	Poor bond on bent portion only.	Thin black layer, shallow metal loss, trapped solution.
1 B.4	Very minor surface corrosion.	Poor bond on bent portion only.	Mostly bright steel, no visible metal loss, trapped solution.
1 B.5	Minor surface corrosion, small and large blisters.	Very poor bond on bent portion and partly on straight ends.	Extensive spreading, thin black layer, very shallow metal loss.
3 B.6	Very minor surface corrosion, many blisters.	Poor bond on bent portion and partly on straight ends.	Mostly bright steel, no visible metal loss, thin black layer.
2 B.7	Minor surface corrosion, many variable size blisters.	Very poor bond on bent portion and most of straight ends.	Moderate spreading, very shallow metal loss, trapped solution.
3 B.8	Concentrated rib and surface degradation and pitting on straight ends. More corrosion on top than on bottom side.		
2 B.9	Very minor surface corrosion, many blisters.	Slightly poor bond on bent portion only.	Slight spreading, no visible metal loss.
1 B.10	Minor surface corrosion, many variable size blisters.	Poor bond on bent portion and partly on straight ends.	Moderate spreading, no visible metal loss, thin black layer, trapped solution.
3 B.11	Very minor surface corrosion, many blisters.	Slightly poor bond on bent portion only.	Mostly bright steel, shallow metal loss.

Table A.17 Observations of macrocell 13-mm (#4) bar specimens, two year exposure.

Specimen	Bar Surface Condition	Coating Adhesion	Undercutting
1 A.1	Concentrated rib and surface degradation and pitting (0.8 mm deep). Equal corrosion on top and bottom sides. Brown-black products.		
2 A.2	No apparent corrosion.	Poor bond on bent portion only.	Mostly bright steel, some darkening, no visible metal loss.
1 A.3	Minor pitting, cracking along continuous rib, blisters.	Very poor bond on bent portion and on most of straight ends.	Black layer around damage, some surface darkening away, stain along continuous rib.
2 A.4	No apparent corrosion.	Poor bond on bent portion only.	Mostly bright steel, no visible metal loss.
3 A.5	Minor pitting, small blisters.	Very poor bond on bent portion only.	Extensive spreading on bent portion, trapped solution.
3 A.6	No apparent corrosion, small blisters.	Very poor bond on bent portion only.	Extensive spreading, no visible metal loss.
2 A.7	Minor surface corrosion, small blisters.	Very poor bond on bent portion only.	Extensive spreading on bent portion, worse on bottom side.
2 A.8	Concentrated rib and surface degradation and moderate pitting (around 1 mm). More corrosion on bottom than on top side. Brown-black products.		
2 A.9	Very minor corrosion, small and large blisters.	Poor bond on bent portion and partly on straight ends.	Mostly bright steel, some darkening, trapped solution.
2 A.10	Minor surface corrosion, numerous corrosion spotting.	Poor bond on bent portion and on most of straight ends.	Black layer around damage, some surface darkening away, stain along continuous rib.
2 A.11	Very minor corrosion, small blisters.	Poor bond on bent portion only.	Mostly bright steel, no visible metal loss.

Table A.18 Observations of macrocell 25-mm (#8) bar specimens, two year exposure.

Specimen	Bar Surface Condition	Coating Adhesion	Undercutting
1 B.1	Concentrated rib and surface degradation with severe pitting (1.5 mm) and significant loss of section. More corrosion on top than on bottom side.		
1 B.2	Very minor surface corrosion, small blisters.	Very poor bond on bent portion and most of straight ends.	Top side black, bottom side dull, very shallow metal loss, trapped solution.
3 B.3	Moderate pitting (1-1.2 mm deep), small blisters.	Very poor bond on bent portion and half of straight ends.	Top side black, bottom side dull, shallow metal loss, trapped solution.
2 B.4	Very minor surface corrosion, small blisters.	Very poor bond on bent portion and straight ends.	Top side black, bottom side dull, very shallow metal loss, corrosion deposits.
2 B.5	Slight pitting (0.8-1 mm deep), small and large blisters.	Very poor bond on bent portion and straight ends.	Top side black, bottom side dull, shallow metal loss, trapped solution.
1 B.6	Very minor surface corrosion inside of bend, many blisters.	Extremely poor bond on bent portion and straight ends.	Top side black, bottom side dull, very shallow metal loss, trapped solution.
3 B.7	Slight pitting (0.8-1 mm deep), small and large blisters.	Very poor bond on bent portion and straight ends.	Top side black, bottom side brown or dull, shallow metal loss,trapped solution.
2 B.8	Concentrated rib and surface degradation with severe pitting (1.5 mm) and significant loss of section. More corrosion on top than on bottom side.		
1 B.9	Very minor surface corrosion, small and large blisters.	Poor bond on bent portion and most of straight ends.	Top side black, bottom side dull, very shallow metal loss, trapped solution.
3 B.10	Slight pitting (0.8-1 mm deep), large number of blisters.	Poor bond on bent portion and half of straight ends.	Top side black, bottom side dull, very slight pitting, trapped solution.
1 B.11	Large number of pinhole corrosion.	Very poor bond on bent portion.	Black and dull steel, very shallow metal loss.

Table A.19 Observations of macrocell 13-mm (#4) bar specimens, 4.5 year exposure.

Specimen	Coating Surface Condition	Coating Adhesion	Undercutting
3 A.1	Extensive surface degradation, rust build-up, and concentrated deep pitting (2 mm). More damage on straight legs. More corrosion on bottom than on top side. Top of bent portion was practically uncorroded. Black, brown, and reddish-brown products.		
3 A.2	Minor rust spots and blisters on bent portion and patched areas. Remaining surface with no apparent corrosion.	Very poor bond on bent portion and about on half-length of straight ends.	Black corroded surface with shallow pitting and slight loss of metal on bent portion mainly. Scattered orange and brown products. More corrosion on bottom side.
3 A.3	No apparent corrosion (one small stain on straight leg). Damaged area is uncorroded.	Very poor bond on bent portion and on most of straight ends.	Mottled surface on bent portion and most of straight ends. Orange and brown products on one straight leg.
3 A.4	No apparent corrosion. Few, small stains, and few blisters on one leg. Very small stains on patched areas.	Very poor bond on bent portion and partly on straight ends.	Mottled surface on most of bent portion. Black corroded surface with orange and brown products on one straight leg.
1 A.5	Scattered rust spotting, mainly on bottom side. Relatively uncorroded top side. Dark rusting and acidic solution on damaged areas.	Extremely poor bond on bent portion and straight ends..	Uniform black corroded surface with shallow pitting and slight metal consumption. Accumulation of whitish products on straight leg and part of bent portion. Scattered white and yellowish-brown products.
2 A.6	Many small stains and extensive blistering on bottom side. Apparently uncorroded top side (but corroded beneath the coating)	Poor bond on bent portion and about on half-length of straight ends.	Black corroded surface with shallow pitting and moderate metal consumption on bent portion and part of straight ends. Accumulation of whitish and yellowish-brown products. More corrosion on bottom side.
3 A.7	No apparent corrosion, only a few blisters and stains. Uncorroded damaged areas.	Very poor bond on bent portion and about on half-length of straight ends.	Mottled surface on outside of bent portion and on straight legs. Dark corroded surface with scattered whitish, orange, and brown products on inside of bent portion.
3 A.8	Extensive surface degradation, rust build-up, and localized deep pitting (2 mm) and metal depletion mainly on straight legs and on parts of outside bend. More corrosion on bottom than on top side. Top of bent portion and part of bottom bent was uncorroded. Black, brown, reddish-brown, and orange products.		
3 A.9	Minor corrosion. Scattered small stains and blisters on bottom side. Apparently uncorroded top side. Rust staining on patched area.	Very poor bond on bent portion and most of straight ends.	Dark corroded surface on bent portion and one straight leg. Scattered orange and brown products mainly on top side. Mottled surface on other straight leg. Similar corrosion on top and bottom sides.
1 A.10	Many small stains and blisters on bottom side (bent portion and one straight leg). Apparently uncorroded top side. Dark rusting on patched area.	Extremely poor bond on bent portion and straight ends.	Dark corroded surface with accumulation of large whitish, brown, and orange products on bent portion and one straight leg. Mottled surface on remaining straight leg. Portions with rust build-up and slight metal depletion. More corrosion on bottom side. Acidic solution.
3 A.11	Apparent minor corrosion, several large and small blisters. Limited staining.	Extremely poor bond on bent portion and straight ends.	Dark corroded surface on bent portion and part of one straight leg. Scattered reddish-brown products. Slight metal consumption. Mottled surface on straight legs. Slightly more corrosion on bottom side.

Table A.20 Observations of macrocell 25-mm (#8) bar specimens, 4.5 year exposure.

Specimen	Coating Surface Condition	Coating Adhesion	Undercutting
3 B.1	Extensive surface degradation with rust build-up and visible metal depletion, mainly on straight legs and bottom side of bent portion. Several large pits. Top side of bent portion was practically uncorroded. Mainly black and reddish-brown products.		
3 B.2	Top side with no apparent corrosion. Extensive blistering and brown staining along bottom side. Coating cracking along rib. Rust staining of patched areas.	Extremely poor bond on bent portion and straight ends.	Uniform dark corroded surface with extensive shallow pitting and moderate metal consumption. Many scattered rust products. Acidic solution. Top side nearly as corroded as bottom side. More corrosion on outside of bent portion.
2 B.3	Severe corrosion on damaged spots (rust build-up and metal loss). Scattered large and small blisters and stains. Coating cracking along rib. Top side apparently more corroded.	Extremely poor bond on bent portion and straight ends.	Uniform dark corroded surface. Darker top side. Many scattered corrosion products. Corrosion more severe on outside of bent portion, with metal depletion and shallow to moderate pitting. Slightly more corrosion on bottom side (condition opposite from coating surface).
3 B.4	Top side with minor corrosion. Staining and extensive blistering on bottom side. Coating cracking along rib. Rust staining on patched areas.	Extremely poor bond on bent portion and straight ends.	Black and dull surfaces with shalow pitting, rust build-up, and metal depletion. Many brown, reddish-brown, and orange products scattered. Acidic solution. Similar corrosion between top and bottom sides. Slightly more corrosion on outside of bent portion.
3 B.5	Extensive dark staining on top side. Spread but less dense staining on bottom side. Small blisters and coating cracking along rib. Dark rust build-up on damaged areas.	Extremely poor bond on bent portion and straight ends..	Uniform black corroded surface with appreciable metal depletion and shallow pitting. Many widespread, scattered brown, orange, and white products. Acidic solution. Small mottled surface on one leg. Similar corrosion between top and bottom sides. Much more corrosion on the outside of bent portion.
2 B.6	No apparent corrosion on top side. Scattered staining and many blisters along bottom side. Dark rust evident on induced coating cracks on outside of bend.	Extremely poor bond on bent portion and straight ends..	Uniform dark corroded surface with little metal consumption, a few shallow pits, and slight rust build-up. Large yellowish-brown stains (thin rust film) on outside of bend. Scattered orange, brown, and whitish products. Acidic solution. Similar corrosion between top and bottom sides.
1 B.7	Light staining spread along bottom of bent portion. Extensive dark rusting on damaged areas. Few large and small blisters.	Extremely poor bond on bent portion and straight ends..	Uniform dark corroded surface with shallow pitting and slight metal consumption and rust build-up. Extensive staining (thin rust film) on outside of bend. Scattered orange, brown, and whitish products. Acidic solution. Small mottled surfaces on straight ends. Similar corrosion between top and bottom sides.

Table A.21 Observations of bar trace on macrocell concrete specimens.

Specimen	Concrete on Top Side of Bar	Concrete on Bottom Side of Bar
A series - Control bars	Porous, dusty, adhering to bar. Exudation of corrosion products extended beyond bar location.	More porous and dusty than on top side, adhering to bar. Exudation of corrosion products extended beyond bar location. A few dark-greenish spots visible immediately after opening.
A series - Coated bars	Smooth, shiny (glossy), minimum pores, clear rib marks, lack of bond with bar. Corrosion products mainly at locations of exposed steel areas in some specimens. Few blisters developed at voids or air pockets.	More pores than on top, less clear rib marks, sometimes with latence or whitish deposits adhering to bar. Corrosion products mainly at locations of exposed steel areas, but sometimes spread along bent portion and part of straight ends. Few blisters developed at voids or air pockets.
B series - Control bars	Porous, dusty, adhering to bar. Exudation of corrosion products extended beyond bar location. A few dark-greenish spots visible immediately after opening.	More porous and dusty than on top side, surface latence filling rib marks, adhering to bar. Exudation of corrosion products extended beyond bar location. A few dark-greenish spots visible immediately after opening.
B series - Coated bars	Smooth, shiny (glossy), minimum pores, clear rib marks, lack of bond with bar. Corrosion products mainly at locations of exposed steel areas, but sometimes spread along bent portion and longitudinal rib. In a few cases, sparse corrosion products reached the top surface. Blisters of variable sizes developed at voids or air pockets.	More pores than on top, less clear rib marks, sometimes with latence or whitish deposits adhering to bar. Corrosion products spread throughout bent portion and straight ends, concentrating more at locations of exposed steel areas and along longitudinal rib. Blisters of variable sizes developed at voids or air pockets.

REFERENCES

1. Clear, K.C. *Effectiveness of Epoxy-Coated Reinforcing Steel–Interim Report*. Canadian Strategic Highway Research Program. Ottawa: C-SHRP, 1992.

2. Sagüés, A.A., R.G. Powers, and A.M. Zayed. "Marine Environment Corrosion of Epoxy-Coated Reinforcing Steel." In *Corrosion of Reinforcement in Concrete*. eds. C.L. Page, K.W.J. Treadaway, and P.B. Bamforth. New York: Elsevier, 1990: 539–549.

3. Zayed, A.M., A.A. Sagüés, and R.G. Powers. "Corrosion of Epoxy-Coated Reinforcing Steel in Concrete." *Corrosion 89*. National Association of Corrosion Engineers. Paper No. 379. Houston: NACE, 1989.

4. Jones, Denny A. *Principles and Prevention of Corrosion*. New York: Macmillan, 1992.

5. Mehta, P. Kumar, and Paulo J.M. Monteiro. *Concrete. Structure, Properties, and Materials*. 2nd ed. Englewood Cliffs: Pretince, 1993.

6. ACI Committee 222. "Corrosion of Metals in Concrete." In *ACI Manual of Concrete Practice*. Part I. Detroit: American Concrete Institute, 1996. 5 Vols.

7. Virmani, Y.P., K.C. Clear, and T.J. Pasko Jr. *Time-to-Corrosion of Reinforcing Steel in Concrete Slabs, V.5: Calcium Nitrite Admixture or Epoxy-Coated Reinforcing Bars as Corrosion Protection Systems*. Vol. 5. U.S. Federal Highway Administration. Report No. FHWA/RD-83/012. Washington, 1983. 5 Vols.

8. Concrete Reinforcing Steel Institute. *CRSI Performance Research: Epoxy-Coated Reinforcing Steel*. Interim Report. Schaumburg: CRSI, 1992.

9. Holm, J. "Comparison of the Corrosion Potential of Calcium Chloride and a Calcium Nitrate Based Non-Chloride Accelerator --A Macrocell Corrosion Approach." *Corrosion, Concrete, and Chlorides. Steel Corrosion in Concrete: Causes and Restraints*. American Concrete Institute. Special Publication SP-102-9. Detroit: ACI, 1987: 35–48.

10. Fontana, Mars G., and Norbert D. Greene. *Corrosion Engineering*. New York: McGraw, 1978.

11. Hededahl, P., and D.G. Manning. *Field Investigation of Epoxy-Coated Reinforcing Steel*. Report No. MAT-89-02. Ontario Ministry of Transportation. Research and Development Branch. Ottawa: MTO, 1989.

12. Clear, K.C., and Y.P. Virmani. "Corrosion of Nonspecification Epoxy-Coated Rebars in Salty Concrete." *Public Roads*. 47, No. 1 (June 1983): 10.

13. Sagüés, A.A. *Corrosion of Epoxy-Coated Rebar in Florida Bridges*. University of South Florida. Interim Summary Report. State Job No. 99700-7556-010. Tampa, 1992.

14. Sagüés, A.A. *Mechanism of Corrosion of Epoxy-Coated Reinforcing Steel in Concrete–Final Report*. University of South Florida. Report No. FL/DOT/RMC/0543-3296. Tampa, 1991.

15. Kahhaleh, K.Z., H.Y. Chao, J.O. Jirsa, R.L. Carrasquillo, and H.G. Wheat. *Studies on Damage and Corrosion Performance of Fabricated Epoxy-Coated Reinforcement*. National Technical Information Service. Report No. FHWA/TX-93+1265-1. Spingfield: NTIS, 1993.

16. Escalante, E., and S. Ito. "Measuring the Rate of Corrosion of Steel in Concrete." *Corrosion Rates of Steel in Concrete*. Eds. N.S. Berke, V. Chaker, and D. Whiting. American Society for Testing and Materials. ASTM STP 1065. Philadelphia: ASTM, 1990: 86–102.

17. American Society for Testing and Materials. *Standard Specification for Epoxy-Coated Reinforcing Steel Bars*. ASTM A775/A775M-90. Philadelphia: ASTM, 1990.

18. American Society for Testing and Materials. *Standard Specification for Epoxy Coated Reinforcing Steel*. ASTM D3963/D3963M-87. Philadelphia: ASTM, 1987.

19. American Association of State Highway Transportation Officials. *Standard Specification for Epoxy-Coated Reinforcing Bars*. AASHTO M284-86. Washington: AASHTO, 1986.

20. **.**Concrete Reinforcing Steel Institute. *Guidelines for Inspection and Acceptance of Epoxy-Coated Reinforcing Bars at the Job Site*. Schaumburg, Ill: CRSI, 1986.

21. "Discussion of ACI Forum: Influence of Chlorides in Reinforced Concrete." *Corrosion, Concrete, and Chlorides. Steel Corrosion in Concrete: Causes and Restraints*. American Concrete Institute. Special Publication SP-102-9. Detroit: ACI, 1987: 143–153.

22. Erlin, B., and W. Hime. "Chloride-Induced Corrosion." *Corrosion, Concrete, and Chlorides. Steel Corrosion in Concrete: Causes and Restraints*. American Concrete Institute. Special Publication SP-102-9. Detroit: ACI, 1987: 155–159.

23. Kahhaleh, Khaled Z. *Corrosion Performance of Epoxy-Coated Reinforcement*. 3 Vols. Ph.D. Diss., The University of Texas at Austin, 1994.

24. Broomfield, J.P., J. Rodriguez, L.M. Ortega, and A.M. Garcia. "Corrosion Rate Measurement and Life Prediction for Reinforced Concrete Structures." *Proceedings of 5th International Conference on Structural Faults and Repair*. V.2. University of Edinburgh, 1993: 155–163.

25. Clear, K.C., and Y.P. Virmani. "Solving Rebar Corrosion Problems in Concrete. Research Update: Methods and Materials." *Solving Rebar Corrosion Problems in Concrete*. National Association of Corrosion Engineers. Paper no. 4. Seminar Reprints. Houston, 1983.

26. Rasheeduzzafar, F.H. Dakhil, M.A. Bader, and M.M. Khan. "Performance of Corrosion Resisting Steels in Chloride-Bearing Concrete." *ACI Materials Journal*. 89, No. 5 (Sept.–Oct. 1992): 439-448.

27. Hime, W.G. "The Corrosion of Steel- Random Thoughts and Wishful Thinking." *Concrete International*. 15, no. 10 (Oct. 1993): 54–57.

28. Wheat, H.G., and Z. Eliezer. "Some Electrochemical Aspects of Corrosion of Steel in Concrete." *Corrosion*. 41, No. 11 (Nov. 1985): 640–645.

29. Al-Qadi, I.L., J.E. Peterson, and R.E. Weyers. "A Time to Cracking Model for Critically Contaminated Reinforced Concrete Structures." *Proceedings of 5th International Conference on Structural Faults and Repair*. V.3. University of Edinburgh, 1993: 91–99.

30. Kobayashi, K., and K. Takewaka. "Experimental Studies of Epoxy-Coated Reinforcing Steel for Corrosion Protection." *The International Journal of Cement Composites and Lightweight Concrete*. 6, No. 2 (May 1984): 99–116.

31. Erdogdu, S., and T.W. Bremner. "Field and Laboratory Testing of Epoxy-Coated Reinforcing Bars in Concrete." *Transportation Research Circular: Epoxy-Coated Reinforcement in Highway Structures*. No. 403. National Research Council. Transportation Research Board. Washington, 1993: 5–16.

32. Treadaway, K.W.J., and H. Davies. "Performance of Fusion-Bonded Epoxy-Coated Steel Reinforcement." *The Structural Engineer*. 67, No. 6 (Mar. 1989): 99–108.

33. Swamy, R.N., S. Koyama, T. Arai, and N. Mikami. "Durability of Steel Reinforcement in Marine Environment." *Concrete in Marine Environment*. Ed. V.M. Malhotra. American Concrete Institute. Proceedings, 2nd International Conference, St. Andrews by-the-Sea, Canada. ACI SP-109. Detroit: ACI, 1988: 147–161.

34. McKenzie, M. "The Effect of Defects on the Durability of Epoxy-Coated Reinforcement." *Transportation Research Circular: Epoxy-Coated Reinforcement in Highway Structures*. No. 403. National Research Council. Transportation Research Board. Washington, 1993: 17–28.

35. Malasheskie, G.J., D.A. Maurer, D.B. Mellott, and J.L. Avellano. *Bridge Deck Protective Systems-Final Report*. Federal Highway Administration. Report No. FHWA-PA-88-001+85-17. Washington, 1988.

36. Pfeifer, D.W., R. Landgren, and P. Krauss. "Performance of Epoxy-Coated Rebars: A Review of CRSI Research Studies." *Transportation Research Circular: Epoxy-Coated Reinforcement in Highway Structures, No. 403*. National Research Council. Transportation Research Board. Washington, 1993: 57–65.

37. Collacott, R.A. *Structural Integrity Monitoring*. London-New York: Chapman and Hall, 1985.

38. Zayed, A.M., and A.A. Sagüés. "Corrosion at Surface Damage on an Epoxy-Coated Reinforcing Steel." *Corrosion Science*. 30, no. 10 (1990): 1025-1044.

39. Sagüés, A.A., and R.G. Powers. "Effect of Concrete Environment on the Corrosion Performance of Epoxy-Coated Reinforcing Steel." *Corrosion 90*. National Association of Corrosion Engineers. Paper No. 311. Houston: NACE, 1990.

40. Smith, L.L., R.J. Kessler, and R.G. Powers. "Corrosion of Epoxy-Coated Rebar in a Marine Environment." *Transportation Research Circular: Epoxy-Coated Reinforcement in Highway Structures*. No. 403. National Research Council. Transportation Research Board. Washington, 1993: 36–45.

41. Sohanghpurwala, A., and K.C. Clear. "Effectiveness of Epoxy Coatings on Minimizing Corrosion of Reinforcing Steel in Concrete." *Transportation Research Board, 69th Annual Meeting*. Paper No. 890432. Washington: TRB, 1990.

42. Leidheiser, Henry Jr. "Corrosion of Painted Metal–A Review" *Corrosion*. (July 1982): 374–383. Reprinted in Ed. Coburn, Seymour K. *Corrosion. Source Book*. American Society for Metals and National Association of Corrosion Engineers. ASM: Metals Park, OH, 1985: 215–224.

43. Schieβl, Peter. "Review of the KCC-Inc. Reports on Effectiveness of Epoxy-Coated Reinforcing Steel." Private communication. Copy of report prepared for C-SHRP. Germany, 1992.

44. Weyers, Richard E., Wioleta Pyc, and Michael Sprinkel. "Corrosion Protection Performance of Bridge Decks and Marine Substructures Constructed with Epoxy Coated Reinforcing Steel in Virginia." *Proceedings of the Seventh International Conference on Structural Faults and Repair*. Vol. 1. Ed. Professor M.C. Forde. Edinburgh: Engineering Technics Press, 1997: 249–261. 3 Vols.

45. Vaca-Cortes, Enrique, Miguel A. Lorenzo, James O. Jirsa, Harovel G. Wheat, and Ramon L. Carrasquillo. "Adhesion Testing of Epoxy Coating." The University of Texas at Austin. Bureau of Engineering Research. Center for Transportation Research. Unpublished Research Report No. 1265-6. Austin, 1998.

46. Andrade, C., J.D. Holst, U. Nürnberger, J.D. Whiteley, and N. Woodman. *Protection Systems for Reinforcement*. CEB Bulletin D'Information No. 211. Switzerland, 1992.

47. Rostam, S. "Service Life Design- The European Approach." *Concrete International*. 15, No. 7 (July 1993): 24–32.

48. Vaysburd, A.M. "Some Durability Considerations for Evaluating and Repairing Concrete Structures." *Concrete International*. 15, No. 3 (Mar. 1993): 29–35.

49. Fraczek, John. "A Review of Electrochemical Principles as Applied to Corrosion of Steel in a Concrete or Grout Environment." *Corrosion, Concrete, and Chlorides. Steel Corrosion in Concrete: Causes and Restraints*. Ed. F.W. Gibson. American Concrete Institute. Special Publication SP-102-9. Detroit: ACI, 1987: 13–24.

50. Hime, W., and B. Erlin. "Some Chemical and Physical Aspects of Phenomena Associated with Chloride-Induced Corrosion." *Corrosion, Concrete, and Chlorides. Steel Corrosion in Concrete: Causes and Restraints*. Ed. F.W. Gibson. American Concrete Institute. Special Publication SP-102-9. Detroit: ACI, 1987: 1–12.

51. Hamad, B.S., J.O. Jirsa, and N.J. D'Abreu D'Paolo. *Effect of Epoxy Coating on Bond and Anchorage of Reinforcement in Concrete Structures*. Research Report No. 1181-1F. The University of Texas at Austin. Center for Transportation Research. Austin, 1990.

52. Cady, P.D., and R.E. Weyers. "Chloride Penetration and the Deterioration of Concrete Bridge Decks." *Cement, Concrete and Aggregates*. CCAGDP. 5, no. 2 (Winter 1983): 81–87.

53. Sagüés, Alberto A. *Corrosion of Epoxy Coated Rebar in Florida Bridges*. University of South Florida. Final Report to Florida DOT WPI No. 0510603. Tampa, 1994.

54. Clear, Kenneth C., William H. Hartt, Jack McIntyre, and Seung Kyoung Lee. *Performance of Epoxy-Coated Reinforcing Steel in Highway Bridges*. National Research Council. Transportation Research Board. NCHRP Report 370. Washington: National Academy Press, 1995.

55. Lehmann, J. "Cathodic Protection (Corrosion Control) of Reinforced Concrete Structures Using Conductive Coatings." *Corrosion, Concrete, and Chlorides. Steel Corrosion in Concrete: Causes and Restraints*. Ed. F.W. Gibson. American Concrete Institute. Special Publication SP-102. Detroit: ACI, 1987: 127–141.

56. Neville, A.M. *Properties of Concrete*. New York: Wiley, 1996.

57. Biczók, Imre. *Concrete Corrosion and Concrete Protection*. 5th ed. New York: Chemical Publishing, 1967.

58. Reis, Robert A. *In Service Performance of Epoxy Coated Steel Reinforcement in Bridge Decks*. California Department of Transportation. Report No. FHWA/CA/TL-96/01-MINOR. Sacramento, 1995.

59. Vaca-Cortes, Enrique, Hengching Chen, James O. Jirsa, Harovel G. Wheat, and Ramon L. Carrasquillo. "Repair of Epoxy-Coated Reinforcement." The University of Texas at Austin. Bureau of Engineering Research. Center for Transportation Research. Unpublished Research Report No. 1265-5. Austin, 1998.

60. ACI Committee 318. Building Code Requirements for Reinforced Concrete (ACI 318-89) and Commentary (ACI 318R-89). American Concrete Institute. Detroit, 1989.

61. American Association of State Highway and Transportation Officials. Deformed and Plain Billet-Steel Bars for Concrete Reinforcement. AASHTO M31. Washington.

62. American Society for Testing and Materials. Standard Specification for Deformed and Plain Billet-Steel Bars for Concrete Reinforcement. ASTM A615- 87a. Philadelphia: ASTM, 1987.

63. American Society for Testing and Materials. Standard Method for Nondestructive Measurement of Film Thickness of Pipeline Coatings on Steel. ASTM G12-83. Philadelphia: ASTM, 1983.

64. American society for Testing and Materials. Standard Test Methods for Determining the Effects of Chemical Admixtures on the Corrosion of Embedded Steel Reinforcement in Concrete Exposed to Chloride Environment. ASTM G109-92. Philadelphia: ASTM, 1992.

65. American Association of State Highway and Transportation Officials. Rapid Determination of the Chloride Permeability of Concrete. AASHTO T277-83. Washington: AASHTO, 1983.